Cell Biology of the Mammalian Ttyh1 Protein

By

Clayton Ashley Matthews

A thesis submitted for the degree of

Doctor of Philosophy

of The Australian National University

May 2007

Statement

All of the experimental work presented in this thesis was performed by the author, unless specifically stated otherwise in the text.

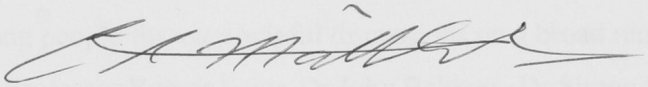

Clayton Ashley Matthews

Acknowledgements

I would like to thank my supervisors, Dr Hugh Campbell and Dr Michael Crouch, for giving me the opportunity to pursue this exciting project within the Molecular Genetics and Evolution group, and at TGR BioSciences. I am grateful for the time and expertise they have provided over the past four years.

I would also like to thank my co-supervisor, Professor Ian Young, for his technical advice and reference for my membership into professional societies. I would like to thank my advisor Dr Anthony Dyer for his support and enthusiasm.

I thank the following people for very helpful discussions on a broad range of topics related to this thesis: Professor Robert Saint, Dr John Bekkers, Dr Simon Koblar, Dr Klaus Matthaei, Dr Ron Osmond, Dr Michael Murray, Dr Mark De Nichilo, Dr Charles Claudianos, Dr Stuart Archer, and Dr Matthew Chong.

Finally, I would like to thank my parents, Ray and Rita, and my family for their encouragement throughout the course of my academic studies. I convey extra thanks to Anita and Les Miller for their financial support which was greatly appreciated. I am also thankful to Jenny for her selflessness and great cooking.

Non est ulla vita usitata,

tantum vita ipsa.

Abbreviations

aa	amino acid residue
AP1	affinity purified N-terminal Ttyh1 antibody
AP2	affinity purified C-terminal Ttyh1 antibody
AQP	aquaporin water channel
bp	base pair
CD49e	human homologue of the integrin alpha 5 subunit
DMEM	Dulbecco's modified Eagles medium
DTT	dithiothreitol
ECM	extracellular matrix
EDTA	ethylenediamine tetra-acetic acid
ELISA	Enzyme-Linked ImmunoSorbent Assay
EST	expressed sequence tag
FA	focal adhesion
FAK	focal adhesion kinase
FCS	fetal calf serum
fli	the *Drosophila melanogaster* flightless gene
GFP	green fluorescent protein
GRAVY	grand average of hydropathy
GTP	guanine triphosphate
HEK293	human embryonic epithelial kidney cell line
HRP	horseradish peroxidase
Ig	immunoglobin
IHC	immunohistochemistry
ILK	integrin linked kinase
IRM	interference reflection microscopy
kb	kilobase
kDa	kilodalton
MALDI-TOF	Matrix Assisted Laser Desorption Ionization Time-of-flight mass spectrometry

MCS	6-maleimidocaproic acyl N-hydroxysuccinimide ester
MQH_2O	Milli-Q^{TM} reverse osmosis purified water
mRNA	messenger ribose nucleic acid
MW	molecular weight
NCAM	neural cell adhesion molecule
PAGE	polyacrylamide gel electrophoresis
PBS	phosphate buffered saline
PCR	polymerase chain reaction
RGD	consensus sequence that supports cell adhesion
RT-PCR	reverse transcriptase polymerase chain reaction
SDS	sodium dodecyl sulphate
SH3	src homology 3 domain
TNT	tunnelling nanotube
TNFR	tumour necrosis factor receptor
TRAF	tumour necrosis factor associated factor
Tris	tris (hydroxymethyl) aminomethane
TRITC	photo-bleach resistant analogue of the Texas-Red fluorophor
Tty	the *Drosophila melanogaster* tweety gene
Ttyh1	the human homologue of isoform 1 of the tweety gene
VRAC	volume regulatory anion channel

Abstract

Homologues of the *Drosophila melanogaster* tweety (tty) gene are present in mammals and *Caenorhabditis elegans*. The available EST expression data suggests that the human homologue of tty isoform 1, Ttyh1, is expressed almost exclusively in the brain and testis, and hydrophobicity analysis predicted that Ttyh1 is a member of a novel family of transmembrane proteins. The encoded proteins have five predicted membrane-spanning regions and recent findings suggest that some family members may be chloride channels. In *Drosophila*, flies lacking tty and several nearby genes had a lower viability than the wild type controls, and exhibited uncoordinated behavior. A complete understanding of the role of transmembrane proteins in the human brain will be essential for the advancement of therapies aimed at disorders involving cell communication, development and cell adhesion.

The aim of the research presented in this thesis was to investigate and characterize the cellular role of the mammalian Ttyh1 protein. There appears to be at least three homologues of tty in human and mouse, two homologues in *D. melanogaster* and one homologue in *C. elegans*. The Ttyh2 isoform is upregulated in renal cell carcinoma, and examination of EST data indicates that Ttyh1 is upregulated in astrocytoma, glioma and several other cancers of predominately neuronal cell types. The prediction of C-terminal variants of Ttyh1 derived by alternative splicing of mRNA was supported by Western blot analysis. Two variants of Ttyh1 were identified, with the N-terminal anti-Ttyh1 antibody detecting proteins of 51 kDa and 49 kDa and the C-terminal anti-Ttyh1 antibody detecting only the 49 kDa protein. Ectopic Ttyh1 expression in several cell lines showed membrane localization which concurred with protein hydrophobicity and topography predictions. Following translocation to the cell membrane, Ttyh1 expression induced dramatic morphological changes similar to those observed by the over-expression of actin assembly genes. Filopodia rich in F-actin protruded from the periphery of cells making contact with the substrate and surrounding cells.

Upon cell migration, Ttyh1-rich deposits were left behind on the substrate and on surrounding cells as filopodia were torn from their adhesive contacts. The Ttyh1 trails deposited by migrating cells were reminiscent of integrin-rich deposits that are left by migrating fibroblasts. Immunohistochemical analysis revealed that points of concentrated Ttyh1 were almost completely coincident with CD49e, the human homologue of the α5 subunit of the α5β1 integrin complex, suggesting that Ttyh1 was spatially and perhaps functionally associated with integrins. In Ttyh1-expressing cells, microtubules were observed to be orientated towards the cell membrane, and often terminated directly behind Ttyh1-induced protrusions. It is possible that the Ttyh1 protein was transported to the membrane via microtubules since Ttyh1 could be seen in discreet packages along peripherally radiating microtubules. Ttyh1 was often observed to be highly concentrated at the interface between cells suggesting a role in cell communication or cell-cell adhesion.

It has previously been shown that trailing edge detachment is the rate-limiting step of cell migration. Real-time microscopy revealed that expressed Ttyh1 was highly concentrated in nascent focal adhesions at the trailing edge of cells. The expression of Ttyh1 either directly or indirectly caused a significant increase in the rate of cell migration. The localization and dynamics of endogenously expressed Ttyh1 in neuronal cultures and in rat brain slices corresponded to those observed in exogenous expression studies. It is possible that Ttyh1 is an F-actin-modulating adhesion molecule or receptor that can regulate neuronal adhesion dynamics and cell migration in the mammalian brain.

Table of Contents

Chapter 4: Detection of endogenous Ttyh1 using immunohistochemistry

Chapter 5: General Discussion

Chapter 1

General Introduction

1.1 Introduction

The *Drosophila melanogaster* tweety gene (tty) was originally discovered as a transcription unit adjacent to the flightless I gene (Campbell et al. 1993). Deletion of this part of the genome containing the tty gene and some adjacent genes such as dodo, penguin and flightless I caused a dramatic loss in fly viability. Transgenic replacement of flightless I did not restore full viability (Campbell et al. 1993), indicating that other genes in this region may be functionally important during development. The possibility that deletion of tty contributed to the significantly lowered viability and uncoordinated behaviour observed following flightless I gene transgenic rescue has not been excluded (Maleszka et al. 1996), although the exact function of tty is unknown. In *Drosophila* and *C. elegans*, at least 60 % of transcription units are not vital for development into adulthood (Goebl and Petes 1986). The 79 % viability compared with controls that was observed following combined tty, dodo and penguin gene knockouts (Fig. I) may attest to the compensatory mechanisms which are prevalent in both prokaryotic and eukaryotic genomes (Soriano 1995; Maleszka et al. 1996).

There appears to be at least three homologues of tty in human and mouse, one homologue in *C. elegans* and a second homologue in *D. melanogaster* (Campbell et al. 2000; Rae et al. 2001; Suzuki and Mizuno 2004). The proteins contain five predicted transmembrane regions arranged in a characteristic 2-2-1 pattern (Campbell et al. 2000) except in the case of Ttyh3 which reportedly contains six transmembrane segments (Suzuki and Mizuno 2004). The Ttyh1 protein is a human homolog of tty which is predominately expressed in the brain, exhibits lower expression levels in the testis and is expressed at very low levels elsewhere. Ttyh1 is located on human chromosome 19 at position q13.4, is predicted to contain 450 amino acid residues (Campbell et al. 2000) and is up-regulated in astrocytoma, glioma and several other cancers (Matthews et al. 2007). The human Ttyh1 gene shows 91 % identity to mouse Ttyh1, 85.7 % identity to rat Ttyh1 and 27 % identity to *Drosophila* tty (Campbell et al. 2000; unpublished data). Mouse Ttyh1 exhibits 91.8 % identity to rat Ttyh1 with the N-terminal and the C-terminal 15 peptides being 100 % identical (unpublished data).

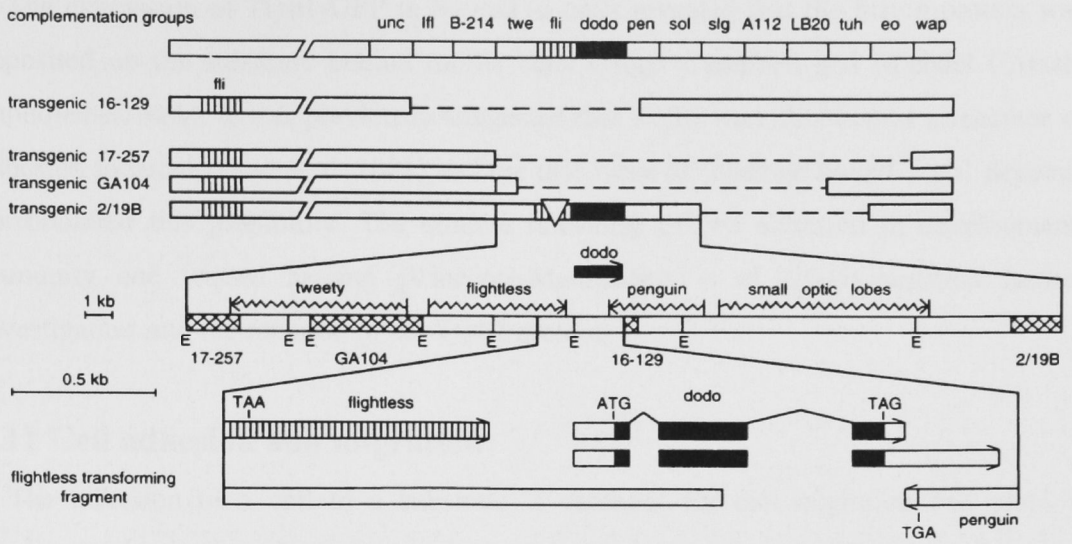

Fig. I A genetic and molecular map of the flightless (fli) region in *D. Melanogaster* and the location of re-arranged chromosomes are illustrated. Chromosome 2/19B carried a 5.4kb insertion in the fli transcription unit and a deficiency outside of this region (top). The five complete transcription units, the EcoRI (E) restriction sites, and the extent of the four chromosomal breakpoints (cross-hatched boxes) are indicated (middle). Intron-exon structure of the dodo transcription unit and the positions of the termination codons in the flightless, dodo, and penguin genes are shown (bottom) (taken from Maleszka et al. 1996).

The human Ttyh2 isoform shows the same 2-2-1 transmembrane protein pattern as Ttyh1, is 48 % homologous and is up-regulated in renal cell carcinoma (Rae et al. 2001). The amino terminus is predicted to be extracellular and Ttyh2 is highly expressed in the brain, testes and, to a lesser extent, the heart (Rae et al. 2001). Uniquely, the Ttyh2 protein contains an RGD motif which has been shown to mediate binding to integrins in other proteins thereby facilitating cell adhesion events (Rae et al. 2001). The highest level of variation between the Ttyh proteins is in the intracellular C-terminus, and Ttyh2 has a C-terminal extension of 84 amino acids compared with Ttyh1 (Rae et al. 2001). A recent paper indicates that some human tweety homologues may have novel chloride ion channel activity (Suzuki and Mizuno 2004). However, the evidence presented is not conclusive and will be discussed in detail later.

The expression of Ttyh1-GFP in Swiss3T3 cells revealed that the fusion protein was deposited on the substrate behind motile cells (Hugh Campbell and Michael Crouch, unpublished data). It was previously suggested that Ttyh1 may function as a receptor or adhesion molecule (Rae et al. 2001) and the discovery of substrate bound Ttyh1 deposits corroborated this possibility. The clinical relevance of cell adhesion in development, immunity and wound healing (Vincente-Manzanares et al. 2005) justified further investigation into the function of the Ttyh1 protein.

1.11 Cell adhesion and migration

The adhesion of a cell to a substrate is essential for cell migration and plays a fundamental role in embryonic morphogenesis, angiogenesis, inflammation and wound healing (Yang et al. 1995; Sheetz et al. 1998; Rossiter et al. 1997). Studies which used interference reflection microscopy (IRM) (Curtis 1964) were the first to show that cells do not attach to a surface uniformly, but rather by specialized foci, the largest of which are termed focal adhesions (FA) (Izzard and Lochner 1980; Burridge et al. 1988). Using the interference patterns of IRM it was estimated that the separation between the cell and the substrate at FA's was 10-15 nanometers and that the immobility of FA's relative to the substrate was consistent with an adhesive function (Izzard and Lochner 1980). In experiments where cells were mechanically sheared from the substrate, FA's were often left isolated and remained attached to the surface on which the cells were grown (Avnur et al. 1983; Neyfakh and Svitkina 1983).

It has now been established that FA's are the complex molecular assemblies linking the actin cytoskeleton to the extracellular matrix via transmembrane receptors called integrins (Schoenwaelder and Burridge 1999; Zamir and Geiger 2001). The integrins are cell surface receptors for extracellular matrix molecules which include vitronectin, fibronectin, laminin and collagen (De Nichilo and Yamada 1995). Combinations of α and β integrin subunits determine specificity, and upon binding to their specific ligands, integrins associate with the actin cytoskeleton to organise the generation of FA's (De Nichilo and Yamada 1995). The ILK protein is a major component of integrin mediated cellular processes which include substrate adhesion, anchorage dependent cell cycle

progression and fibronectin matrix assembly (Li et al. 1999). Identification of the components of FA's which began with vinculin (Geiger 1979), and now contains over fifty distinct proteins (Zamir and Geiger 2001) (Fig. II), has made it possible to study adhesion sites using fluorescent probes and high resolution microscopy techniques (Anderson and Cross 2000). It has also become apparent that FA's are only one of a growing number of adhesion complexes that exist in migrating cells (Zhang 2002).

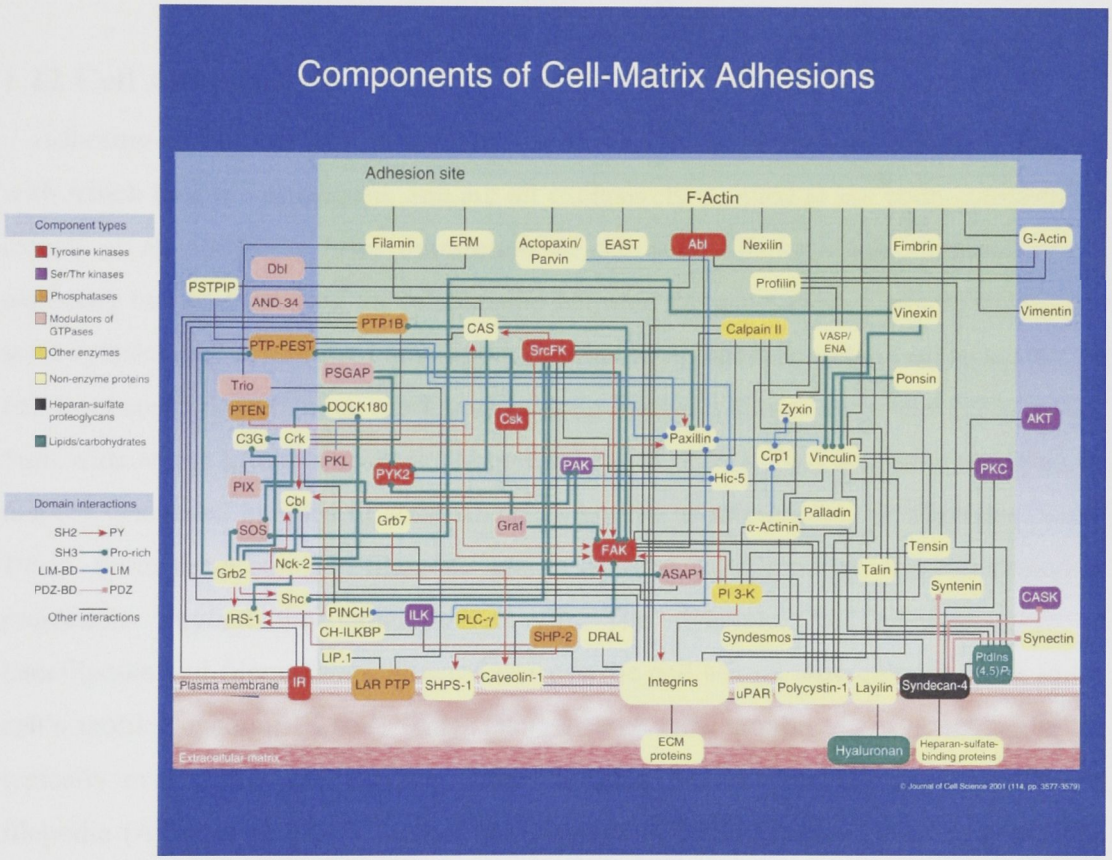

Fig. II A schematic representation of molecules involved in cell-ECM adhesions. The properties of each component are specified by the colour of its box, and the kind of interaction between the components is represented by the colour and style of the interconnecting lines. Molecules known to be associated with cell-matrix adhesion sites have been placed within the green box, while proteins that affect matrix adhesions but are not stably associated with them have been placed within the blue frame. (taken from Zamir and Geiger 2001)

The process of cell migration requires precise control of integrin mediated adhesions and involves coordinated attachment to the substrate at the leading edge, and detachment at the rear (Lauffenberger and Horwitz 1996; Sheetz et al. 1999). The focal adhesions, actin cytoskeleton and intracellular signalling pathways work in unison to mediate cell migration. Collectively they must respond to a diverse range of extracellular signals and translate them into a finely regulated intracellular response (Stokes et al. 1990). Implementation of this response requires complex interactions between the extracellular matrix, transmembrane molecules and the actin cytoskeleton.

1.12 Cell Adhesion Foci

Adhesion complexes can be classified according to the assemblies of actin filaments with which they are associated, and are all exclusively coupled to the actin cytoskeleton (Small et al. 1998). A brief description of the actin filament sub-compartments is necessary before discussing the relationship between the generation of adhesion sites and actin cytoskeleton assembly. Lamellipodia, including membrane ruffles, at the advancing cell front consist of a laminar meshwork of actin filaments (Small and Celis 1978) around 5μm wide and 0.2μm in thickness (Abercrombi et al. 1971). This is often punctuated by radially orientated bundles of actin filaments known as microspikes or filopodia (Small 1981). From these bundles, filaments merge into the lamellipodium and can extend in projections beyond the lamellipodium tip. The dynamic, fast growing ends of lamellipodia and filopodia are directed towards the cell's front where they engage in the cell's motile functions (Small 1981). The adhesive focal complexes in lamellipodia are typically oval shaped and are sometimes elongated beneath microspikes and adherent filopodia (Allen et al. 1997). Behind the filopodium, actin filaments are organized into one of at least five types of bundled arrays or more loosely packed actin networks (Small et al. 1998). These consist of stress fibres which traverse the cytoplasm, concave bundles at the cell,s edge, convex bundles at the cells edge, polygonal networks and dorsal arcs (Gloushankova et al. 1997). Unlike lamellipodia and filopodia, these arrays contain anti-parallel actin that is associated with myosin II and is therefore contractile (Wollert et al. 2002). Concave bundles and stress fibres are anchored to the substrate via elongated adhesion sites which correspond to the focal adhesions visible by IRM. Since polygonal

arrays and dorsal arcs are not directly associated with the substrate (Heath and Holifield 1993; Rathke et al. 1979) they will not be discussed further.

1.13 Adhesion complexes and small GTPases

The Rho family of small GTPases are essential in the regulatory pathways that signal to induce actin cytoskeleton assembly and the formation of adhesion complexes (Hall 1998). Briefly, RhoA signals the formation of focal adhesions which are associated with actin stress fibre bundles, Rac1 signals the construction of focal complexes associated with lamellipodia and cdc42 signals the creation of focal complexes associated with filopodia (Carton et al. 2003). It has also become apparent that there is a balance between Rho GTPase activities influenced by mutual antagonism which is essential in the determination of cytoskeletal organisation and patterns of cell adhesion (Moorman et al. 1999). The activities of Rho GTPases have a dramatic effect on actin filament bundle assembly and the relative proportions of lamellipodia and filopodia at the cells leading edge (Allen et al. 1997). Bundle assembly is further modulated by two downstream targets of RhoA. The first is Rho kinase which signals for thick, compact bundles, and the second is mDia which signals for parallel arrays of fine bundles (Watanabe et al. 1999). The relationship between Rho GTPase activity and adhesion formation was demonstrated in live 3T3 fibroblasts by labelling adhesions with rhodamine tagged vinculin (Rottner et al. 1999). Adhesion sites, recognised by vinculin accumulation, begin as small focal complexes behind the leading edge of the lamellipodium and beneath the actin array. Molecules which have been localised to these focal complexes include vinculin, paxillin, α5-integrin, β1-integrin, α-actinin and FAK (Lee and Jacobson 1997). These studies showed that the formation of focal complexes could be induced in lamellipodia by the injection of constitutively active Rac1 and that these could be converted into focal adhesions by the addition of RhoA (Rottner et al. 1999). It was also shown that the injection of dominant negative Rac1 could cause the suppression of focal complexes and membrane ruffling accompanied by an increase in the size of focal adhesions in normal migrating fibroblasts (Rottner et al. 1999). The inhibition of Rho kinase in non-motile fibroblasts expressing only focal adhesions could induce lamellipodia protrusions with transient focal complexes (Rottner et al. 1999). The Rac1-dependent membrane ruffling

could also be suppressed by the introduction of constitutively active cdc42 exemplifying the reciprocal antagonism between Rho family members (Allen et al. 1997).

The fate of a focal complex depends on whether it forms in front of the cell body, in the central region or at the cells edge. In the central region focal complexes remain stationary relative to the substrate and disassemble as the cell moves over them. They may also be removed from the substrate as the trailing edge of the cell rolls upward upon cell migration (Anderson and Cross 2000; Anderson et al. 1996). If focal complexes form in the vicinity of the lamellipodium, which flank the cell body, they fuse together at the trailing edge to create large adhesions resembling complete focal adhesions. The lateral adhesions are mobile, transient, and are drawn towards the flanks of the cell body in a sliding motion which is driven by the contractile bundles of laterally orientated actin filaments (Anderson et al. 1996; Lee et al. 1994). These data provide a good example of the recycling nature of adhesion sites and prompted the question of whether the trailing, lateral adhesions served a purpose in cell motility. Experimental evidence suggests that these adhesions are necessary for the generation of lateral tension which is required to develop traction within the cell body (Svitkina et al. 1997). Hypotonicity can also activate Rac and cdc42, and thereby induce membrane protrusions and actin remodelling (Carton et al. 2003). It is possible that integrin disruption is the hypertonicity sensor leading to reduced inhibition of Rac and the observed cellular response. However, it is unlikely that actin remodelling is involved in the activation of ion transporters or channels that contribute to regulatory volume decrease (Carton et al. 2003). There is no correlation between activation of volume regulatory anion channels (VRAC) and actin remodelling (Pederson et al. 1998; Tilly et al. 1996). F-actin reorganization and VRAC activation appear to be swelling induced phenomena which are not causally or mechanistically coupled (Carton et al. 2003).

1.14 Intracellular tension in cell adhesion

The development of tension in the actin cytoskeleton via actin-myosin interactions is a prerequisite for the formation of focal adhesions (Chrzanowska-Wodnicka and Burridge 1996). Similarly, the formation of focal complexes and their exertion of traction upon the

substrate is dependent on actomyosin tension (Rottner et al. 1999; Beningo et al. 2001). Experiments have shown that by the application of an external mechanical force on live cells, adhesion sites can be induced which are similar to those generated by intracellular contractility (Riveline et al. 2001). Recently it was demonstrated that FAK performs a mechanosensory function and is required for persistent migration in fibroblasts (Li et al. 2002). Furthermore, the application of shear stress induced a transient activation of FAK, recruitment to focal adhesions and lamellipodia induction at the cell periphery implicating it as a key molecule in the transduction of mechanosensory signals (Li et al. 2002).

During cell migration, tension in the actin cytoskeleton is required for adhesion at the leading edge as illustrated by the leading edge retraction which can be induced by myosin inhibitors (Cramer and Mitchison 1995). Inhibition of myosin also causes the retraction of the trailing edge of the cell body in the final phase of motility (Dunn 1980). The use of flexible substrates has facilitated quantitation of the forces exerted at adhesion sites by living cells. These forces are the result of actomyosin contraction, occur on a time scale of fractions of a second and are determinants of focal adhesion assembly (Balaban et al. 2001). In migrating fish fibroblasts, leading edge focal complexes and early focal adhesions exert a greater force than mature focal adhesions (Pelham and Wang 1999). This was demonstrated by the decreased substrate deformation at the trailing edge of migrating fibroblasts and the sliding of the trailing edge during cell edge retraction (Zamir et al. 2000). Other studies have clearly indicated that integrin signalling is dependent on cellular contractility (Felsenfeld et al. 1999). Taken together, these experiments illustrate the central role intracellular tension plays in the generation and dissociation of cell adhesion complexes, and in the activation of their associated signalling cascades.

1.15 Adhesion foci and cytoskeletal communication

The depolymerisation of cytoskeletal microtubules in fibroblasts causes cells to become less polarised in terms of shape (Vasiliev and Gelfand 1976), an increase in cytoskeletal contractility (Danowski 1989) and an increase in the size of focal adhesions

(Chrzanowska-Wodnicka and Burridge 1996). These responses are correlated with RhoA activation (Bershadsky et al. 1996), while re-polymerisation of microtubules is associated with Rac1 activation (Waterman-Storer et al. 1999). This implies a link between microtubule polymerisation and the Rho GTPases that control actin cytoskeletal organisation and substrate adhesion. Studies using living cells in which adhesion components and microtubules had been fluorescently labelled revealed that microtubules target adhesion foci as they polymerise towards the cell membrane (Kaverina et al. 1998). The interface between microtubules and focal adhesions is in close proximity since focal adhesions are able to capture and temporarily stabilise microtubules against depolymerisation induced by exposure to nocodazole (Kaverina et al. 1998). More recently, by using total internal reflection fluorescence microscopy, microtubules over adhesion sites were captured dipping into the evanescent wave formed within 150 nanometers of the substrate (Toomre and Manstein 2001).

Data suggest that the intimate cross-talk between microtubules and focal adhesions serves the purpose of modulating adhesion site dynamics (Kaverina et al. 2000), and it has been demonstrated that the targeting of focal complexes or focal adhesions by microtubules retards their growth or promotes their disassembly (Kaverina et al. 1999). The focal adhesion disassembly associated with microtubule targeting can also be mimicked by applying inhibitors of myosin contractility at the cell's edge (Kaverina et al. 1999). It was revealed that cells lacking microtubules that were structurally depolarised could be re-polarised and induced to move by the asymmetrical addition of the same myosin inhibitor (Kaverina et al. 2000). These data imply that microtubules influence cell polarisation by modulation of adhesion site turnover via the point delivery of signals that antagonise myosin contractility at adhesion sites. Microtubule disruption has also been shown to induce focal adhesions and stress fibre formation which could be prevented by the inhibition of cell contractility via RhoA (Bershadsky et al. 1996).

1.16 Leading edge component delivery

Integrins and other membrane components of focal adhesions may be delivered to adhesion assembly sites via microtubule driven membrane traffic (Bretscher 1996). It has

been shown that blocking vesicle transport along microtubules inhibits cell spreading and delivery of integrins to the cell membrane (Roberts et al. 2001). Our understanding of the means of replenishment of the cell membrane at the leading edge remains to be clarified and could involve members of the Rab family of small GTPases. It should be noted however that cell spreading can occur in the absence of microtubules, and thus is not always dependent on microtubule related vesicle trafficking (Spaargaren and Bos 1999).

1.17 Filopodia and cell surface protrusions

A complete understanding of the actin dynamics at the leading edge of cultured cells is considered to be the key to understanding cell locomotion. The biochemistry underlying these processes is complex and includes actin polymerisation via the Arp2/3 complex and depolymerisation involving cofilin (Pantaloni et al. 2001). In migrating cells actin polymerisation underlies the protrusion of lamellipodia (ruffles) at the leading edge and the rearward flow of F-actin (Watanabe and Mitchison 2002). Actin polymerisation is promoted within 1 micrometer of the leading edge, but polymerisation and depolymerisation occur at a higher rate as F-actin flows toward the rear (Watanabe and Mitchison 2002). Studies have shown that G-actin is actively transported to the leading edge for polymerisation and incorporation into F-actin during cell protrusion (Zicha et al. 2003). However, this transport does not rely on microtubule based motors or motor proteins of the myosin superfamily and disruption of microtubules does not stop rapid transport of actin to the leading edge (Zicha et al. 2003). Non-muscle myosin II is unlikely to transport actin directly, though it is required for cell body contraction which appears to be necessary for G-actin transport (Zicha et al. 2003). The polymerization of actin at the cell's leading edge is accompanied by the creation of complexes that connect extracellular signals to regions of actin assembly (Rottner et al. 2001). Among the structural molecules, talin is a major activator of integrin and a direct linker of integrin and actin (Vicente-Manzanares et al. 2005; Nayal et al. 2004).

Components of the non-enzymatic zyxin protein support its role as a regulator of actin dynamics at the leading edge (Hobert et al. 1996). The zyxin protein contains polyproline-rich stretches in the amino terminus which provide binding sites for the SH3

domain of the guanine nucleotide exchange factor for Rho GTPases (Hobert et al. 1996). These polyproline rich domains also provide docking areas for Ena/VASP family proteins which are recruited to the distal edge of lamellipodia in quantities that directly correlate with actin protrusion rates (Rottner et al. 1999). Ectopic expression of zyxin causes the induction of actin rich protrusions which can be reduced by the expression of a zyxin mutant lacking functional Ena/VASP binding sites (Drees et al. 2000). By blocking the interaction of zyxin with α-actinin, retraction of the leading edge, migration and cell spreading are perturbed (Drees et al. 1999). Membrane targeting of zyxin induces local actin assembly, and cell-cell interactions via cadherins have also been shown to involve the LIM domains of zyxin in regulating junction assembly via VASP (Hansen and Beckerle 2006).

Other actin-associated proteins such as WASP and WAVE are important for the regulation of actin filament reorganization in response to extracellular stimuli (Takenawa and Miki 2001). Activation of N-WASP induces filopodia formation (Fig. III) while WAVE2 activation leads to the formation of lamellipodia (Takenawa and Miki 2001). We are only beginning to understand some of the complex interactions which control adhesion induced cytoskeletal rearrangements via these modulators. The recent discovery of novel filopodia, termed tunnelling nanotubes (TNT), exemplifies the diversity of cell protrusions as well as the necessity of a complete understanding of their interactions. TNT's are capable of directly shuttling lipid-containing organelles and cell surface proteins between physically separated cells (Onfelt et al. 2005). These long distance channels can move proteins between cells without the need for the machinery normally required to move proteins across the hydrophobic cell membrane barrier (Onfelt et al. 2005).

A large number of proteins are involved in the formation or stabilization of surface protrusions. These include actin membrane linkers such as ponticulin (Shutt et al. 1995) and the ERM protein family which includes ezrin, moesin and radixin (Bretscher 1999). The formation of protrusions is potentiated by actin assembly and bundling proteins in

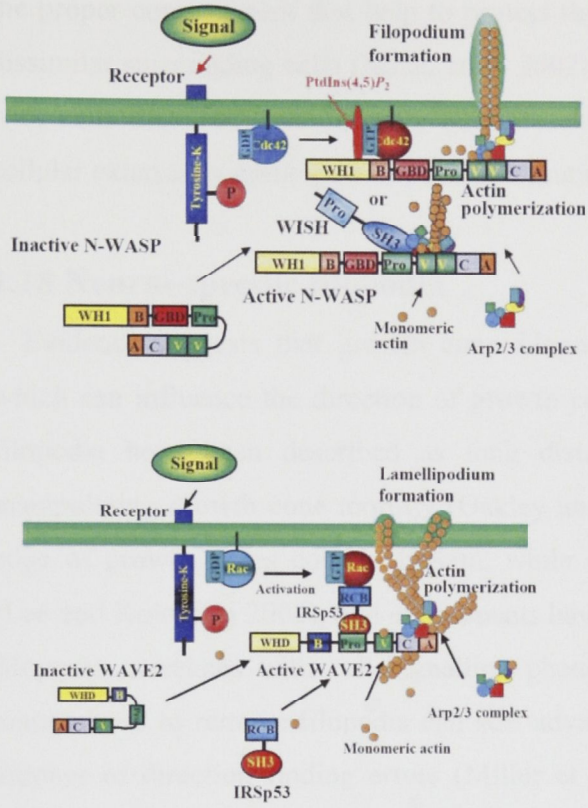

Fig. III A schematic representation of the mechanism of activation of N-WASP and WAVE2 and the consequent induction of actin polymerization during the formation of filopodia or lamellipodium, respectively. Activation of N-WASP induces filopodia formation while WAVE2 activation leads to the formation of lamellipodia (taken from Takenawa and Miki 2001).

the vicinity of the plasma membrane (Furukawa and Fechheimer 1997). Upregulation of F-actin bundling proteins such as fascin (Yamashiro et al. 1998), villin (Frank et al. 1990) or supervillin (Wulfkuhle et al. 1999) causes dramatic changes in cell morphology and results in the formation of long, spiky protrusions at the cell membrane. In a recent publication the expression of the adhesion molecule α5 integrin-GFP appears to have induced the formation of long, branched filopodia, though this induction may have been overlooked and was not discussed in the paper (Laukaitis et al. 2001). Another function of cell surface protrusions can be observed in developing Drosophila embryos. If cells are placed into an inappropriate environment in Drosophila imaginal discs, they can form extensions which reach into

the proper compartment that help to protect the cells from apoptosis induced by the dissimilar surrounding cells (Milan et al. 2002). Long projections are also associated with cells that move directionally (Ribeiro et al. 2002), and there is evidence that cellular extensions participate in guided migration (Rorth 2003).

1.18 Neural-specific filopodia

Evidence suggests that growth cone filopodia in neural cells act as chemosensors which can influence the direction of growth cone migration (Miller et al. 1995). These filopodia have been described as long distance sensors that can guide axons by manipulating growth cone motility (Oakley and Tosney 1993). Filopodia at the leading edge of growth cones contain F-actin, while the core contains polarized microtubules (Lee and Kolodziej 2002), and experiments have shown that the function of growth cone filopodia correlates with cell signalling phenomena. Growth cones which have been manipulated to remove filopodia can still advance, but they make a dramatically larger number of direction finding errors (Miller et al. 1995). Data from a diverse range of systems suggests that thin filopodia play a sensory role (Miller et al. 1995) though details of this function remain largely unknown. Claims of a possible sensory role for filopodia are substantiated by the induction of neurite-like outgrowths by the overexpression of receptors such as SREC (Shibata et al. 2004). Other suggestions for the roles of these protrusions include the formation of precise binary connections and the coupling of intracellular signalling with physical force (Rorth 2003).

Direct contact mediated interactions make possible a mutual exchange of information between two cells to the exclusion of surrounding cells. An example of this can be seen in the interaction between myopodia and axon growth cones which allows an initial transient contact between two cells to be stabilized before maturation into a neuromuscular junction (Ritzenthaler et al. 2000). Integrins are capable of acting synergistically with cell membrane receptor systems to finely modulate cell adhesive activities in response to environmental signals (Schmid and Anton 2003), and membrane bound adhesion molecules have been found to trigger synapse formation (Fu et al. 2003). The action of these adhesion molecules is not limited to initial contact formation but can

also perform the function of specific target recognition (Shen et al. 2004). An ideal synaptogenic cell adhesion molecule would be concentrated at the tips of synapses and could mediate heterophilic adhesion between axons and dendrites, or another specific cell type (Kim et al. 2006). The cytosolic region would be expected to interact with scaffold proteins to enable a coupling of adhesion events with the recruitment of synaptic proteins (Kim et al. 2006).

1.19 Trailing edge dynamics of migrating cells

The behaviour of integrins in the cell-substrate adhesion structures at the rear of the cell have been shown to influence cell migration (Chen 1981), and the velocity of cell locomotion is approximately equal to the rate of rear detachment (Palecek et al. 1998). Adhesion site dissociation is highly regulated and depends not only on events mediated by mechanical forces, but also on numerous tyrosine kinases and phosphatases that modulate integrin affinity for extracellular matrix (ECM) molecules (Kirfel et al. 2004). Other mediators of rear detachment include cytosolic adapter proteins, proteases such as calpain which can cleave the adhesion complex, and ADAM family sheddases (Kirfel et al. 2004). Intracellular calcium levels have also been associated with the substrate release of migrating neutrophils (Maxfield 1993, Vincente-Manzanares et al. 2005). In this case the calcium/calmodulin dependent phosphatase, calcineurin, is responsible for αvβ3 integrin detachment and its recycling to the front of the cell (Maxfield 1993). In fish keratinocytes calcium fluctuation has been shown to arise from the activation of stretch activated calcium channels (Lee et al. 1999); however, it is still mostly unknown how these highly localized transient calcium levels are generated.

The proteolytic release of membrane anchored cell surface proteins, known as ectodomain shedding, is crucial for developmental events (Yamamoto et al. 1999) and is mediated by membrane resident sheddases of the ADAM family (Werb and Yan 1998). The discovery that collagen XVII/BP 180, an epithelial adhesion molecule, is shed by an ADAM family member implicates the involvement of sheddases in rear detachment (Franzke et al. 2004). Motile fibroblasts have been shown to deposit integrins in a process known as membrane ripping which leaves α5β1 integrin-rich migration trails in their

wake (Palecek et al. 1996). The formation of these macroaggregates is thought to depend on actin cytoskeleton disruption leading to the fragmentation of cylindrical cell extensions into periodic chains of pearls (Bar-Ziv et al. 1999). The anchorage of macroaggregate-resident integrins to the ECM must therefore be maintained during the process of rear release thereby contributing to the creation of migration trails. It is possible that substrate deposited materials fulfil physiological roles such as guidance for other cells or chemotactic signalling for axonal pathfinding.

1.20 Cell adhesion dysfunction

The process of cell migration exhibits many regulatory steps, and any deficiency, either ectopic activation or modification by pathogens, can impair or enhance cell migration dynamics with catastrophic consequences. Diseases which are the result of aberrant cell migration control include chronic inflammation, vascular disease, cancer and mental retardation (Vincente-Manzanares et al. 2005). Studies in *D. Melanogaster* have shown that a deletion of βPS, the ortholog of the integrin β1 subunit in vertebrates, results in embryonic muscle-attachment defects (Brown 1994). Similar defects are seen in deletions of other focal adhesion molecules such as the ILK (Zervas et al. 2001) and PINCH (Clark et al. 2003) orthologs. Flies deficient in βPS and PINCH have defects in dorsal closure indicating an impairment of cell migration (Brown 1994, Kadrmas et al. 2004). Chimeric flies also show a blistering phenotype which is indicative of a loss of cell adhesion to the ECM (Kadrmas et al. 2004). The loss of function of β1 integrin or PINCH results in embryonic lethality, but mutants show subtle differences in phenotype indicating distinct defects (Liang et al. 2005). Knockout of the *C. Elegans* ILK homolog, pat4, results in paralysis and arrest of elongation which is similar to the α- and β-integrin knockout phenotype observed in the same model (Li et al. 1999). Embryonic lethality of PINCH null mice correlates with an increase in endodermal cell apoptosis demonstrating a cell survival role for PINCH (Li et al. 2005).

Live studies of embryonic dorsal closure show actin cables and dynamic filopodia expressed at the leading edge of epithelial cells (Jacinto et al. 2000). Suppression of the assembly of the actin-rich filopodia by down regulation of cdc42 results in the failure of

the zipping together of opposing epithelial sheets (Jacinto et al. 2000). The 'purse string'-like function of F-actin cables in dorsal closure is recapitulated in wound healing in the mammalian cornea, embryonic skin and in tissue culture monolayers (Danjo and Gipson 1998). Blocking of this process by the inactivation of Rho results in aberrant cable assembly and severe impairment of wound healing (Brock et al. 1996). Studying adhesion molecule mutants in animals has been difficult due to their often embryonic lethal phenotype. To elucidate the modes of action of such mutants, embryoid bodies were used to study adhesion molecule knockouts. It was found that β1 integrin mutants failed to deposit basement membrane due to defects in laminin synthesis (Li et al. 2002) while ILK and PINCH mutants showed defects in epiblast polarization and cavity formation (Li et al. 2005, Sakai et al. 2003). Knockouts of various α and β integrin subunits in the mammalian brain cause phenotypes which include impaired neuronal migration, abnormal radial glial differentiation, altered neuron-glia interaction, disorganised cortical plates and dysfunctional neural tube closure (Schmid and Anton 2003).

1.21 The Ttyh1 protein

The Ttyh1 protein contains consensus sequences for the binding of various SH domain proteins and protein phosphorylation sites. Some interesting consensus sequences recognized in Ttyh1 include TRAF2 (TLEE, SLEE) which is located in extracellular loops in both instances. In addition to the TRAF2 motif detected in the mouse, the human Ttyh1 sequence contains a TRAF6 (FAPQEQEYQ) binding site just on the extracellular side of the cell membrane at amino acids 32-40 as predicted by the eukaryotic linear motif resource tool (ELM, http://elm.eu.org). Members of the tumor necrosis factor receptor (TNFR) superfamily initiate intracellular signaling by recruiting the C-domain of the TNFR-associated factors (TRAFs) through their cytoplasmic tails. Another interesting consensus sequence present in the C-terminal cytosolic region of Ttyh1 is a PDZ domain. The neuronal cell adhesion molecules, neurexin and neuroligin, bind to cytosolic PDZ domain-containing scaffold proteins via their C-termini (Kim et al. 2006). This association of presynaptic neurexin and post synaptic neuroligin induces bidirectional synaptic differentiation (Kim et al. 2006).

Algorithm based structure prediction (PSORT II, http://psort.nibb.ac.jp/) indicates that the Ttyh1 C-terminus is located in the cell cytoplasm. Ttyh1 contains five transmembrane helices, and topography prediction using the method of Rost et al. (1996) generates the following representation:

Amino acid	Membrane Position
1-47	outside region 1
48-66	membrane helix 1
67-90	inside region 1
91-108	membrane helix 2
109-216	outside region 2
217-235	membrane helix 3
236-245	inside region 2
246-265	membrane helix 4
266-391	outside region 3
392-411	membrane helix 5
412-450	inside region 3

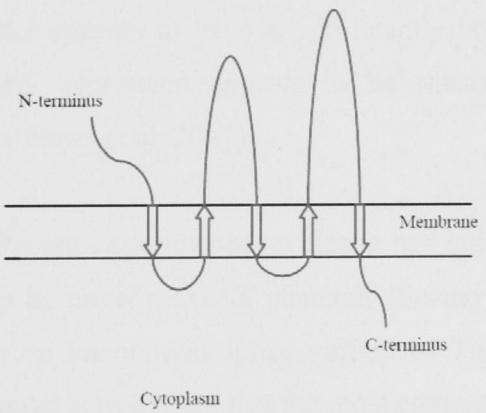

Analysis of the Ttyh1 protein also revealed a positive grand average of hydropathy (GRAVY) score of 0.269. The grand average of hydropathy value for a peptide or protein is calculated as the sum of hydropathy values of all the amino acids, divided by the number of residues in the sequence, and provides valuable information about a protein's conformation (Kyte and Doolittle 1982). Of particular interest in this case, it should be

noted that analysis of anion channels is known to generate a negative GRAVY score (Millar et al. 2001).

Three tty-related genes, Ttyh1 (Campbell et al. 2000), Ttyh2 (Rae et al. 2001) and Ttyh3 (Suzuki and Mizuno 2004) occur in the mouse at chromosomal locations 7A1, 11E2 and 5G2 respectively (Matthews et al. 2007). Examination of data on the sources of ESTs summarized by the UniGene EST ProfileViewer (http://www.ncbi.nlm.nih.gov/UniGene) indicated that Ttyh1 is mainly expressed in the brain, eye, spinal cord and testis, with much lower levels detected in pancreas, pituitary gland, mammary gland and liver. The UniGene EST expression profile for human Ttyh1 showed a very similar picture, with expression being detected in brain, eye, ovary and testis, and at lower levels in muscle, placenta, liver and lung. UniGene EST expression profiles indicated that all of the Ttyh genes are expressed strongly in brain and eye (except for weak Ttyh2 expression in the latter) but that Ttyh2 and Ttyh3 have broader ranges of expression than Ttyh1. For example, at least three of four of the Ttyh2 and Ttyh3 genes are expressed in heart, lung, muscle, placenta and skin, but Ttyh1 expression is generally not detected in these tissues. Ttyh3 appears to have a significantly broader expression profile than the others, while Ttyh1 expression appears to be substantially restricted to neural tissue and testis (Matthews et al. 2007).

Recent experimental evidence has indicated that some human Ttyh family members may be novel maxi-Cl^- channels (Suzuki and Mizuno 2004). In that study, it was found that an uncommon splice variant of Ttyh1 (hTtyh1sv) had volume-sensitive maxi-Cl^- channel activity, but that the most common form of Ttyh1 (Campbell et al. 2000) did not. The hTtyh1sv gene sequence was isolated from a retinal library while RT-PCR revealed that mTtyh1, but not mTtyh1sv, is expressed in the hippocampus and hypothalamus (Suzuki 2005). Data suggest that Ttyh1sv may function independently of the canonical Ttyh1 isoform (Suzuki 2005). It is likely that the intracellular C-terminal regions of the Tty-related proteins confer functional specificity (Rae et al. 2001). However, the C-terminal region in the hTtyh1sv splice variant is altered compared to the more common forms (Suzuki and Mizuno, 2004), and therefore may have affected the function of the

protein. Chloride channel activity was detected in the hTtyh3 isoform (Suzuki and Mizuno, 2004). However, this function should not be extrapolated to include the other Ttyh isoforms, considering that Ttyh3 is most distantly related to Ttyh1 and Ttyh2 (Suzuki 2005, Matthews et al. 2007), Ttyh3 contains six transmembrane segments (Suzuki 2005) and is expressed in a wide range of non-neural tissues (Matthews et al. 2007).

It has been reported that there are more than 600 known proteins with five transmembrane domains (Campbell et al. 2000). The high affinity iron transporter protein FTR1, its homologue FTH, and the neurotensin receptor NTSR1 share a similar arrangement of transmembrane segments with Ttyh1 (Campbell et al. 2000). This led to the proposal that Ttyh1 may function as a membrane bound receptor (Rae et al. 2001). The Ttyh2 isoform, which is also highly expressed in the brain, has a similar pattern of transmembrane segments to Ttyh1, but in addition, has an RGD consensus sequence in the second extracellular domain (Rae et al. 2001). Many proteins that are involved in cell adhesion contain RGD motifs which can mediate the binding of integrins and affect cell adhesion events (D'souza et al. 1991).

1.22 Aim of the thesis

The aim of this project was to understand the cellular function of the mammalian Ttyh1 protein using genetic, cellular biological and biochemical approaches. The human and mouse homologues of the *D. Melanogaster* tweety gene were cloned and expressed in several cell lines to elucidate the cellular location, over-expression phenotype, Ttyh1-associated proteins and the effects of Ttyh1 expression on cell function. Antibodies directed against the N- and C-terminal peptides were validated and used to detect Ttyh1 in neuronal cultures and *in situ* using thin brain slices. The effect of Ttyh1 expression on cell adhesion and migration was analysed and will be discussed.

Chapter 2

Detection of Ttyh1 and Ttyh1-Associated Proteins

2.1 Introduction

The aim of the work presented in this chapter was to use Ttyh1 anti-peptide antibodies to detect the Ttyh1 protein in rat brain and cell lines, and to identify Ttyh1-associated proteins using co-immunoprecipitation and other co-association methods. Anti-Ttyh1 antibodies designed to recognize Ttyh1 N- and C-terminal peptides were produced in sheep and purified by affinity chromatography for use in Western blotting, immunohistochemistry and immunoprecipitation experiments. Each antibody was used to detect Ttyh1 by Western blotting in rat brain lysates and available cell lines. Bands were considered to be specific if they were the correct molecular weight and could be blocked by competitive binding of the antibody to its cognate antigen peptide.

The identification of Ttyh1 binding partners would guide our research and help to elucidate the cellular function of the Ttyh1 protein. To facilitate this, the Ttyh1 gene was cloned into the mammalian expression vector pEGFP-N1 and expressed in HEK293 cells. The protein product of pEGFP-N1-Ttyh1 was an enhanced green fluorescent protein fused to the N-terminus of Ttyh1. Ttyh1-specific antibodies, AP1 and AP2, and a generic anti-GFP antibody were used to immunoprecipitate native Ttyh1 from brain lysates and ectopically expressed Ttyh1-GFP from HEK293 cell cultures. Antibodies were cross-linked to protein G-agarose to discriminate Ttyh1 from the 50 kDa antibody heavy chain that results from antibody heavy and light chain dissociation during SDS-PAGE. Whole brain lysates were incubated with protein G-agarose-antibody complexes in an effort to isolate binding partners using the highly concentrated Ttyh1-GFP product of ectopic cell expression. The composition of lysis buffer was adjusted and procedures were carried out at 4°C in an attempt to preserve protein-protein interactions between Ttyh1 and its binding partners. The use of yeast-2-hybrid systems for the detection of interacting proteins was investigated, and related systems that were designed for use with membrane proteins were considered.

2.2 Materials and methods

Throughout the methods and results section, methods are described once and are thereafter applicable to subsequent experiments in which the same procedure was used.

2.21 Ttyh1 anti-peptide antibodies

Antibodies raised against the N- and C- terminal regions of Ttyh1 were prepared as follows. The peptides MGAPPGYRPSAWVHC and CPQESKRFVQWQSSI, which consist of the 14 N-terminal and C-terminal residues of Ttyh1 (GenBank Accession No. NP_067299) respectively, were synthesized by Mimotopes Pty. Ltd. (Melbourne, Australia). These N- and C- terminal peptides are also identical in rat Ttyh1 (GenBank Accession No. XP_218263) and human Ttyh1 isoform 1 (GenBank Accession No. NP_065710). An N-terminal cysteine residue was added to each peptide for conjugation reactions. Each peptide was conjugated to diphtheria toxoid, and used to raise sheep polyclonal antibodies (IMVS, Adelaide, Australia). The crude antisera were affinity purified at Mimotopes (Melbourne) on columns consisting of the corresponding peptide conjugated to Thiopropyl Sepharose 6B using MCS. The purified N-terminal (AP1) and C-terminal (AP2) antibodies were assayed by ELISA for reactivity to the antigenic peptides, and stored at -80 °C.

2.22 Gel electrophoresis and Western blotting

Brain sections from adult Evans or Wistar rats and some common cell lines were dissolved in NuPAGE SDS lysis buffer (Invitrogen, Australia). Lysates were centrifuged at 10,000 g and the supernatant was loaded on a 4-12 % Bis/Tris polyacrylamide gel (NuPAGE, Invitrogen, Australia). Electrophoresis was carried out at 150 V for 1 hour followed by electrophoretic transfer to nitrocellulose membrane (Hybond-C Extra, Amersham, USA) at 30 V for 1 hour. Non-specific antibody binding sites were blocked by gently rocking nitrocellulose membranes in TBS-T blocking buffer (150 mM NaCl, 10 mM Tris/HCL, 1 mM $MgCl_2$, 1 mM EGTA, 0.05 % (v/v) Tween 20, 5 % non-fat milk powder) for 1 hour at room temperature. Antibodies AP1 and AP2 were used as primary antibodies to detect the Ttyh1 protein at a dilution of 1:200 in blocking buffer unless otherwise indicated. Primary antibody binding was achieved by sealing the nitrocellulose membrane in a plastic bag along with TBS-T blocking buffer and antibody, and rocking overnight at 4°C. HRP-conjugated anti-sheep antibody (Silenus or Jackson, USA) was used as the secondary antibody at a 1:1500 dilution in blocking buffer, unless indicated otherwise, to visualise the protein bands. To confirm antibody specificity, controls were

included that utilised antigen-saturated AP1 or AP2 antibodies which had been incubated with 50 µg/ml of their corresponding antigen peptides for 1 hour at 4°C prior to their use. Protein bands were considered to be specific if they were of the predicted molecular weight and could be blocked when the peptide-saturated antibodies were used.

2.23 Construction of the Ttyh1-GFP fusion vector

The mouse cDNA clone MNCb-1314 (GenBank Accession No. AF190991) contains the translation initiation codon and most of the coding sequence for the 450 amino acid residue form of Ttyh1 (GenBank Accession No. NP_067299) but lacks the region encoding the stop codon and C-terminal 7 amino acids as it has an alternative C-terminus (116). Oligonucleotide HDC270 (5′-CGC GGA TCC GCG ATG GAA GAC TGC CAC TGC ACA AAG CGT TTG GAT TCC TGA GG-3′) was used with primer HDC220 (5′-CTT CTG CTC TAA AAG CTG CG-3′), specific for the vector pME18S-FL3 (GenBank Accession No. AB009864) sequence flanking the 5′-end of the insert to amplify a 1.4 kb fragment from MNCb-1314 plasmid DNA. PCR was carried out using Taq polymerase with 200 µM dNTPs, 10 pmol of each primer and 1 ng of MNCb-1314 plasmid DNA as template in a reaction volume of 50 µl. After 2 min at 95°C, 40 cycles of 94°C (30 sec), 55°C (30 sec), and 72°C (1.5 min) were carried out, followed by 5 min at 72°C. The 1.4 kb product was gel purified, digested with EcoRI and BamHI, and ligated between the EcoRI and BamHI sites of the pEGFP-N1 expression vector (Clontech, USA). The 1.4 kb inserts in individual clones were sequenced. A clone without PCR errors was selected for use as a mammalian Ttyh1-GFP expression vector and named pEGFP-N1-Ttyh1.

2.24 Culture and transfection of HEK293 cells

Cells were seeded on glass cover slips in 24-well plates at 5×10^4 cells per well and cultured overnight in antibiotic-free DMEM (Sigma, Australia) containing 10 % FCS at 37°C in a 5 % CO_2 humidified atmosphere. Immediately prior to transfection, cells were washed in 1 ml of pre-warmed (37°C) sterile PBS, then 500 µl of pre-warmed (37°C) serum-free, antibiotic-free DMEM was added to each well. The plasmids pEGFP-N1-Ttyh1 and pEGFP-N1 (160 ng) or plasmid-free controls were mixed with 50 µl of serum-free, antibiotic-free DMEM. A 2 µl aliquot of Lipofectamine2000 (Invitrogen, Australia)

was added to 50 µl of serum-free, antibiotic-free DMEM for each well. The plasmid and Lipofectamine2000-containing media were mixed and incubated for 20 minutes at room temperature. The combined 100 µl of reagent was added to each well of cells in the 24-well plate and incubation continued for 5 hours at 37°C in a 5 % CO_2 humidified atmosphere. After 5 hours, the medium was removed and 1 ml of DMEM containing 10 % FCS was added. Cells were incubated at 37°C in a 5 % CO_2 humidified atmosphere for 48 hours prior to analysis.

2.25 Immunoprecipitation of endogenous and ectopic Ttyh1

The following protocol was applied to immunoprecipitate Ttyh1 from brain and cell lysates. Samples were kept at 0 - 4°C throughout the procedure. PBS-washed cell cultures containing 10^7 cells were lysed in 1 ml of Triton-X lysis buffer (10 mM Tris/HCl pH 8.0, 0.3 % (vol/vol) Triton-X100, 300 mM sucrose, 1.5 mM $MgCl_2$, 0.23 mM PMSF, 16.8 mM $Na_4P_2O_7$, 20 mM NaF, 0.14 mM Na_3VO_4, ± 0.1 – 0.3 % SDS). Lysates were centrifuged at 20,000 g and supernatant was transferred to a new tube. Protein G-agarose (25 µl) was washed twice in 1.5 ml of PBS then centrifuged at 4000 g. The resulting pellet was resuspended in 37.5 µl of PBS and used to clear endogenous antibodies by adding it to the lysates and gently mixing for 45 minutes at 4°C. The G-agarose-antibody conjugates were centrifuged for 1 minute at 4000 g, and the supernatant was decanted to a new tube. This clearing step was repeated. A further 3 ml of lysis buffer was added to the supernatant before adding the specific antibody for immunoprecipitation. Affinity-purified antibodies, AP1 and AP2, were added at a concentration of 2.5 µl per 4 ml of total lysate, and anti-GFP monoclonal antibody (Sigma, Australia) was added at 2 µl per 4 ml of total lysate for each immunoprecipitation experiment. Samples were rotated on a wheel overnight at 4°C, then washed protein G-agarose (50 µl per sample) was added to each Ttyh1-antibody-lysate mixture and allowed to bind by rotating the sample for a further 1 hour at 4°C. Following antibody binding, the G-agarose beads were pelleted by centrifugation for 2 minutes at 4000 g. Supernatant was discarded, and the pellet was washed sequentially in 1.5 ml of lysis buffer, 1.5 ml of PBS containing 50 mM Tris/HCL (pH 8.0), and finally in 1.5 ml of PBS. Sample buffer (2×) was added at a volume of 30 µl per pellet and the sample was incubated at 100°C for 4 minutes. Each sample was

finally centrifuged at 12,000 g for 2 minutes and 20 µl of the supernatant was subjected to SDS-PAGE for analysis.

The cross-linker, BS^3, is the water soluble analog of the homobifunctional N-hydroxysuccinimide ester known as DSS. In some experiments BS^3 was used to covalently bond antibodies to protein G-agarose prior to Ttyh1 immunoprecipitation in order to stop the antibody heavy chain from dissociating and covering the 50 kDa position in subsequent Western blot analyses. This was achieved by washing 25 µl of protein G-agarose twice with 1.5 ml of PBS, centrifuging the washed protein G-agarose at 4000 g and resuspending the pellet in 37.5 µl of PBS (~50 µl total). Antibody (2-5 µl) was added to the washed G-agarose in a total volume of 100 µl per reaction made up with PBS, and mixed on a wheel at 4°C for 1 hour. Excess antibody was removed by washing G-agarose 3 times in 1.5 ml of PBS and centrifuging the sample at 4000 RPM between each wash. The BS^3 crosslinker was added to the antibody-G-agarose complex at a concentration of 5 mM, mixed and incubated at room temperature for 30 minutes. The reaction was quenched by the addition of 15 mM of Tris/HCl pH 7.5 and a further incubation at room temperature for 15 minutes. The cross-linked antibody-G-agarose complex was washed 3 times with 1.5 ml of PBS before being added to cleared lysates along with 3 ml of lysis buffer. The antibody-G-agarose complexes were allowed to bind the Ttyh1 or Ttyh1-GFP protein by rotational mixing overnight at 4°C. Following binding, the antibody-G-agarose complex was pelleted by centrifugation for 2 minutes at 4000 g. Supernatant was discarded, and the pellet was washed sequentially in 1.5 ml of lysis buffer, 1.5 ml of PBS containing 50 mM Tris/HCL pH 8.0, and finally in 1.5 ml of PBS. Sample buffer (2×) was added at a volume of 30 µl per pellet, and the sample was incubated at 100°C for 4 minutes. Each sample was finally centrifuged at 12,000 g for 2 minutes, and 20 µl of the supernatant was subjected to SDS-PAGE for analysis.

2.26 Silver nitrate staining

Protein-antibody-G-agarose complexes were dissociated by boiling for 4 minutes in 30 µl of 2× NuPage sample buffer containing 7.5 mg/ml DTT (Invitrogen, Australia), and electrophoresis was performed as previously described. Polyacrylamide gels were washed

with 100 ml of MQH_2O for 30 minutes and fixed in 50 % methanol containing 5 % acetic acid for 30 minutes. Following fixation, gels were washed with MQH_2O for 30 minutes and sensitized by immersion in 0.02 % sodium thiosulphate for 1 minute. Gels were washed with MQH_2O for 2×30 seconds and then stained with 0.1 % chilled silver nitrate solution for 20 minutes. Gels were washed with MQH_2O for 2×30 seconds and then developed by immersion in 2 % sodium carbonate monohydrate containing 0.014 % formaldehyde with gentle rocking for 5-10 minutes. The reaction was stopped by incubation in 1 % acetic acid for 10 minutes, and then gels were dried by immersion in gel drying solution (30 % methanol, 5 % glycerol) for 30 minutes. Cellophane was briefly soaked in gel drying solution before the gel was mounted between two sheets of soaked cellophane and dried at room temperature for 1 hour.

2.3 Results

2.31 Optimization of Ttyh1 detection

Polyacrylamide gel electrophoresis was used for the initial separation of Ttyh1 from whole rat brain lysate, and the optimization of reagent concentrations for Ttyh1 detection. Western blot analysis was carried out following protein transfer to nitrocellulose using the N- and C-terminal antibodies designated AP1 and AP2, respectively. Rat brain was weighed, lysed in NuPage lysis buffer (Invitrogen, Australia) containing 7.5 mg/ml DTT as the reducing agent, and proteins separated by SDS-PAGE and Western blotted using Ttyh1 antibodies. Ttyh1 was detected at 51 kDa with a second smaller band at 49 kDa by using antibody AP1 as the primary antibody (Fig. 2.1). These bands were close to the predicted molecular weight of 49.029 kDa for rat Ttyh1. The 51 kDa band was named Ttyh1a and the 49 kDa band was named Ttyh1b to simplify discussions. The detection of two bands using the N-terminal antibody was in agreement with RNA splicing analysis (unpublished data) which predicted that at least two Ttyh1 variants existed with alternatively spliced C-terminal regions. If the two separate Ttyh1 bands were the result of glycosylation or association with other proteins, we would expect both antibodies to show two bands. However, the antibodies appear to be predominately detecting either the large band (AP1) or the small band (AP2). The best protein band separation was achieved using 0.3 mg/well of brain lysate, and this concentration was used for most Western blots

that followed. The antibody concentrations which gave the clearest results were 1:200 for both of the primary Ttyh1 antibodies and 1:1500 for the secondary anti-sheep HRP conjugated antibody (Silenus, USA).

Western blot analysis using the C-terminal primary antibody, AP2, revealed one main band at 49 kDa which appeared to be the same size as the Ttyh1b band that was detected by AP1 (Fig. 2.1). Due to the similarity of size and shape, this band was also named Ttyh1b. In order to determine if these bands were specific, the cognate antigen peptides which were used to produce each Ttyh1 antibody were added in serial dilutions to block the Ttyh1 bands. Antibody blocking was achieved by incubation of each antibody with its peptide antigen for 1 hour at 4°C on a rotating wheel prior to use as a primary antibody for Western blotting. A concentration of 50 μg/ml of peptide 802 was sufficient to block the Ttyh1 band detected by antibody AP1 and 25 μg/ml of peptide 806 was sufficient to block the Ttyh1 band detected by antibody AP2 (Fig 2.1). A peptide concentration of 50 μg/ml was chosen to block Ttyh1 bands in subsequent experiments. The use of peptide 802 to block binding of the AP1 antibody produced a dark background in some Western blots and computer analysis of the 15 amino acid sequence revealed that it was more hydrophobic than peptide 806. In some experiments, a number of the minor bands that appeared on the western blots were also partially blocked by the antigenic peptide, indicating some cross-reactivity with much more abundant proteins. However, as indicated later in this chapter, further experiments showed that the Ttyh1 antibodies specifically recognize Ttyh1 when expressed ectopically. This reinforces that the bands seen in brain tissue, which were the correct molecular weight and the most immunoreactive, were almost certainly endogenous brain Ttyh1 isoforms.

Western blot analysis of nine available cell lines was performed in an attempt to find a cell line which expressed Ttyh1 endogenously and could thereafter be used in cell based studies of the protein. The cell lines analyzed were HEK293, Swiss3T3, ARPE-19, CHO, COS-7, IMR-32, Kelly, PC-12 and SK-N-SH (Fig. 2.2). The ARPE-19 cell line was a retinal pigmented epithelial line while IMR-32, Kelly and SK-N-SH were neuroblastoma cell lines. None of the cells lines analyzed expressed endogenous Ttyh1, so it was

decided that the cell biology of the Ttyh1 protein would be studied by ectopic expression in a transfectable cell line. The endogenous protein was later detected in primary brain cell cultures, and will be discussed in chapter four.

2.32 Preparation for Ttyh1-GFP expression and immunoprecipitation

The pEGFP-N1-Ttyh1 plasmid was transfected into electro-competent DH5α *E. Coli* bacteria, and a plasmid maxi-prep kit (Qiagen, Australia) was used to isolate and purify concentrated pEGFP-N1-Ttyh1 plasmid. Correct insertion of the Ttyh1 gene was checked by EcoR1/BamH1 double digestion and the Ttyh1 product ran at the predicted size of 1.4 kb (Fig. 2.3). DNA sequencing (performed at the BRF facility, JCSMR, Australian National University) revealed that the Ttyh1 gene was correctly inserted and that there were no altered DNA bases. Lysis buffers were tested using whole brain to establish a suitable buffer for use in immunoprecipitation experiments that would free the Ttyh1 protein and allow it to be isolated with the lysate supernatant rather than leaving it in the insoluble pellet (Fig. 2.4). The most suitable buffers were RIPA buffer and Triton-X100 buffer supplemented with 0.3 % SDS. Since RIPA buffer contains very powerful detergents, it could not be used for co-immunoprecipitation experiments as it would dissociate weak protein-protein interactions. The Triton-X100 buffer supplemented with various concentrations of SDS was chosen for use in immunoprecipitation experiments. Interestingly, Triton-X100 buffer alone did not dissociate Ttyh1 from the pellet so Ttyh1 was not detected in the supernatant. It is known that TritonX-100 does not dissolve F-actin and other components of the cytoskeleton whereas SDS does. Following the addition of 0.3 % SDS to the Triton-X100 lysis buffer Ttyh1 was dissolved and could be detected in the lysate supernatant.

2.33 Ttyh1-GFP expression in HEK293 cells

The pEGFP-N1-Ttyh1 plasmid was transfected into HEK293 cells as described, the cells were lysed, and Western blot analyses of the expressed fusion protein were performed (Fig. 2.5). The pEGFP-N1 control cells showed a high level of GFP protein expression which was detected at the predicted molecular weight of 27 kDa using the anti-GFP antibody. The pEGFP-N1-Ttyh1 transfected cells produced the Ttyh1-GFP

fusion protein at the expected molecular weight of around 76 kDa but at a lower concentration than observed in the GFP-only control cells. This was to be expected as the empty pEGFP-N1 vector contains a significantly shorter transcript than the pEGFP-N1-Ttyh1 vector. The number of cells loaded for SDS-PAGE was 10^3 cells per well in order to avoid protein overloading in the GFP control lane. For a direct comparison of the expressed fusion protein and the native Ttyh1 protein, brain lysates and lysates from HEK293 cells ectopically expressing Ttyh1-GFP were run side by side in the same gel (Fig. 2.6).

In whole brain lysates, the Ttyh1a and Ttyh1b isoforms were detected by the AP1 antibody and blocked by its antigen peptide 802, and the Ttyh1b isoform was detected by the AP2 antibody and blocked by its antigen peptide 806. Both antibodies detected the same expressed canonical Ttyh1 fusion protein in HEK293 cell lysates indicating that the expressed protein is antigenic to both the AP1 and AP2 antibodies.

2.34 Immunoprecipitation of Ttyh1-GFP

The size of the Ttyh1 protein lies within 49-51 kDa. This is the same size as the dissociated antibody heavy chains from the AP1, AP2 and anti-GFP antibodies. Therefore immunoprecipitation experiments would not allow the direct observation of the native Ttyh1 protein. In order to overcome this problem, antibodies were covalently cross-linked to protein G-agarose so that they could be used to isolate the Ttyh1 protein from lysates, and then be removed from the lysate themselves along with the protein G-agarose beads. A concentration of 5 mM of the BS^3 cross-linker was sufficient to bond antibodies to protein G-agarose and thereby remove the antibody heavy chains from lysates prior to gel electrophoresis (Fig. 2.7). Cross-linked anti-GFP antibody was used to immunoprecipitate Ttyh1-GFP and GFP from transfected HEK293 cells. The amount of GFP recovered from lysates was high but the amount of Ttyh1-GFP recovered was much lower. The recovered Ttyh1-GFP protein was not visible by silver staining so the proteins were transferred to nitrocellulose for Western blot analysis. By using anti-GFP as the primary antibody, both the GFP and the Ttyh1-GFP protein were visible, although the concentration of Ttyh1-GFP was around 100 times lower than the concentration of GFP

alone (Fig. 2.8). The amount of Ttyh1-GFP recovered by cross-linked immunoprecipitation was deemed insufficient to be of use in co-immunoprecipitation experiments.

A series of experiments were performed using non cross-linked antibody-G-agarose complexes in order to increase the yield of Ttyh1-GFP fusion protein. Three strong Ttyh1-GFP bands of the same molecular weight were detected following immunoprecipitation with AP1, AP2 and anti-GFP (Fig. 2.9). The Ttyh1-GFP band was visible despite the large number of dissociated antibody and other non-specific protein bands detected by silver staining. The immunoprecipitated Ttyh1-GFP along with associated proteins was analysed by Western blot and probed with AP2 as the primary antibody. Strong Ttyh1-GFP bands were detected by AP2 after immunoprecipitation using AP1, AP2 and anti-GFP antibodies. This confirmed that the expressed Ttyh1-GFP protein that was immunoprecipitated by the AP1 antibody was also antigenic to the AP2 antibody, and therefore confirmed the specificity of both antibodies (Fig. 2.9). Two unidentified high molecular weight proteins at around 130-160 kDa were co-immunoprecipitated using all three antibodies. Since these protein bands were detected using primary AP2 antibody in the Western blot, it is likely that some Ttyh1-GFP remained attached to the unidentified proteins to have enabled detection, or that they were detected by the secondary anti-sheep antibody. In the corresponding silver stained gel, only small bands were detected at this high molecular weight. The recovered co-immunoprecipitated proteins could not be separated from contaminating non-specific bands which were present in all samples. Ttyh1-GFP-associated high molecular weight proteins were also detected in other IP experiments between 180 and 220 kDa (Fig. 2.10).

In order to increase the concentration of co-immunoprecipitated proteins, protein G-agarose-bound antibodies which were also bound to Ttyh1-GFP, were incubated with whole rat brain lysates. The high concentration of G-agarose-bound Ttyh1-GFP was used in an attempt to bind unknown proteins present in rat brain. Although Ttyh1-GFP was clearly visible by silver staining, no co-immunoprecipitated proteins were isolated from the rat brain lysate (Fig. 2.11).

Due to the low recovery rate of Ttyh1-associated proteins using the co-immunoprecipitation method with Ttyh1-GFP, alternative methods were investigated to elucidate novel protein-protein interactions. The yeast-2-hybrid system commonly used to detect protein interactions in the nucleus could not be used to investigate Ttyh1 protein binding partners as Ttyh1 was predicted to localize to the cell membrane. The split-ubiquitin system (Fig. 2.12) which is designed to detect protein-protein interactions at the cell membrane (Stagljar et al. 1998, Suter et al. 2006) was considered for use with the Ttyh1 protein. The Ttyh1 gene was cloned into the yeast expression vector pCXJ29 (a kind donation from Des Clark-Walker, RSBS) for optimization of yeast protocols. However, upon receiving a quote of above $10,000AUS for the purchase of the split-ubiquitin system, I decided that the cost was prohibitively expensive and ceased this line of investigation.

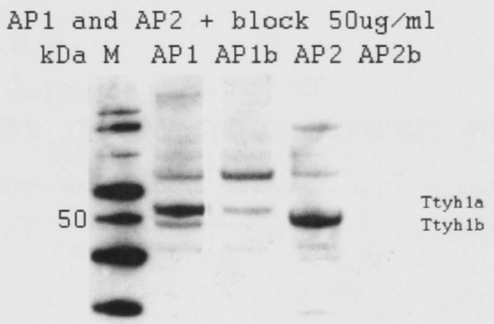

Fig. 2.1 The figure shows proteins separated by gel electrophoresis followed by Western blot analysis. Endogenous Ttyh1 in whole rat brain lysates was detected by each antibody, and blocked by the addition of antigenic peptides. The primary antibodies, N-terminal AP1 and C-terminal AP2, were used at a concentration of 1:200 and secondary anti-sheep antibody was used at a concentration of 1:1500 to detect endogenous Ttyh1. The symbol M represents protein size standards in kilodaltons. Specific blocking of Ttyh1 bands was achieved by incubating each antibody with its cognate peptide antigen, designated AP1b and AP2b, at a concentration of 50 μg/ml for 1 hour prior to use. The detection of isoform Ttyh1a was mostly blocked by the addition of the peptide while the detection of isoform Ttyh1b was completely blocked for each antibody.

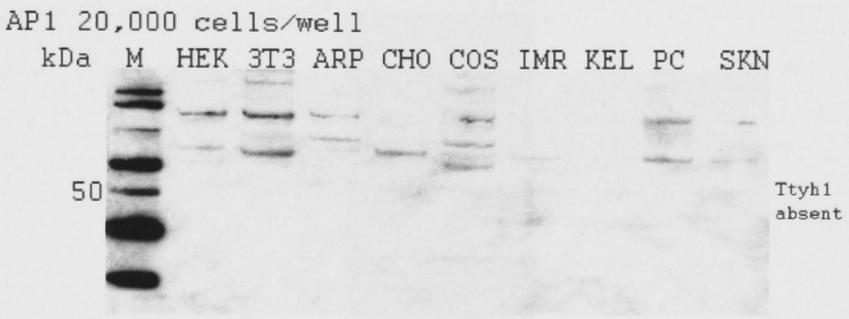

Fig. 2.2 The figure shows proteins from cell lysates separated by gel electrophoresis, followed by Western blot analysis to detect the expression of endogenous Ttyh1. The cell lines analyzed were HEK293, Swiss3T3, ARPE-19, CHO, COS-7, IMR-32, Kelly, PC-12 and SK-N-SH. ARPE-19 is a retinal pigmented epithelial cell line and IMR-32, Kelly and SK-N-SH are neuroblastoma cell lines. The symbol M represents protein size standards in kilodaltons. No endogenous Ttyh1 was detected.

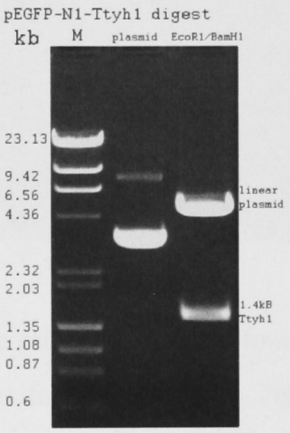

Fig 2.3 The pEGFP-N1-Ttyh1 plasmid maxiprep before and after double digestion with the EcoR1 and BamH1 restriction enzymes. The DNA was separated by size using agarose gel electrophoresis. The symbol M represents DNA size standards in kilobases. The digest was performed at 37°C for 75 minutes, and 1µl of plasmid was separated by electrophoresis on a 10 % agarose gel and visualized using ethidium bromide staining.

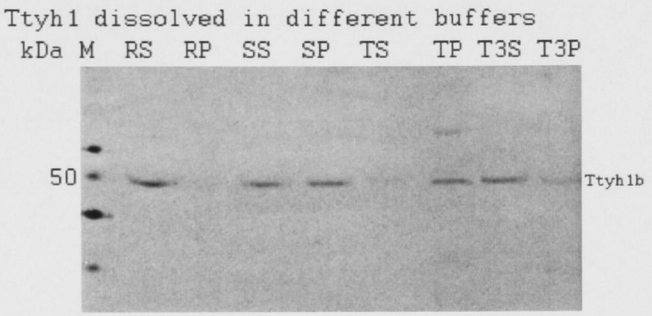

Fig. 2.4 A Western blot of whole rat brain lysed in four different kinds of lysis buffer to determine the optimal conditions for releasing the Ttyh1 protein into the supernatant. AP2 was used as the primary antibody. The symbol M represents protein size standards in kilodaltons. Each lane contains the supernatant or pellet after centrifugation at 12,000 g of whole brain lysate in each lysis buffer. Lanes contain the following combinations: RS, RIPA buffer supernatant; RP, RIPA buffer pellet; SS, NuPAGE sample buffer supernatant; SP, NuPAGE sample buffer pellet; TS, Triton-X100 buffer supernatant; TP, Triton-X100 buffer pellet; T3S, Triton-X100 buffer plus 0.3 % SDS supernatant; T3P, Triton-X100 buffer plus 0.3 % SDS pellet. The addition of SDS released Ttyh1 into the supernatant.

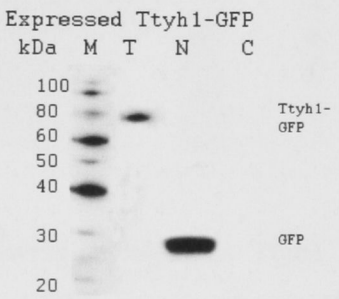

Fig. 2.5 A Western blot of cells expressing the Ttyh1-GFP plasmid and the GFP-only control plasmid. Lysates of 1×10^3 HEK293 cells were loaded into each well to check that the proteins were properly expressed. The symbol M represents protein size standards in kilodaltons. Lanes contain the following lysates: T, Ttyh1-GFP transfected cells; N, control cells transfected with the empty pEGFP-N1 plasmid; C, untransfected control cells. The primary anti-GFP antibody detected the Ttyh1-GFP fusion protein close to the predicted molecular weight of 76.5 kDa and the GFP protein at 27 kDa.

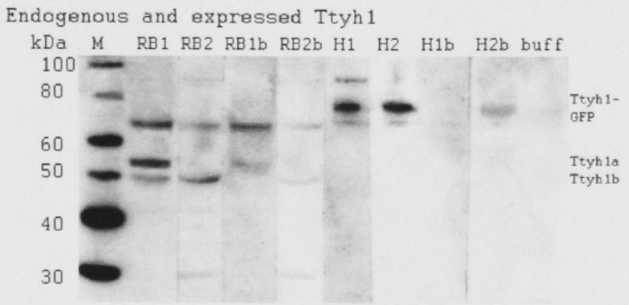

Fig. 2.6 A Western blot showing endogenous Ttyh1 protein from rat brain lysates alongside the expressed Ttyh1-GFP protein from HEK293 cell lysates for direct comparison. The symbol M represents protein size standards in kilodaltons. Lanes represent the following conditions: RB1, rat brain lysate probed with the AP1 primary antibody; RB2, rat brain lysate probed with the AP2 primary antibody; RB1b, rat brain lysate probed with the blocked AP1 primary antibody; RB2b, rat brain lysate probed with the blocked AP2 primary antibody; H1, lysate of Ttyh1-GFP-expressing HEK293 cells probed with the AP1 primary antibody; H2, lysate of Ttyh1-GFP-expressing HEK293 cells probed with the AP2 primary antibody; H1b, lysate of Ttyh1-GFP-expressing HEK293 cells probed with the blocked AP1 primary antibody; H2b, lysate of Ttyh1-GFP-expressing HEK293 cells probed with the blocked AP2 primary antibody; buff, sample loading buffer-only control. In all lanes either 0.3 mg of rat brain or 2.5×10^4 HEK293 cells were loaded.

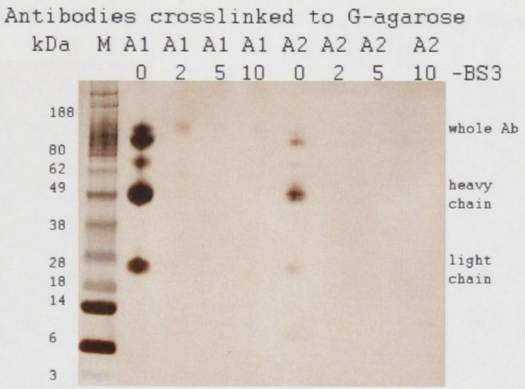

Fig. 2.7 Silver stained polyacrylamide gel displaying Ttyh1 antibodies, AP1 or AP2, cross-linked to protein G-agarose using incremental concentrations of the BS^3 cross-linker. The symbol M represents protein size standards in kilodaltons. The lanes marked A1 represent 5 µl of antibody AP1 and the lanes marked A2 represent 5µl of antibody AP2 while the numbers correspond to the concentration (mM) of BS^3 used in the cross-linking reaction. A concentration of 5 mM of BS^3 was sufficient to cross-link the antibodies to protein G-agarose and remove the antibody heavy and light chains from the sample before electrophoresis.

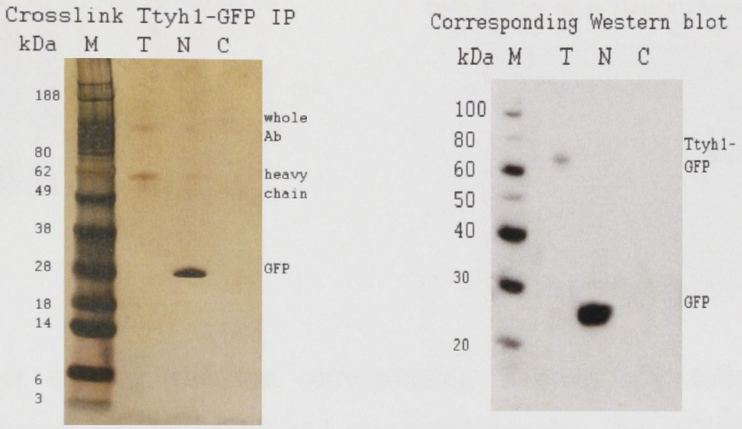

Fig. 2.8 Silver stain and Western blot following the immunoprecipitation of Ttyh1-GFP and GFP-only from HEK293 cells using a cross-linked anti-GFP-G-agarose complex. The symbol M represents protein size standards in kilodaltons. Lanes contain the immunoprecipitated products of the following lysates: T, Ttyh1-GFP-transfected cells; N, GFP-only-transfected cells; C, untransfected cells. Each immunoprecipitation was performed using lysates of 4×10^6 cells, and the Western blot was probed with a 1:30,000 concentration of anti-GFP antibody. The cross-linked antibody precipitated a very small amount of Ttyh1-GFP.

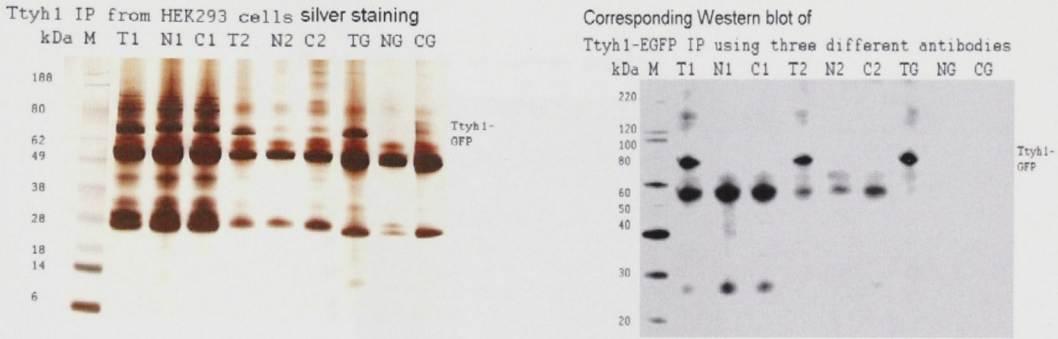

Fig. 2.9 Silver staining and the corresponding Western blot following the co-immunoprecipitation of Ttyh1-GFP and associated proteins from HEK293 cells using non-cross-linked AP1, AP2 and anti-GFP antibodies. The symbol M represents protein size standards in kilodaltons. Lanes contained immunoprecipitated products of the following lysates: T, Ttyh1-GFP transfected cells; N, GFP-only transfected cells; C, untransfected cells. The number 1 represents immunoprecipitation using AP1, the number 2 represents immunoprecipitation using AP2 and the letter G represents immunoprecipitation using the anti-GFP antibody. For each immunoprecipitation 2.7×10^7 cells were lysed and the SDS concentration of the lysis buffer was reduced to 0.1 % to maintain protein-protein interactions. The Ttyh1-GFP protein was precipitated along with high MW unknown proteins. The antibody heavy and light chains appear as strong bands at around 50 kDa and 25 kDa respectively. The Western blot, which used AP2 as the primary antibody, revealed high MW proteins associated with Ttyh1-GFP.

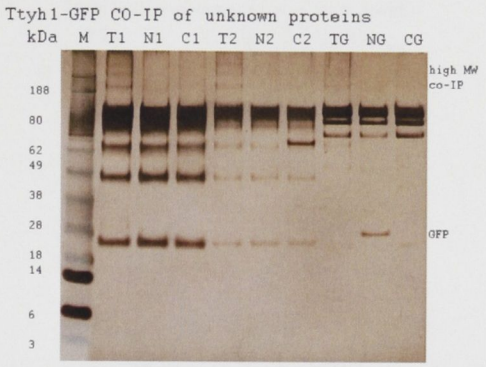

Fig. 2.10 Co-immunoprecipitation of Ttyh1-GFP from transfected HEK293 cell lysates, followed by SDS-PAGE and silver staining revealed the presence of high molecular weight Ttyh1-GFP-associated proteins. The symbol M represents protein size standards in kilodaltons. Lanes contained the following lysates: T, Ttyh1-GFP transfected cells; N, GFP-only transfected cells; C, untransfected cells. The number 1 represents immunoprecipitation using AP1, the number 2 represents immunoprecipitation using AP2 and the letter G represents immunoprecipitation using anti-GFP antibody. For each immunoprecipitation 4×10^6 cells were lysed to reduce the amount of background protein and improve the resolution of co-immunoprecipitated proteins.

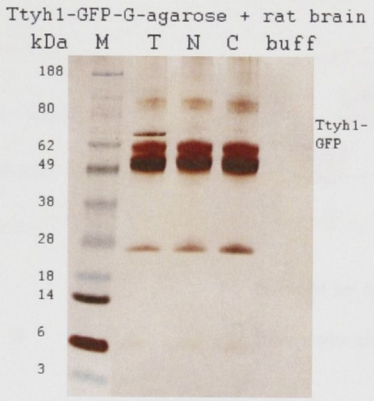

Fig. 2.11 Silver staining following the co-immunoprecipitation and SDS-PAGE of G-agarose-bonded, antibody-fusion-protein complex, following overnight incubation with rat brain lysate to detect endogenous Ttyh1-binding proteins. During the initial immunoprecipitation of Ttyh1-GFP, the non cross-linked anti-GFP antibody was used, and the immunoprecipitation was performed using lysates from 2.5×10^6 Ttyh1-GFP transfected HEK293 cells. Following the initial immunoprecipitation of Ttyh1-GFP, the Ttyh1-GFP-G-agarose covalently bonded complex was incubated with 0.25 mg of rat brain in Triton-X100-0.1 % SDS lysis buffer. Some Ttyh1-GFP was recovered from the complex but no extra bands due to Ttyh1 interacting proteins were detected.

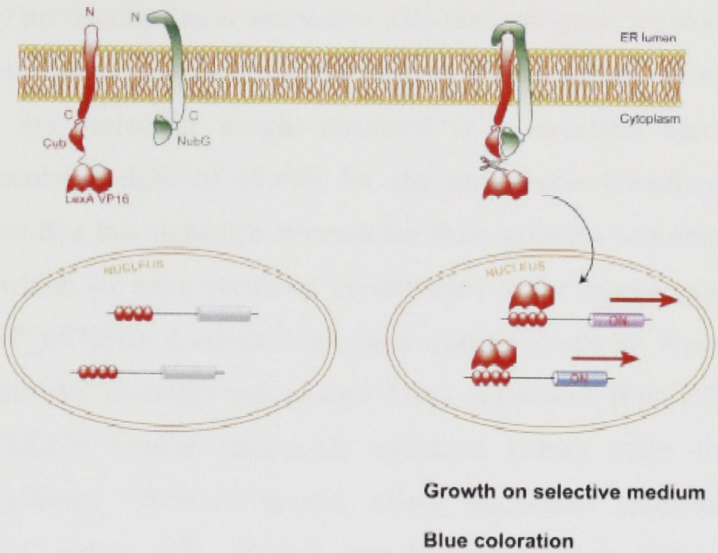

Fig. 2.12 The DualSystems split-ubiquitin assay would be a useful tool in identifying Ttyh1-interacting proteins. This system takes advantage of a protein complementation assay, the split-ubiquitin system (Johnson and Varshavsky 1994), to detect the interaction of two heterologously expressed fusion proteins in the yeast *Saccharomyces cerevisiae*. In contrast to conventional yeast-two-hybrid assays, there is no requirement for the interacting proteins to be located in the nucleus. In the figure, the C terminal of an ubiquitin recognition site (Cub) attached to the LexA VP-16 transcription factor could be fused to Ttyh1. A cDNA library could be used to generate possible interacting proteins fused to the N terminal of the ubiquitin recognition site (Nub). If the protein fused to Nub interacted with Ttyh1, the whole ubiquitin recognition site (Nub+Cub) would be in close proximity and would be recognised and cleaved by ubiquitin. The transcription factor would be released and activate marker genes in the nucleus so that yeast containing the interacting partner cDNA could be isolated and the protein identified.

2.4 Discussion

Western blotting of whole rat brain lysates using the affinity purified antibodies AP1 and AP2 revealed strong bands close to the predicted size of the Ttyh1 protein. Bands were blocked by pre-incubation of antibodies with their antigenic peptides (Fig. 2.1). The 49 kDa band corresponded to the canonical form of the mammalian protein (Campbell et al. 2000), and the molecular weight observed is in excellent agreement with the calculated molecular weight of 49.029 for the rat protein (GenBank accession no. XP_218263; note that this sequence is predicted from genomic sequence and contains a short insertion which we have corrected by reference to the mouse sequence, GenBank accession no. NP_067299). Available cell lines were analysed by Western blotting and immunohistochemistry to detect endogenous Ttyh1 expression (Fig. 2.2). The cell lines tested were HEK293 human embryonic epithelial kidney cells, Swiss3T3 mouse embryonic fibroblasts, ARPE-19 human retinal pigmented epithelium cells, CHO Chinese hamster ovary cells, COS-7 transformed monkey kidney cells, PC-12 (neuronally differentiated and undifferentiated) cells derived from a pheochromocytoma of the rat adrenal medulla and several retinoblastoma cell lines. No endogenous Ttyh1 expression was detected by Western blotting in any of these cell lines. A curious artefact was detected in ARPE-19 cells at around 51 kDa. However, detection of this protein could not be blocked, even by the addition of up to 1 mg/ml of blocking peptide to the antibody (data not shown), and the protein band was therefore considered to be a non-specific artefact.

The existence of C-terminal variants of rat Ttyh1 derived by alternative splicing of mRNA, as occurs in the mouse, is supported by our Western blot results with antibodies directed against N- and C-terminal peptides corresponding to one of the major mammalian isoforms. The N-terminal antibody detected a 51 kDa band and a 49 kDa band, while the C-terminal antibody only detected the 49 kDa band. It is likely that modification of the C-terminus has altered the peptide target of AP2 in the 51 kDa isoform. Removal of C-terminal residues would result in a protein which could only be detected by the N-terminal antibody. Since the C-terminal antibody detected a 49 kDa band with a very similar intensity to the 51 kDa band detected by AP1 using the same

brain lysate, it is likely that both proteins are alternatively spliced from a single gene transcript. This suggests that in rat brain, there are two major splicing variants, one which contains the AP2 C-terminus and one which has an altered C-terminus so as to be undetectable using the AP2 antibody. The C-terminal splice variant is consistent with the data indicating that mouse Ttyh1 (and human Ttyh1) exhibits significant alternative splicing of the region encoding the C-terminus. Antibody AP1 consistently detected a comparatively faint band corresponding to the Ttyh1b isoform, though AP2 demonstrated that significant amounts of Ttyh1b were present in the lysate. It is likely that an splice variant of the N-terminus also exists in the native protein. Alternatively, the C-terminal domain may be post-translationally modified. It appears that the presence of the N-terminal peptide corresponds to the alteration of the C-terminal peptide. In figure 2.1, blocking of the 51 kDa Ttyh1 isoform by the addition of the antigenic peptide 802 to the AP1 antibody is only partial, while blocking of the 49 kDa isoform is complete. This occurred because the concentration of 50 μg/ml of peptide 802 was too low to completely block the 51 kDa band. Increased concentrations of this peptide above 100 μg/ml could completely block the 51 kDa band, but also blocked some non-specific bands, therefore a concentration of 50 μg/ml was chosen for most experiments.

Dissociation of the cell membrane using Triton-X100 based lysis buffer was not sufficient to free the Ttyh1 protein from brain tissue. The addition of 0.3 % SDS to the same lysis buffer allowed Ttyh1 to be released indicating that Ttyh1 may be associated with actin or another cellular component which cannot be dissolved by Triton-X100, but which is dissolved by SDS (Patton et al. 1989). Both the Ttyh1-GFP and the GFP protein alone were expressed at high levels and at the predicted molecular weight in HEK293 cells. The Ttyh1-GFP fusion protein was detected by each of our affinity purified Ttyh1 antibodies and a generic anti-GFP antibody at around 76 kDa. This result further validated that the canonical form of the Ttyh1 protein was antigenic to each of our affinity purified antibodies. The blocking of the Ttyh1-GFP band by the addition of the antigen peptides to the antibodies prior to use indicated that protein binding was specific. Interestingly, a second weaker band was detected just below the 76 kDa Ttyh1-GFP band separated by a similar distance as that observed between the Ttyh1a and Ttyh1b isoforms

in the endogenous protein. Whether this represents a genuine Ttyh1 isoform or a degradation product remains to be clarified, but the band was also blocked by the addition of antigen. It should be noted that other weak bands can sometimes be blocked by the addition of antigen, and at a high concentration of antigen all non-specific bands can be blocked.

The cross-linking of antibody to protein G-agarose was performed to remove interfering antibody heavy chain bands from gel electrophoresis experiments. The heavy chain is generally the same size as the native Ttyh1 protein, and it can be difficult to discriminate between the two bands. Many immunoprecipitation experiments with varied buffer conditions, protein concentrations and experimental protocols were performed but the covalently cross-linked antibody-G-agarose complex failed to yield enough Ttyh1-GFP for use in co-immunoprecipitation experiments. It is possible that the cross-linking process disrupted the conformation of the antibodies reducing their capacity for antigen binding. The cross-linking approach was abandoned and the use of non-cross-linked antibody with protein G-agarose was pursued. This simplified method produced better results and immunoprecipitation of Ttyh1-GFP revealed a strong band at the expected size. It was possible to see the Ttyh1-GFP protein in silver stained gels as the molecular weight of the fusion protein was 76 kDa and was therefore not covered by the interfering antibody heavy chain. Western transfer and probing with Ttyh1-specific antibodies revealed that immunoprecipitation using all three antibodies had successfully isolated a substantial amount of Ttyh1-GFP.

The molecular weight of the immunoprecipitated protein and the associated high molecular weight bands was the same for all antibodies used to immunoprecipitate Ttyh1-GFP. Along with the Ttyh1-GFP bands, two extra bands were detected at around 130-160 kDa. Since the Western blot was probed with AP2, it is likely that the co-immunoprecipitated bands contained proteins that had not dissociated completely from the Ttyh1-GFP protein and were therefore detected by the Ttyh1-specific probe. It is possible that these high MW bands were detected by the secondary anti-sheep antibody, but since they are only there when Ttyh1-GFP is present, it is most likely that they were

genuine Ttyh1 associated proteins. Reduction of the number of cells used in immunoprecipitation experiments revealed several other high molecular weight bands between 180 and 220 kDa. The bands were weak and did not contain sufficient quantities of protein for identification by standard mass spectrometry, but may contain a suitable amount for identification by MALDI-TOF mass spectrometry.

In order to increase the amount of immunoprecipitated endogenous Ttyh1-associated proteins from whole rat brain lysates, the Ttyh1-GFP protein isolated from transfected HEK293 cells was used as bait, and incubated with rat brain lysate. The use of concentrated Ttyh1-GFP to co-immunoprecipitate Ttyh1-associated proteins failed to reveal any novel proteins. It is possible that buffer constituents may require fine tuning for this kind of experiment, and following several failed attempts at precipitating increased yields of Ttyh1-associated proteins, this line of investigation was halted.

A considerable amount of time was spent investigating the yeast-2-hybrid approach for identification of Ttyh1 binding partners. The Ttyh1 gene was cloned into the yeast expression vector pCXJ29, and experiments were commenced to optimize Ttyh1 expression in yeast. However, since Ttyh1 was predicted to be an integral membrane protein, conventional yeast-2-hybrid methods would not be suitable as they require the protein of interest to enter the nucleus. An option which could be used to overcome this problem involves splitting Ttyh1 into domains and expressing the partial protein which can then be localized to the nucleus. However, this approach tends to produce many false positives as the protein is not in its native conformation and protein binding motifs are exposed which are not normally accessible in the intact protein. A more recent technique designed to study membrane-localized and integral membrane proteins is the split-ubiquitin yeast-2-hybrid system. This method relies on two separate halves of the ubiquitin protein being expressed as fusion proteins; one half fused to the protein of interest and the other half fused to proteins produced by a cDNA library from the tissue of interest. The ubiquitin fragment attached to the protein of interest is also fused to a transcription factor for a reporter gene which is co-transfected into the yeast cell. If an unidentified protein from the library binds to the protein of interest, the two ubiquitin

halves are moved into close proximity, and the ubiquitin protein is recognized by enzymes in the yeast cytoplasm. Upon recognition, these complexes cleave the ubiquitin from the interacting proteins and the attached transcription factor moves into the nucleus where it activates a reporter gene so yeast expressing the novel interacting partner can be isolated. The reason that the split-ubiquitin assay was not pursued was primarily the cost of the assay, which was prohibitively expensive, and the time it would have taken to optimize the protocol. It is likely that the elimination of false positives and problems associated with the expression of a mammalian protein in yeast would have taken more time than was available. However, the split-ubiquitin assay remains the most suitable method for the identification of Ttyh1-associated proteins.

These experiments have validated our antibodies against the native and expressed Ttyh1 protein, and have shown that specific detection of Ttyh1 can be achieved using each antibody. They have also indicated that two splice variants of Ttyh1 exist in the endogenous form. We have prepared and validated the pEGFP-N1-Ttyh1 expression vector for the ectopic expression of Ttyh1-GFP in cell lines. The Ttyh1 protein was not released into the supernatant following Triton-X100 based tissue dissociation, but was released upon the addition of SDS into the lysis buffer. This indicates that it remained bound to proteins that were Triton-X100 insoluble. F-actin is one possible candidate protein since it is a cytoskeletal scaffold protein which associates closely with cell membrane proteins, is not soluble in Triton-X100, but is soluble in SDS. The AP1 and AP2 antibodies have been further validated by their detection of the Ttyh1-GFP fusion protein at the predicted size. The fusion protein was successfully immunoprecipitated using AP1 and AP2, and the specificity of the antibodies was confirmed by immunoprecipitation of the same protein using a generic anti-GFP antibody. Several unidentified Ttyh1-GFP-associated proteins were detected following co-immunoprecipitation experiments, but the concentration of these high MW proteins did not facilitate identification by mass spectrometry.

Chapter 3

Ectopic Ttyh1 Expression in Mammalian Cells

3.1 Introduction

The aim of the work presented in this chapter was to investigate the effects of cellular expression of Ttyh1 and Ttyh1-GFP using confocal and deconvolution microscopy. The Ttyh1-GFP expression plasmid that was validated in chapter 2 was used to express Ttyh1-GFP in HEK293, COS7 and Swiss3T3 cells. A Ttyh1 expression plasmid with the EGFP component removed from the pEGFP-N1-Ttyh1 plasmid was created so that the Ttyh1 gene could be expressed alone. This control was included to ensure that any effects observed during the expression of Ttyh1-GFP were not artefacts resulting from the expression of the fusion protein. Immunohistochemical analysis (IHC) of the expressed protein was used to visualize Ttyh1 localization and cell morphology following transfection. Stable cell lines expressing Ttyh1-GFP were created so that results were not obscured by the presence of excess untransfected cells that would be present in transiently transfected cells. Real-time microscopy experiments were designed to observe cell locomotion in live, stable Ttyh1-GFP-expressing cells. A scratch assay was performed to ascertain whether Ttyh1 expression had an effect on the rate of cell migration. Components of the cytoskeleton were visualized to identify possible Ttyh1-interacting elements and investigate Ttyh1-induced morphological changes. Substrate bound integrins were examined using immunohistochemistry to identify any co-localization with Ttyh1, and the junctions between cells were visualized to reveal possible interactions involving Ttyh1 at the cell membrane.

3.2 Materials and methods

3.21 Removal of GFP from pEGFP-N1-Ttyh1

The excision of the GFP gene from pEGFP-N1-Ttyh1 using the AgeI and NotI endonucleases results in the Ttyh1 gene remaining attached to the vector with the amino acid sequence ADPPGPRL on the 3' end, and a surrogate TAG stop codon being created. The pEGFP-N1-Ttyh1 plasmid was restricted using the AgeI and NotI endonucleases in a double digest reaction. The digested DNA product was subjected to electrophoresis in a 10 % agarose gel, and the p-N1-Ttyh1 band was cut out and purified. Blunt ends were filled in using the Stoffel fragment DNA polymerase with dNTP's at a concentration of 200 μM for 10 minutes at 37°C. The plasmid was re-ligated in the absence of the GFP

gene using T4 DNA ligase (7 µl MQH_2O, 1 µl T4 ligase buffer, 1 µl p-N1-Ttyh1 plasmid (~600 ng/µl), 1 µl T4 ligase (1 unit)). *E. Coli* (DH5α) were electroporated in the presence of 5 µl of the p-N1-Tty1 ligation reaction product and grown on selective media. Bacteria expressing the correct plasmid were identified, sequenced and the p-N1-Ttyh1 plasmid was multiplied and purified using a maxiprep kit (Qiagen, Australia).

3.22 Stable cell transfection

Cultures of HEK293 cells were plated at a density of 1×10^5 cells per ml in a 24-well plate, and transfected with the pEGFP-N1-Ttyh1 plasmid as previously described. After 48 hours, cells were subjected to selection using 400 µg/ml of geneticin (Sigma, USA). After 20 days of selection the concentration of geneticin was reduced to 200 µg/ml and stable Ttyh1-GFP-expressing polyclonal stocks were frozen at -80°C. Monoclonal stably transfected cells were also produced by plating polyclonal Ttyh1-GFP-expressing cells at a density of 1 cell per well in a 96-well plate. Wells which contained a single cell were maintained in selective media until clonal descendants of the original cell filled the well. The monoclonal population was transferred into larger culture dishes to increase the number of cells, and monoclonal stocks were frozen at -80°C.

3.23 Immunohistochemistry

Cultures of COS7, Swiss3T3 and HEK293 cells were fixed by removing culture media and adding 500 µl per well of fixing solution (3.7 % (v/v) formaldehyde, 164 mM sucrose in PBS) and incubating at room temperature for 10 minutes. To increase the rate of cell fixing for the preservation of F-actin structures, a modified solution was used (8 % (v/v) formaldehyde, 1:100 TRITC-phalloidin (Sigma, Australia) in PBS). Glass coverslips, used as the substrate for cell cultures, were transferred to a new 24-well plate, and fixed cells were permeabilised using 1 ml of permeabilisation solution (10 mg/ml BSA and 0.1 % (w/v) SDS in PBS) per well, and were incubated at room temperature for 10 minutes. Permeabilisation solution was aspirated and nonspecific binding sites were blocked by gently agitating coverslips in 500 µl per well of blocking solution (10 mg/ml BSA in PBS) at room temperature for 1 hour. The coverslips were then incubated in 300 µl of blocking solution containing a 1:100 concentration of affinity-purified AP1, AP2,

TRITC-phalloidin (Sigma, USA), anti-human CD49e (Chemicon, USA) or monoclonal anti-alpha-tubulin (Sigma, USA) antibodies for 1 hour at room temperature. The cells were washed 5 times with PBS, and incubated in blocking solution containing a 1:100 concentration of secondary TRITC or Texas Red conjugated anti-sheep or anti-mouse antibody (Jackson, USA) for 1 hour at room temperature. Cells were washed 5 times in PBS and twice in distilled water before mounting on glass microscope slides using 5 µl of Gel Mount Solution (ProSciTech, Australia). Real time microscopy was carried out by allowing pEGFP-N1-Ttyh1-expressing HEK293 cells to grow in 24-well plates with the plastic base removed, and thin glass coverslips glued in their place with epoxy resin. Images of live cells were captured at 5 minute intervals to document cell migration dynamics during Ttyh1-GFP expression.

3.24 Visualization of F-actin

Cells were fixed for 10 minutes at room temperature in PBS containing 3.7 % formaldehyde, then rinsed with PBS. The cells were permeablised in PBS containing 0.2 % Triton-X100 for 4 minutes, then rinsed with PBS. Non-specific binding sites were blocked by incubation in PBS containing 10 % FCS for 30 minutes at room temperature, and then cells were rinsed twice with PBS. Cells were incubated in PBS containing 1 unit of TRITC-phalloidin and 1 % FCS at room temperature for 20 minutes followed by rinsing with PBS. Finally, the cells were rinsed with MQH_2O, mounted onto glass microscope slides with gel mounting solution (ProSciTech, Australia) and F-actin was visualized using the 529 nm TRITC excitation wavelength.

3.25 Deconvolution and confocal microscopy

Microscopic examination of cultured cells by deconvolution microscopy was carried out using an Olympus IX70 microscope fitted with a nano-motion stage (Applied Precision) using a 40, 60 or 100× lens. Confocal microscopy was performed using an Olympus AX70 laser scanning confocal microscope fitted with a Biorad MRC 1024 laser using a 100× lens. Slides were immersed in Nikon type A (nD=1.518) oil and illuminated using an Olympus 100 W high pressure mercury power source (#BH2-RFL-T3) with an Olympus U-ULH burner (#U-ULS100HG), cooled by a Photometrics LCU liquid

nitrogen system. The excitation and emission wavelengths for green fluorescent protein detection were 488 nm and 529 nm respectively. The excitation and emission wavelengths for TRITC and Texas Red based detection were 529 nm and 571 nm respectively. Cells were photographed using a Roper Scientific CH350 digital camera and processed with LaserSharp 2000 software (DeltaVision). A total of 15 images of each frame were captured starting at the surface closest to the glass coverslip, and continuing through each cell in 0.5 μm increments. The deconvolution algorithm was applied 15 times to each stack of photos and the images at the most clearly resolved z coordinates were selected for analysis.

3.26 Scratch assay

Stably transfected HEK293 cells expressing pEGFP-N1-Ttyh1, pEGFP-N1 or no-plasmid control were grown in 24-well plates until they were approximately 80 % confluent. The base of each well was marked with two straight, parallel reference lines separated by 5 mm near the centre of the well. Two scratches were made through the cell cultures perpendicular to the reference lines under sterile conditions by pressing a yellow pipette tip down on the substrate and moving it from one side of the well to the other. Two reference points were chosen at the intersection of a scratch and a reference line for each well, and photographed at 0 hours. Culture plates were returned to the 37°C 5 % CO_2 incubator and subsequent photos were taken at 5 hour intervals at the same reference point for each scratch over a 30 hour period. The rate of closure of the scratch was determined using Photoshop software and the scale bars from the deconvolution microscope images. The scale bar was copied and pasted in consecutive frames between the advancing cell fronts at either side of the scratch until the gap was traversed. The length of the scale bar was multiplied by the number of bars required to traverse the gap. The distance between the advancing cell fronts was measured at 3 positions for each scratch and then averaged. Each new averaged measurement was subtracted from the previous measurement to deduce the average distance the advancing fronts had migrated during the 5 hour interval. Four averaged migration distances from two separate wells were calculated for each of the Ttyh1-GFP, GFP-only and no-plasmid control cells and were themselves averaged to generate a single numerical representation of migration rate

(μm/5hrs). Standard deviations of the four averaged migration rates for each cell type were calculated using Microsoft XL, and a graphical representation of cell migration rate was generated. Statistical analysis was performed using a Students T-test to compare the four averaged migration rate values for Ttyh1-GFP, GFP-only and no-plasmid control cells.

3.3 Results

3.31 Expression of Ttyh1 in HEK293 cells

The mammalian expression plasmids pEGFP-N1-Ttyh1, p-N1-Ttyh1 and pEGFP-N1 were transfected into COS-7, Swiss3T3 or HEK293 cells. The fluorescence of negative control cells lacking the GFP plasmid was almost invisible upon exposure to the GFP excitation wavelength (Fig. 3.1). After 48 hours of expression in transient transfection experiments, cells were fixed, stained using IHC and examined by deconvolution and confocal microscopy. Staining of F-actin with TRITC-phalloidin revealed strong fluorescence using the TRITC excitation wavelength, and bundles of F-actin fibres, actin arcs and small protrusions were clearly visible (Fig. 3.2). The pEGFP-N1 transfected HEK293 cell controls were fibroblast-like in appearance and expressed GFP primarily in the nucleus with some expression in the cytoplasm. These control cells displayed a few small spikes of F-actin around 2-5 μm in length.

The expression of the pEGFP-N1-Ttyh1 and p-N1-Ttyh1 plasmids in all cell lines resulted in dramatic morphological changes at the cell membrane (Figs. 3.3 and 3.4). The Ttyh1-GFP protein was localized to the endoplasmic reticulum or Golgi within 20 hours following transfection. After this time (generally 36–48 h post-transfection) Ttyh1-GFP migrated towards the peripheral membrane of cells where it became concentrated. Upon translocation to the membrane, Ttyh1 expression induced the formation of many long, often branched filopodia, which protruded from the cell and were around 10-20 μm in length. Extending out past the tips of protrusions were what appeared to be migration trails of consecutive dots and dashes of Ttyh1-GFP attached to the substrate. To ensure that the formation of the filopodia-like structures was independent of the GFP portion of the fusion protein, we expressed the p-N1-Ttyh1 plasmid in HEK293 cells followed by

protein detection using antibodies AP1 and AP2 (Fig. 3.5). The expression of Ttyh1 alone confirmed that the morphological changes and migration trails were a genuine result of the expression of the Ttyh1 gene.

Confocal microscopy revealed that Ttyh1-GFP was most concentrated at the peripheral cell membrane between the cell and the substrate. There was also some localization around the outside of the nucleus with no internally nuclear localized Ttyh1-GFP detected. The Ttyh1-GFP protein was specifically associated with fibrous polymers which looked like microtubules or F-actin, rather than being dispersed evenly throughout the cytoplasm (Fig. 3.6).

3.32 F-actin in Ttyh1-induced protrusions

Cells expressing Ttyh1 and Ttyh1-GFP were co-stained with TRITC-phalloidin revealing that the thin Ttyh1-induced filopodia were rich in F-actin. The F-actin extended into protrusions to around half of their total length whereas Ttyh1 was localized throughout the protrusions, and was most concentrated towards the tips (Figs. 3.3 and 3.4). In order to capture F-actin throughout the filopodia, the cell fixation protocol was modified to accelerate the fixing process and preserve F-actin structures by including phalloidin and an increased formaldehyde concentration in the fixative. The modified fixation solution preserved F-actin structures, and F-actin was detected along the entire length of the induced filopodia with Ttyh1-GFP most highly concentrated at the very tips (Fig. 3.7).

Upon cell-cell contact, some filopodia stabilized and filled with F-actin to create thick cables between two or more cells. Ttyh1-GFP was expressed along the length of the cables and was also present at the interface between the ends of the cables and the contacted cell (Fig. 3.8). It was not possible to ascertain whether the long intercellular cables were initiated by Ttyh1 expression or if they were the result of normal F-actin interactions. Ttyh1 may have become localized at the cell-cell interface by a default association with F-actin. Deposits of Ttyh1-GFP were observed on the membranes of nearby cells which had been contacted by filopodia in a similar pattern to the Ttyh1 trails

left on the substrate (Figs. 3.9 and 3.10). In many of the cell-cell interactions involving Ttyh1 protrusions, the contacts appeared to induce an almost seamless link between the F-actin cytoskeletal components of two distinct cells (Fig. 3.9). The Ttyh1-GFP protein and the loose end of the protrusion was scattered around these stabilized F-actin structures appearing as though Ttyh1 had created an opening to allow F-actin to enter the neighboring cell.

The induction of F-actin rich filoplodia often involves the activation of one or more of the small GTPases, Rho, Rac and cdc42 (Carton et al. 2003). Since Ttyh1 expression led to the induction of F-actin rich filopodia, the activation status of RhoA, Rac1 and cdc42 was assayed using a kit which relied on affinity purification of the active GTP-bound forms of each protein. The protocol for purification was carried out according to the manufacturers instructions (Cytoskeleton, Denver, USA) and used the binding of activated RhoA, Rac1 or cdc42 to the Rho binding domain (RBD) of the Rho effecter protein, Rhotekin, or the cdc42 / Rac interactive binding region (CRIB) of the cdc42 / Rac effecter protein, p21 activated kinase 1 (PAK), respectively. A positive control using GTPγS to activate Rho, Rac, or cdc42 was included in each activation assay, and produced a strong signal for each control cell lysate. The negative controls simply replaced GTPγS with GDPγS to generate the inactive form of the GTPase being tested. In addition, cells expressing the GFP protein alone, or containing no plasmid were included as negative controls. No change in the activation status of either of the GTPases was detected in response to Ttyh1 expression (data not shown).

3.33 Ttyh1 migration trails

The Ttyh1 protein was deposited in trails of dots on the substrate along the paths of migrating cells, and was occasionally deposited as an intact network of branched protrusions. However, in contrast to cell-attached filopodia, little or no F-actin could be detected in the deposited networks (Fig. 3.11). Filopodia stretched out from the rear of migrating cells, and trails often extended over distances of several times the cell's diameter. In the intact deposits of filopodial networks that had broken away from cells, Ttyh1-GFP was concentrated at branch points, points of trajectory change, crossover

points with other filopodia and at the ends of protrusions (Fig. 3.11). The points of trajectory change are likely to coincide with adhesive contacts which would be necessary to allow the observed angles to form. There were several instances where cells had been washed from the substrate during the IHC procedure leaving a complete footprint made up of Ttyh1-GFP. The original position and shape of the cell could be easily deduced from these clear footprints (Fig. 3.11).

3.34 Real-time microscopy of live cells

By using real-time imaging of live, stable Ttyh1-GFP-expressing cells, it was evident that the filopodia were dynamic, extending and retracting branched protrusions with substrate contacts at points of trajectory change. A high coincidence of Ttyh1-GFP was observed at the points of trajectory change, branching and at the tips of filopodia. In stationary cells, Ttyh1 was deposited as the filopodia retracted from an initially extended position. The filopodia at the rear of migratory cells seemed to be unable to detach from the substrate, causing stretching and then tearing of the cell membrane from the filopodia tips as the cell moved forward (Fig. 3.12). Upon substrate release, filopodia recoiled towards the cell body leaving a substrate-bound Ttyh1 deposit. In most cases filopodia were attached at many positions along the protrusion, but in some cases they were only attached at the tip distal from the cell body. In these cases filopodia appeared as straight lines attached at the cell body and the tip. The angle of protrusion from the cell body changed as the cell moved, indicating that the adhesive contact was at the very tip of the projection where Ttyh1 was concentrated. By using the fast-fixing protocol, some F-actin rich filopodia were observed in control HEK293 cells, but these projections were considerably shorter and were far less numerous than those seen in Ttyh1-GFP cells. They did not leave GFP deposits upon cell migration and the GFP did not co-localize with F-actin or become concentrated at the tips of projections.

Polymers of F-actin appeared to facilitate the extension of filopodia before retracting back into the cell. The membranous exterior of the protrusion remained extended and disintegrated upon cell migration without its F-actin support, leaving Ttyh1-GFP deposited on the substrate and on the membranes of contacted cells (Fig. 3.12). As cells

moved forward and filopodia were torn from the substrate, membrane-localized Ttyh1-GFP moved in from the periphery at the rear of the cell and became highly concentrated in round circles 5-10 μm in diameter, and around 3 μm in from the trailing edge. These circles appeared to be complete focal adhesions (Fig. 3.12).

3.35 Ttyh1 co-localizes with human α5 integrin

Further analysis of the Ttyh1 trail revealed that areas of Ttyh1 expression were coincident with the human CD49e protein (the α5 subunit of the human α5β1-integrin complex). The CD49e protein was detected directly below filopodia and Ttyh1 deposits, and was nearly always coincident with areas of concentrated Ttyh1 expression (Fig. 3.13). CD49e appeared to be positioned between Ttyh1 and the substrate as Ttyh1-GFP was always above CD49e when incremental points along the z axis of the microscope were photographed (data not shown). The localization of substrate-bound CD49e correlated with dots along filopodia that had a higher Ttyh1 concentration than the rest of the protrusion. Filopodia that were attached to cells appeared to make contact with the substrate via CD49e, and the shape of deposited Ttyh1-GFP trails could be recognized in the patterns of substrate bound CD49e (Fig. 3.14).

3.36 Ttyh1 expression led to an increase in cell migration rate

The widths of cell monolayer scratches were determined for each of the Ttyh1, N1-control or no-plasmid control wells at time points 10, 15 and 20 hours. Two separate scratches were measured and the scratch width was averaged for each well giving a total of four measurements representing each protein expression category. The rate of cell migration was averaged and plotted on a graph representing the migration distance in micrometers per 5 hour interval. The expression of Ttyh1 significantly increased the rate of cell migration into the scratch (Fig. 3.15). Cells stably expressing pEGFP-N1-Ttyh1 migrated at 117.4±9.8 μm / 5hrs, cells stably expressing pEGFP-N1 migrated at 87.7±12.4 μm / 5hrs and untransfected control cells migrated at 89.6±10.4 μm / 5hrs. The increased rate of cell migration observed in Ttyh1-GFP-expressing cells was calculated using ANOVA with multiple comparisons, and was statistically significant with P-values

of 0.019663 for Ttyh1-GFP versus GFP-only and 0.045031 for Ttyh1-GFP versus no-plasmid control.

3.37 The effect of Ttyh1 expression on microtubules

Analysis of cytoskeletal microtubules revealed that Ttyh1-GFP transfected cells contained microtubules that were polarized towards the membrane. Polarized microtubules were frequently orientated in the same plane as Ttyh1 filopodia, with the F-actin-rich protrusions extending out past the tips of the microtubules (Fig. 3.16). In areas where microtubules ran parallel to the cell membrane, Ttyh1 filopodia were not present. Microtubules in untransfected cells tended to run parallel with the cell membrane. In control cells microtubules were sometimes polarized towards the membrane in the direction of migration, and where the occasional small protrusion emanated from the cell. The Ttyh1-GFP fusion protein co-localized with microtubules (Fig. 3.17) and appears to have been transported to the membrane by a microtubule-dependent mechanism.

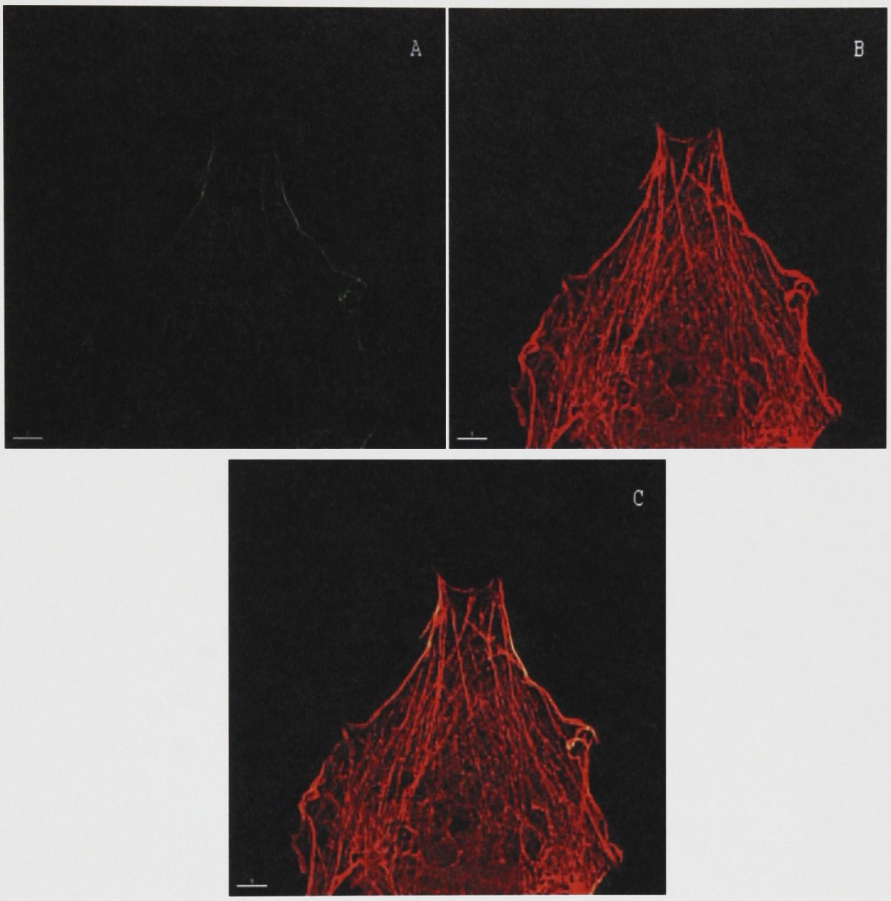

Fig. 3.1 The figure shows de-convoluted confocal images of an untransfected HEK293 cell following staining of cytoskeletal F-actin with TRITC-phalloidin. (A) Visualization using the GFP excitation wavelength shows very little fluorescence. (B) The F-actin cytoskeleton is clearly visible using the TRITC excitation wavelength. (C) The merged image shows mostly red staining indicating that the background GFP fluorescence is low. Scale bars represent 5 μm.

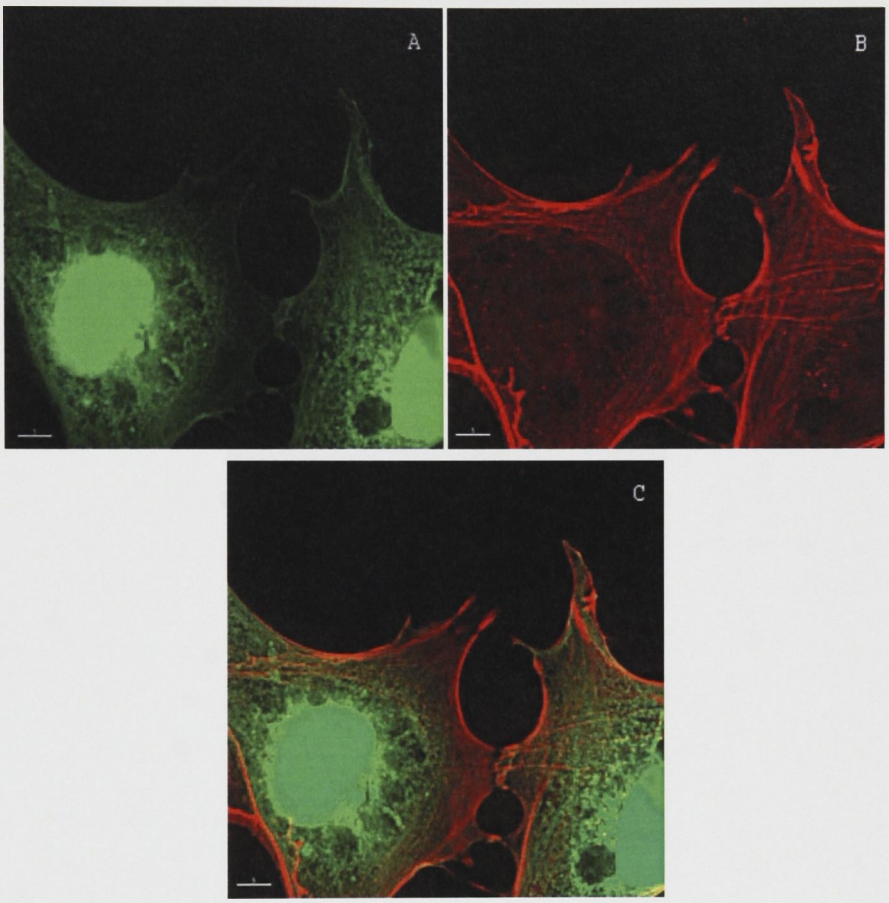

Fig. 3.2 The figure shows de-convoluted confocal images of transfected HEK293 cells expressing the GFP-only control plasmid after staining with TRITC-phalloidin to visualize the F-actin cytoskeleton. (A) The GFP protein localizes mainly to the nucleus with some GFP in the golgi and cytoplasm. (B) F-actin stress fibres and arcs are visible using the TRITC excitation wavelength. (C) The merged image shows orange and yellow fluorescence where GFP and F-actin co-localize. Scale bars represent 5 μm.

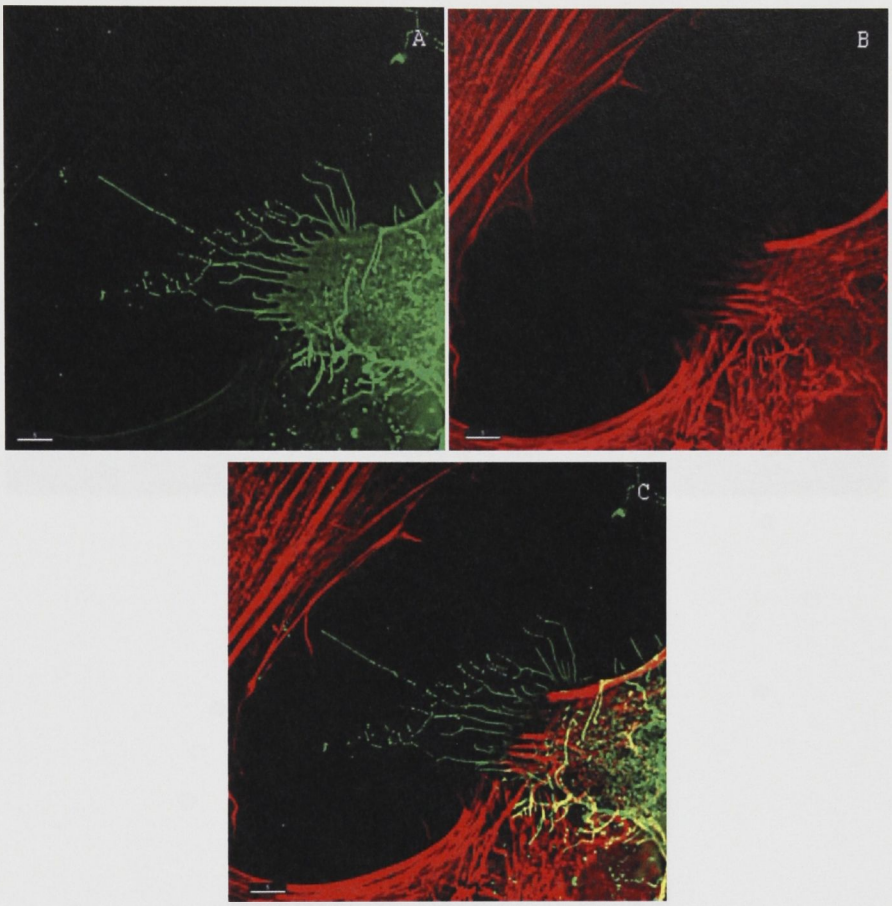

Fig. 3.3 The figure shows de-convoluted confocal images of a transiently transfected HEK293 cell expressing the Ttyh1-GFP protein alongside two un-transfected cells. (A) Filopodia rich in Ttyh1-GFP extend out from the cell membrane and leave substrate-bound trails upon their retraction. The filopodia also contact the neighbouring cell and leave deposits on the cell membrane. (B) Staining with TRITC-phalloidin reveals F-actin protruding into the filopodia and terminating at around half of their length. (C) The merged image shows Ttyh1-GFP protrusions extending beyond the F-actin fibres, and a strong coincidence of Ttyh1-GFP with F-actin at the interface with the neighbouring cell (yellow). Scale bars represent 5 μm.

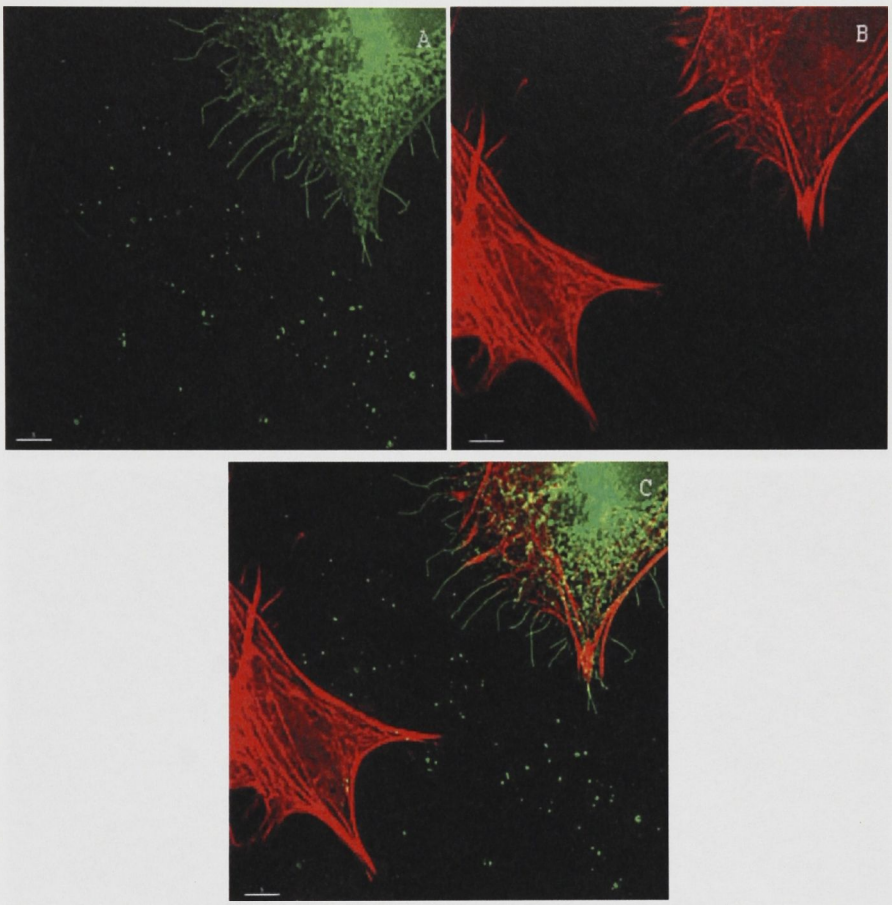

Fig. 3.4 The figure shows de-convoluted confocal images of a transiently transfected HEK293 cell expressing Ttyh1-GFP positioned alongside an un-transfected cell for direct comparison. (A) Filopodia rich in Ttyh1-GFP extend from the cell membrane with Ttyh1-GFP concentrated at the tips. (B) Staining with TRITC-phalloidin shows F-actin protruding almost all of the way into the filopodia. (C) The merged image shows Ttyh1-GFP protrusions on the transfected cell which are absent on the untransfected cell. Scale bars represent 5 μm.

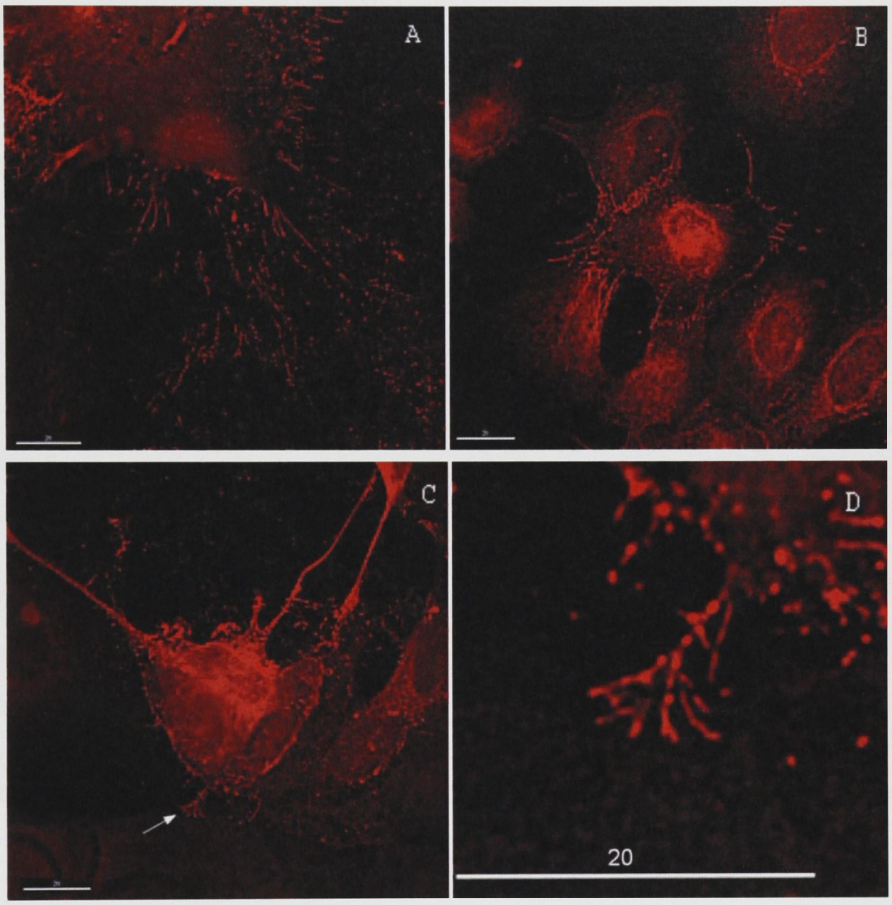

Fig. 3.5 The figure shows de-convoluted confocal images of three HEK293 cells which were transiently transfected with the p-N1-Ttyh1 plasmid lacking the EGFP gene. (A) Cells were stained with the Ttyh1-specific antibody AP1 or (B,C) AP2 and a secondary Texas Red conjugated antibody. The expression of Ttyh1 alone was sufficient to induce the formation of filopodia and leave deposits on the substrate. (D) A close-up of image (C) (arrow); the Ttyh1 protein was highly concentrated at the tips of protrusions at the cell-cell interface. Scale bars represent 20 μm.

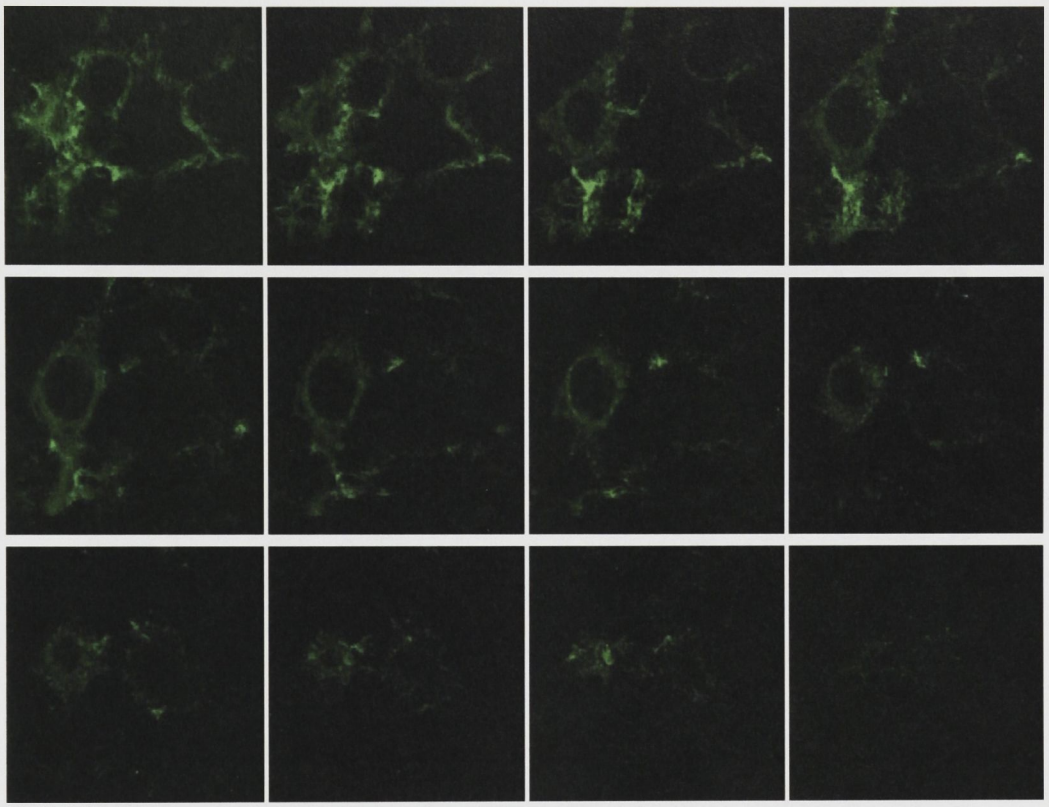

Fig. 3.6 The figure shows standard confocal images of a HEK293 cell expressing Ttyh1-GFP. The first image was taken at the z coordinate closest to the substrate followed by images taken in 0.3 μm increments along the z axis. In the first image, it is apparent that Ttyh1-GFP is highly concentrated close to the substrate and is associated with fibrous cytoskeletal structures. A reduction in the level of Ttyh1 expression was observed as photos were taken at increasing z values moving away from the substrate, exemplifying the substrate localization of Ttyh1-GFP.

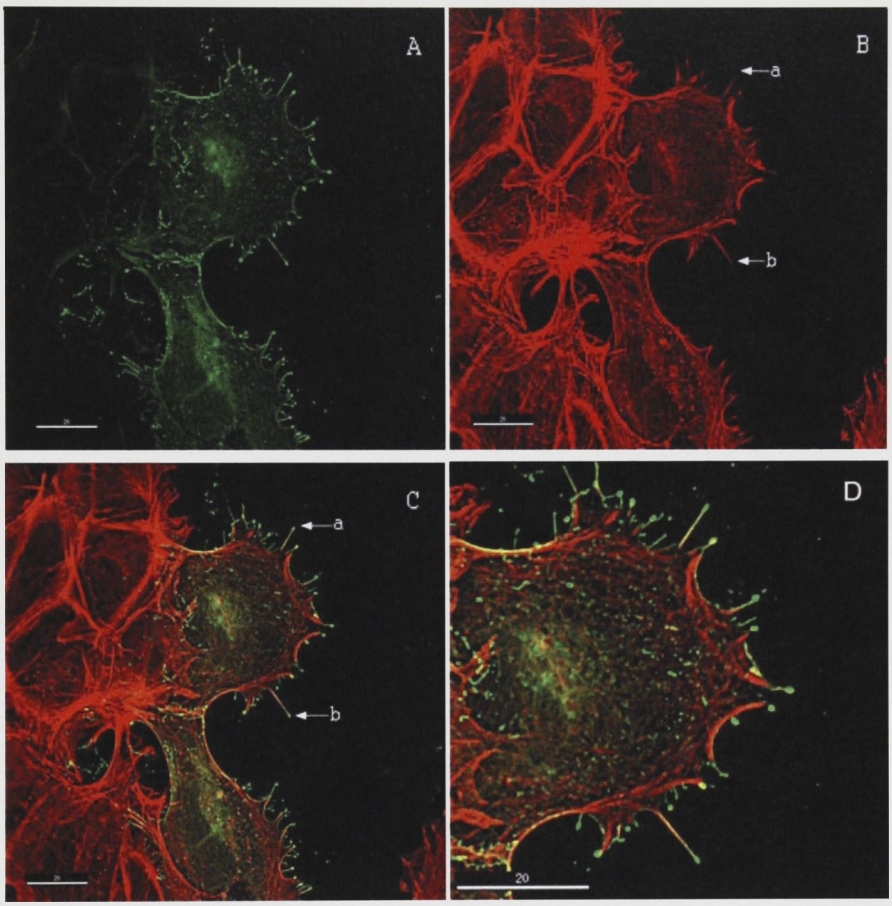

Fig. 3.7 The figure shows de-convoluted confocal images of the co-localization of F-actin throughout Ttyh1-GFP protrusions visualized by preserving F-actin during cell fixing. (A) HEK293 cell expressing Ttyh1-GFP. (B) Detection of F-actin with TRITC-phalloidin and (C) the merged image. Arrows indicate that F-actin is present throughout the protrusion with Ttyh1-GPF at the tips. (D) Close-up view of F-actin and Ttyh1-GFP in the filopodia. Scale bars represent 20 μm.

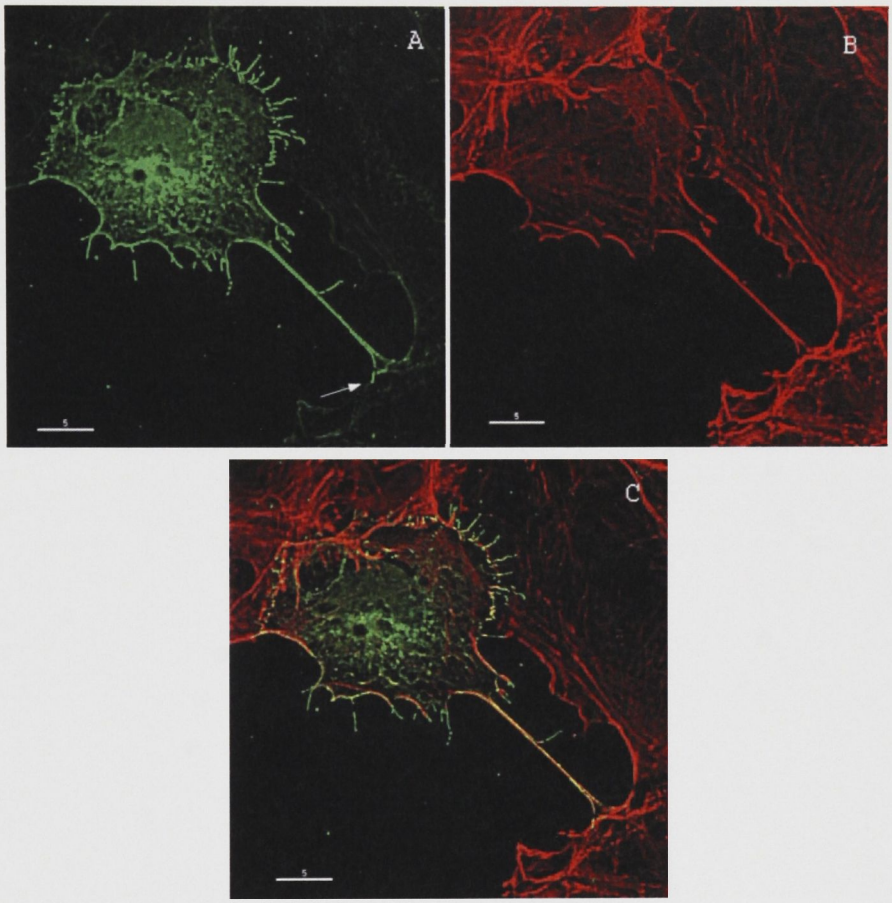

Fig. 3.8 The figure shows de-convoluted confocal images of filopodia which occasionally formed long distance connections with neighbouring cells and filled with F-actin. (A) A HEK293 cell expressing Ttyh1-GFP shows the expressed protein throughout the cable-like protrusion with Ttyh1-GFP concentrated at the interface between the cells (arrow). (B) TRITC-phalloidin labelling revealed that the structural protein within the cables was F-actin. (C) The merged image shows strong co-localization between Ttyh1 and F-actin in the cable. Scale bars represent 5 μm.

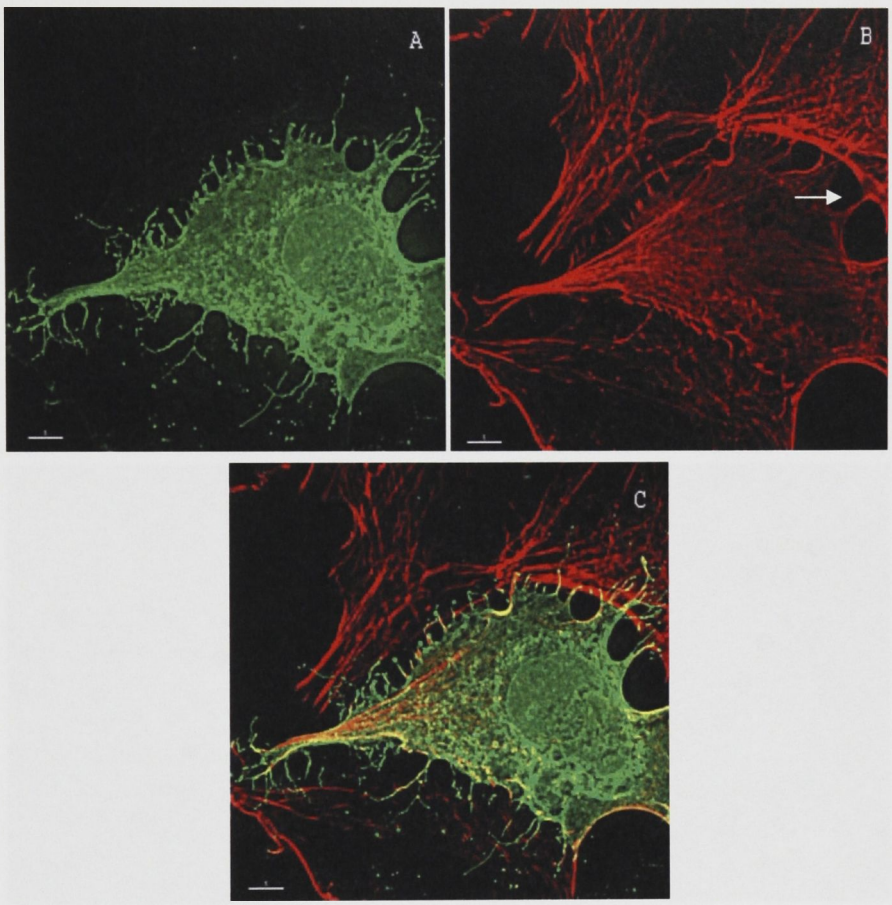

Fig. 3.9 The figure shows de-convoluted confocal images of short distance connections between filopodia and neighbouring cells which contained F-actin and appeared to promote the formation of a direct cytoskeletal link between the cells. (A) A HEK293 cell expressing Ttyh1-GFP makes multiple connections with neighbouring cells. (B) Labelling with TRITC-phalloidin shows what appear to be direct cytoskeletal F-actin connections between cells (arrow). (C) The merged image shows strong co-localization between Ttyh1 and F-actin in the cables. Scale bars represent 5 μm.

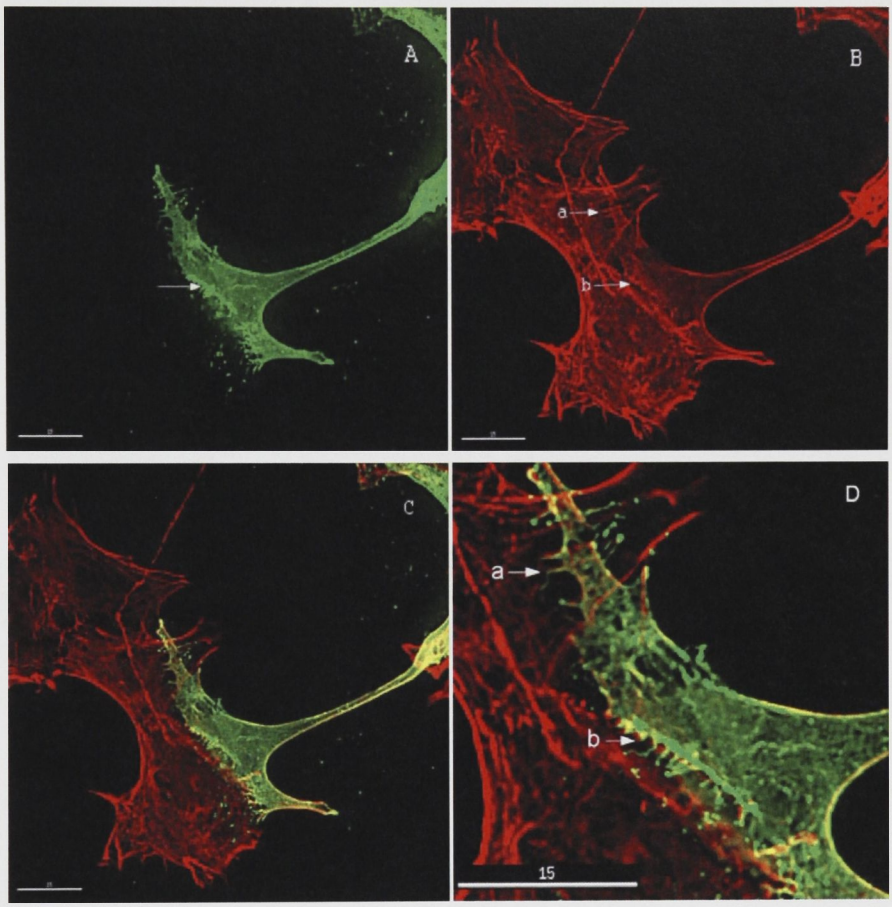

Fig. 3.10 The figure shows de-convoluted confocal images of the interface between a Ttyh1-GFP-expressing HEK293 cell and an untransfected cell. (A) Ttyh1-GFP was highly concentrated close to the cell membrane behind filopodia at the cell-cell interface. (B) F-actin appeared to form a continuous connection between cells (a) and the region of concentrated Ttyh1-GFP was also high in F-actin (b). (C) The merged image shows co-localization of concentrated Ttyh1 and F-actin. (D) Close-up view of the cell-cell interface. Scale bars represent 15 μm.

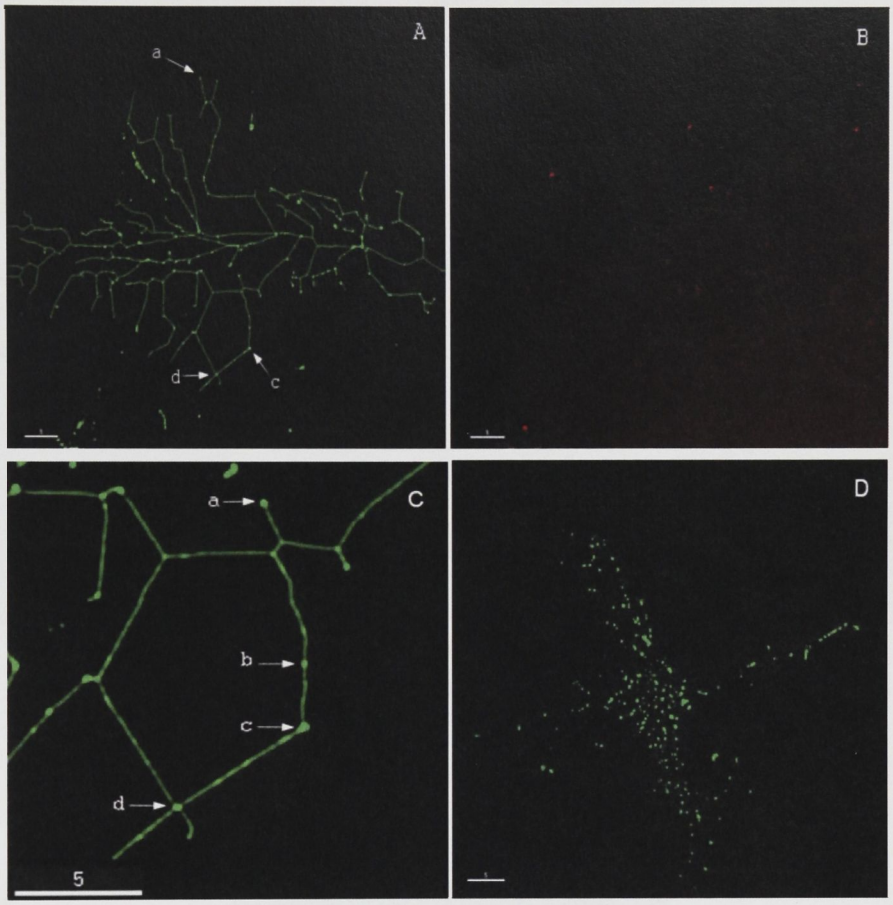

Fig. 3.11 The figure shows de-convoluted confocal images of an intact network of substrate-bound Ttyh1-GFP protrusions deposited upon cell migration. (A) Ttyh1-GFP was most highly concentrated at the tips of filopodia (a), at points of trajectory change (c) and where filopodia made contact with one another (d). (B) Following staining with TRITC-phalloidin, negligible amounts of F-actin were detected in deposits. (C) A close-up of areas where Ttyh1-GFP was most highly expressed. Ttyh1-GFP was not expressed uniformly throughout filopodia, but instead was in discreet packages (b). (D) A footprint of Ttyh1 left where a transfected cell had been washed off the substrate. Scale bars represent 5 μm.

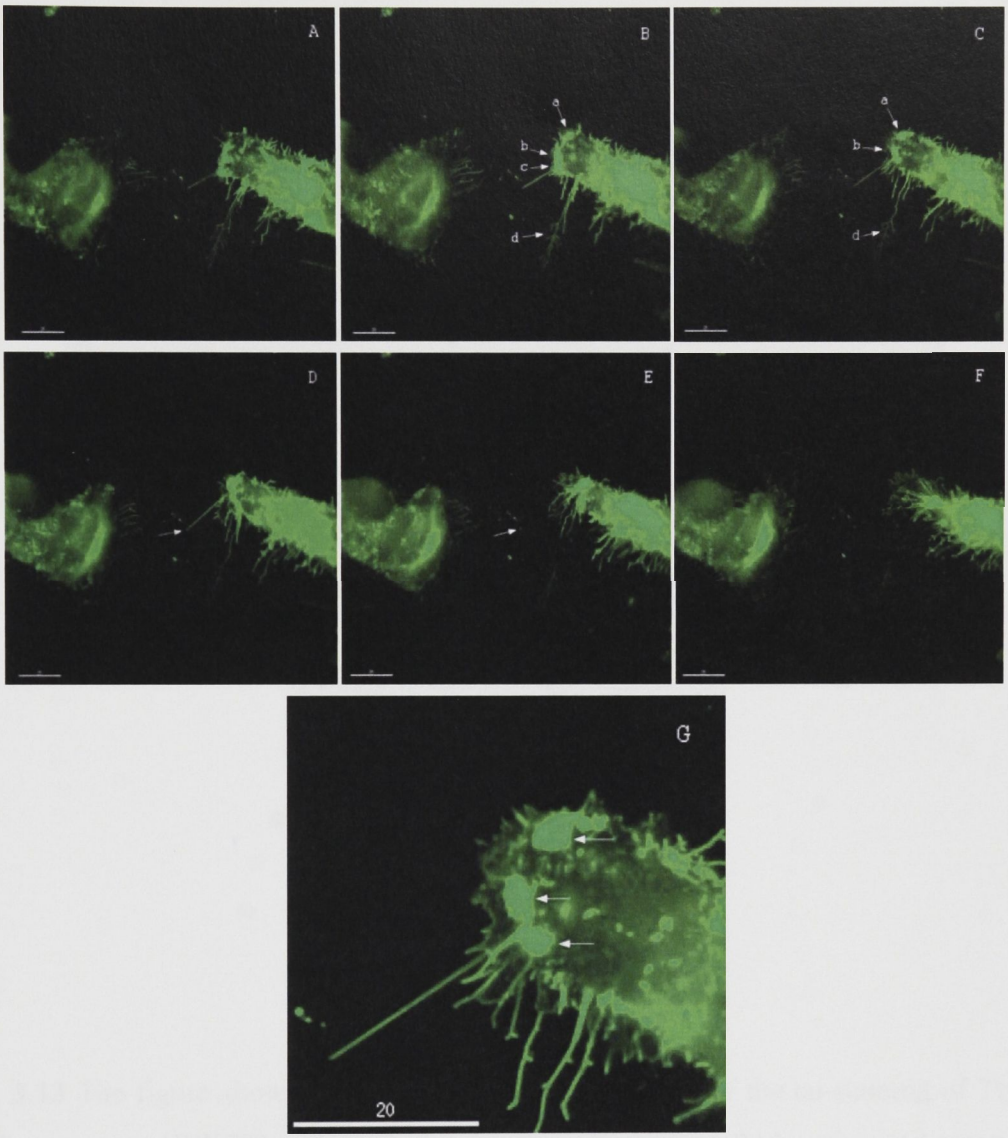

Fig. 3.12 The figure shows consecutive real-time de-convoluted confocal images of live, stably transfected Ttyh1-GFP-expressing HEK293 cells. (A) Photos were taken at 5 minute intervals as the cells migrated. (B,C) Large focal adhesions containing Ttyh1 formed at the rear of the cell (a,b,c) and upon migration, branched filopodia disintegrated (d). (D,E) As the cell moved forward, attached filopodia were stretched and torn from the substrate leaving a Ttyh1 deposit. (G) A close-up view of the trailing edge of the migrating cell revealing highly concentrated Ttyh1-GFP in the nascent focal adhesion complexes. Scale bars represent 20 μm.

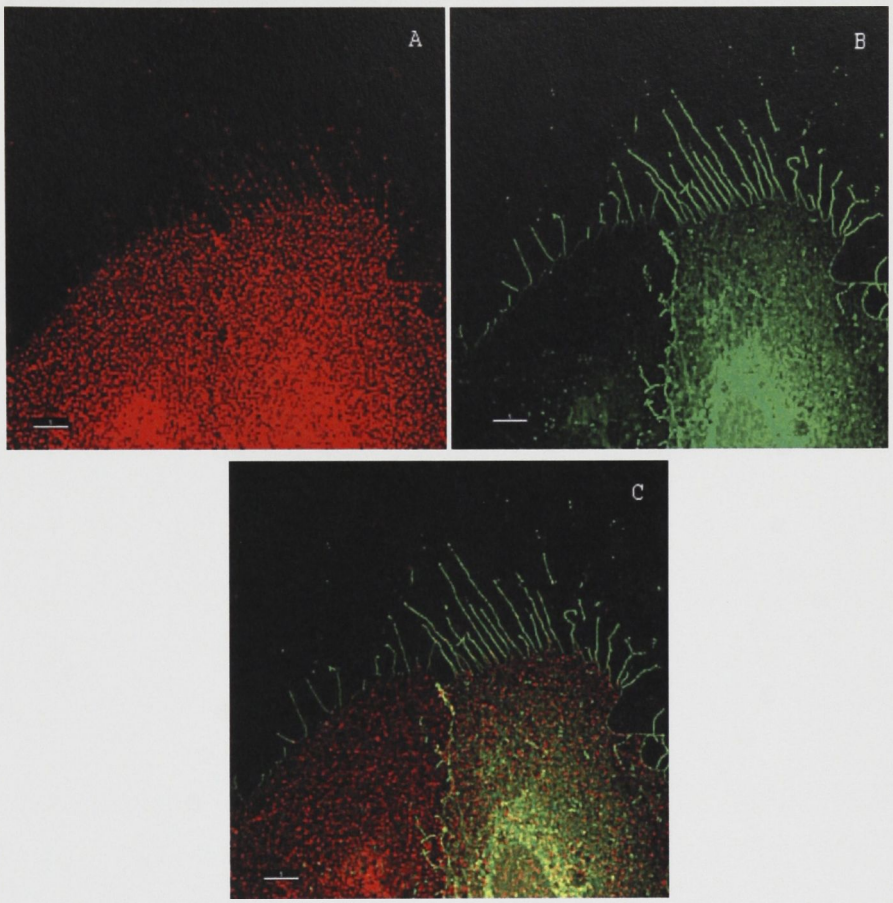

Fig. 3.13 The figure shows de-convoluted confocal images of the co-staining of Ttyh1-GFP-expressing HEK293 cells with anti-CD49e and a Texas Red conjugated secondary antibody. (A) Staining with anti-CD49e revealed substrate bound dots that were coincident with Ttyh1-GFP-induced filopodia. (B) Ttyh1 protrusions were attached to the substrate via integrin complexes containing the human CD49e (α5) integrin subunit. The shape of Ttyh1 filopodia was easily identified by the patterns of integrin attached to the substrate. (C) The merged image shows almost complete co-localization between Ttyh1-GFP and integrin. Scale bars represent 5 μm.

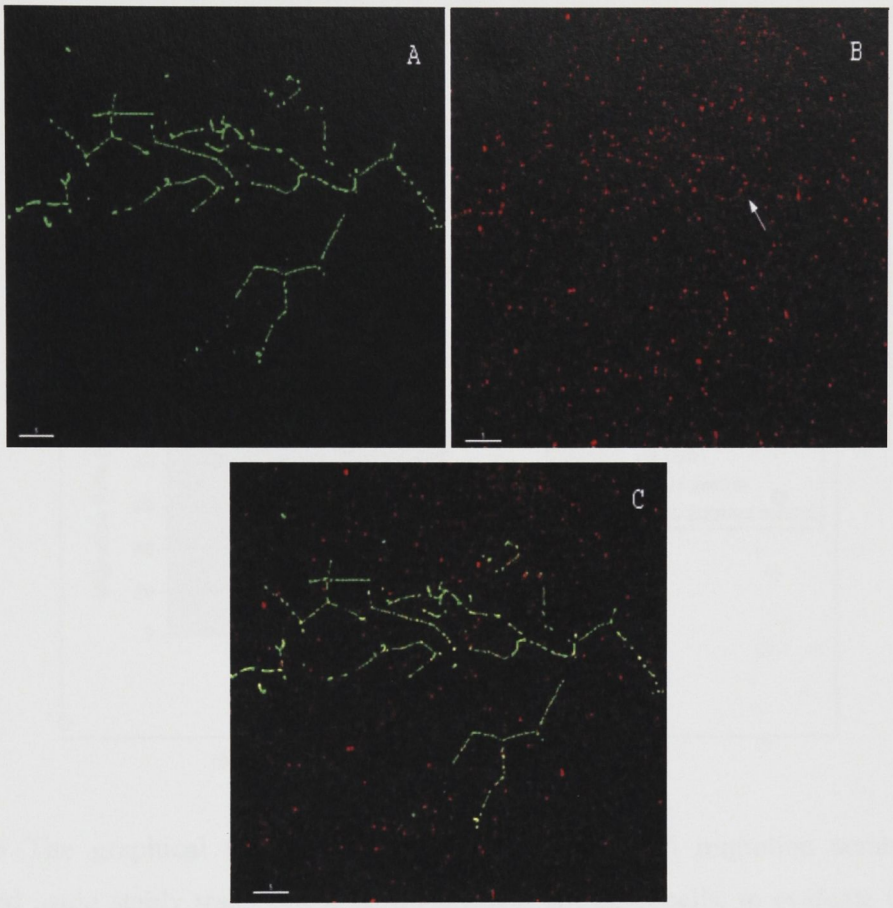

Fig. 3.14 The figure shows de-convoluted confocal images of a Ttyh1-GFP substrate-bound trail. Integrin was present below Ttyh1-GFP trails left by migrating HEK293 cells, and remained attached to the substrate along with Ttyh1-GFP (A) A substrate-bound Ttyh1-GFP cell migration trail. (B) Detection of the CD49e integrin subunit followed by staining with a Texas Red-conjugated secondary antibody reveals that the CD49e protein is coincident with Ttyh1-GFP. The shape of Ttyh1-GFP migration trails could be determined by observing the patterns of deposited integrin remaining on the substrate after cell migration. (C) The merged image shows Ttyh1-GFP covering the integrin trail. Scale bars represent 5 μm.

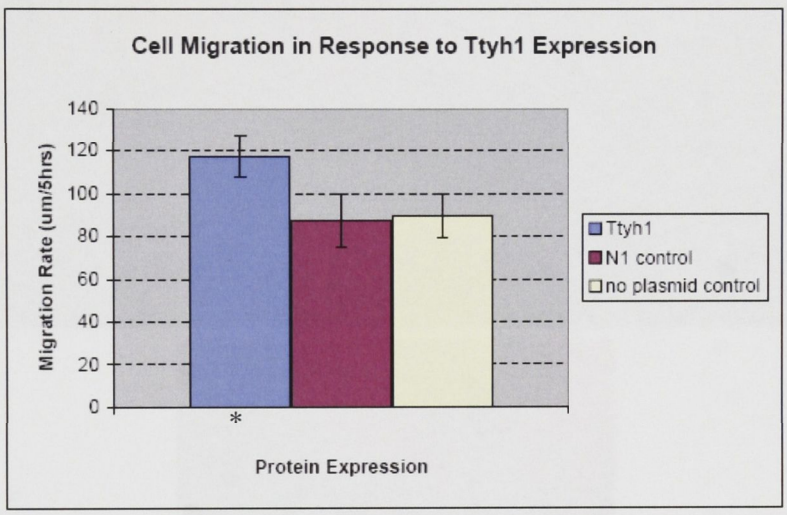

Fig 3.15 The graphical representation of data from a cell migration scratch assay performed using stably transfected, semi-confluent HEK293 cells, to evaluate the effect of Ttyh1 expression on cell migration. Data were generated to represent the scratch width (μm) recorded at 5 hour intervals, and were used to derive the rate of cell migration for Ttyh1-expressing cells and controls. Cells expressing Ttyh1 moved into the scratch at an increased migration rate. The data were significant at the $P<0.05$ level (ANOVA with multiple comparisons*), indicating that Ttyh1 expression resulted in an increased rate of cell migration.

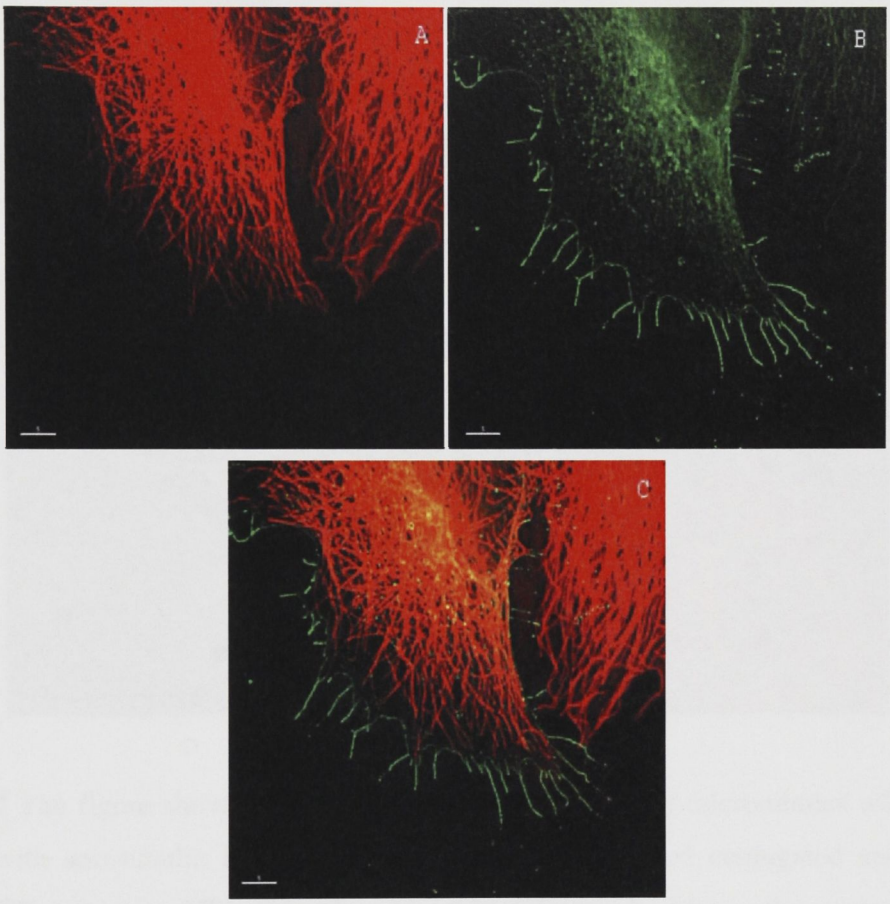

Fig. 3.16 The figure shows de-convoluted confocal images of microtubules which were stained with anti-tubulin followed by a Texas Red conjugated secondary antibody in Ttyh1-GFP-expressing HEK293 cells. (A) The microtubules appeared to be polarized towards the membrane more often in transfected cells than in control cells. (B) A transfected cell can be seen alongside an untransfected cell for comparison. (C) In the merged image microtubules can be seen terminating just behind Ttyh1-GFP protrusions. Scale bars represent 5 μm.

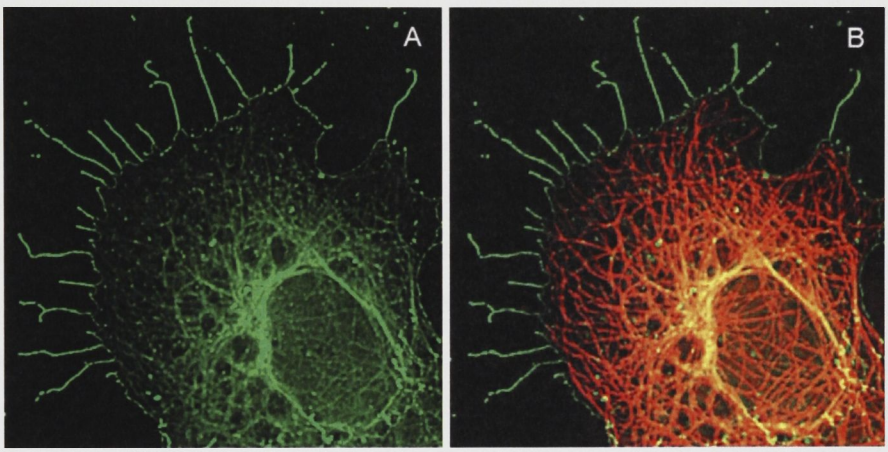

Fig. 3.17 The figure shows de-convoluted confocal images of microtubules which were stained with anti-tubulin followed by a secondary Texas Red conjugated antibody in Ttyh1-GFP expressing HEK293 cells. (A) Ttyh1-GFP can be seen in the same pattern as microtubules, and polarised towards the cell membrane. (B) In the merged image, yellow and orange staining illustrates the high coincidence of Ttyh1-GFP and microtubules.

3.4 Discussion

The expression of Ttyh1-GFP and the Ttyh1 protein alone induced the formation of long cell membrane protrusions in several cell lines. The HEK293 cell line was chosen as the model system for Ttyh1 expression due to the high efficiency with which these cells could be transfected. The F-actin scaffold protein was likely involved in the genesis of Ttyh1-associated protrusions which were similar to those that have been observed in association with lamellipodia at the leading edge of migratory cells. The advancing cell front of migratory cells consists of a meshwork of actin filaments which are around 0.2 μm in diameter (Abercrombi et al. 1971), and are often punctuated by radially orientated bundles of actin microspikes or filopodia (Small 1981). From these bundles, filaments can extend in projections beyond the cell membrane. The formation of such projections can be potentiated by actin assembly and bundling proteins in the vicinity of the plasma membrane (Furukawa and Fechheimer 1997). It has previously been shown that the upregulation of F-actin bundling proteins such as fascin (Yamashiro et al. 1998) and villin (Frank et al. 1990) causes dramatic alterations in cell morphology, and results in the formation of long, spiky protrusions at the cell membrane. It is likely that filopodia play a sensory role in cells, and the induction of similar filopodia by the over-expression of receptors such as SREC substantiate this claim (Shibata et al. 2004). The protrusions induced by Ttyh1 expression appear to be almost identical to those resulting from the expression of several F-actin bundling proteins. The localization of Ttyh1 to the cell membrane along with the induction of long, spiky, F-actin rich filopodia implicates the Ttyh1 protein in F-actin bundling or indirect regulation of F-actin bundling proteins. Since Ttyh1 is a transmembrane protein it may act as a receptor which can induce the polymerization of F-actin and cause filopodial extension.

It is likely that a synaptogenic cell adhesion molecule would be concentrated at the tips of synapses to facilitate heterophilic adhesion between axons and other cell types (Kim et al. 2006). The cytosolic region would interact with scaffold proteins to enable a coupling of adhesion events with the recruitment of synaptic proteins (Kim et al. 2006). Preservation of F-actin structures in Ttyh1 filopodia prior to immunohistochemical analysis revealed that Ttyh1 was particularly concentrated at the very tips of F-actin

protrusions. In ectopic expression studies the Ttyh1 protein appears to fulfil the criteria expected of a synaptogenic adhesion molecule. In addition, Ttyh1 is up-regulated directly behind filopodia in regions of cell-cell contact where the Ttyh1-induced protrusions mediate the formation of direct cytoskeletal F-actin links between cells. In many instances it appeared that Ttyh1 filopodia had somehow opened a pore in the membrane of contacted cells to facilitate the formation of F-actin bridges between the two cells. It was surprising that Ttyh1 expression did not cause an increase in the activation status of Rho family GTPases and may indicate a problem with the experimental protocol or that Ttyh1 affects F-actin polymerization via an alternative activation pathway.

Studies of embryonic dorsal closure have shown F-actin cables and dynamic filopodia expressed at the leading edge of epithelial cells (Jacinto et al. 2000). The function of actin cables in dorsal closure is recapitulated in wound healing in the mammalian cornea, embryonic skin and in tissue culture monolayers (Danjo and Gipson 1998). Long filopodia can be induced by the ectopic transplant of cells into an inappropriate environment. For example, if *Drosophila* imaginal disc cells are placed in the wrong compartment, they can form extensions which reach into the appropriate compartment which helps to protect them from apoptosis that would normally be induced by the dissimilar surrounding cells (Milan et al. 2002). Projections are also associated with cells that move directionally (Ribeiro et al. 2002), and there is evidence that cellular extensions participate in guided cell migration (Rorth 2003). The Ttyh1-induced filopodia occasionally reached over long distances of up to several times the cell's diameter to form stable, F-actin rich connections with remote cells. The Ttyh1 protein was concentrated at the cell-cell interface, and long F-actin cables appeared to be under tension as there were no bends in the cables, and they were positioned above the substrate without adhesive contacts for support. It is possible that one function of these cables is to bridge the gaps between cells in a similar way to that observed during dorsal closure and wound healing. It is also possible that F-actin cables are the result of cells being unable to release their adhesive contacts as they move apart. Another possibility is that the ectopic expression of Ttyh1 in cell types where it is not normally expressed may have led to the formation of these structures. F-actin cables may have been generated in an attempt to

locate 'like' cells and form the desired connections, though this has not been tested. It would be useful to over-express Ttyh1 in neuronal cell types that express endogenous Ttyh1 to see if similar cables are formed.

Motile fibroblasts have been shown to deposit integrins in a process known as membrane ripping which leaves α5β1 integrin-rich migration trails in their wake (Palecek et al. 1996). The formation of these macroaggregates is thought to depend on actin cytoskeleton disruption leading to the fragmentation of cylindrical cell extensions into periodic chains of pearls (Bar-Ziv et al. 1999). Similarly, the expression of Ttyh1 results in the deposition of consecutive spots on the substrate as cells migrate, and pieces of disintegrating filopodia are torn from the cell as observed by real-time microscopy. Interestingly, Ttyh1 was also deposited on surrounding cells. It should be noted that *in vivo*, the surrounding cells and ECM are the substrate. It is likely that Ttyh1 was deposited on these cells in the same way that it was deposited on the glass substrate, and not necessarily to confer information to other cells. However, if a Ttyh1 projection is attached to a neighbouring cell it is likely that mechanical forces would affect signalling events in both cells involved. Confocal microscopy revealed that Ttyh1-GFP was closely associated with fibrous cytoskeletal proteins that appeared to be F-actin. It was also evident that Ttyh1-GFP was most highly concentrated close to the interface between the cell and the substrate at the peripheral cell membrane. These peripheral regions are where the cell first comes into contact with the substrate as it migrates to a new area. If Ttyh1 was functioning as a receptor that could mediate cell adhesion in response to substrate bound environmental cues, this would be a logical area for the transmembrane protein to be expressed.

Analysis of substrate-bound Ttyh1 filopodia revealed that Ttyh1-GFP was highly concentrated at the tips of filopodia, at points of trajectory change, and where filopodia made contact with one another. For a sharp angle to form in filopodia it would be necessary to attach the structure to the substrate at the angles zenith. It is safe to assume that adhesion sites exist at these points of trajectory change, which is exactly where Ttyh1-GFP is concentrated. Deposited filopodia and migration trails did not contain F-

actin. During cell fixing actin retracted back into the cell body very quickly, necessitating a modified protocol to preserve F-actin throughout Ttyh1 protrusions. It appears that upon migration F-actin retracts in the direction of cell migration leaving Ttyh1 filopodia attached to the substrate. Without F-actin support the filopodia disintegrate as the cell moves away. Further analysis of Ttyh1 deposits revealed that they were closely associated with the CD49e (α5) integrin subunit. Filopodia were attached to the substrate via CD49e and Ttyh1 co-localized with the integrin complex. It is possible that Ttyh1 protein expression causes membrane ripping by aberrantly stabilizing integrin binding and thereby interfering with focal complex release. In a recent publication the over-expression of α5 integrin appears to have induced the formation of long, branched filopodia, though this induction may have been overlooked and was not discussed in the paper (Laukaitis et al. 2001). Since the expression of Ttyh1 induces filopodia, the expression of α5 integrin induces very similar filopodia and Ttyh1 co-localizes with α5 integrin, it is likely that both proteins are eliciting the induction of filopodia via a common, cell adhesion associated signalling pathway.

When focal complexes form in the vicinity of lamellipodia which flank the cell body, they fuse together at the trailing edge to create large, oval shaped adhesions resembling complete focal adhesions (Anderson et al. 1996). The lateral adhesions are mobile, transient, and are drawn towards the flanks of the cell body in a sliding motion which is driven by the contractile bundles of laterally orientated actin filaments (Anderson et al. 1996, Lee et al. 1994). One of the most important observations in this chapter is the formation of nascent focal adhesions at the rear of a migrating cell captured by real-time microscopy. The focal adhesions that formed in the Ttyh1-GFP-expressing cell perfectly matched those described previously (Anderson et al. 1996), and sequestered Ttyh1 from the surrounding focal complexes and cytoplasm. The Ttyh1-GFP protein was expressed in these emerging focal adhesions at the highest concentration observed in any cellular region during this study. In some instances when cells had been mechanically removed from the substrate by washing with PBS, perfect Ttyh1-GFP footprints of the cells were observed. This exemplifies the strength of the connection between Ttyh1 and cell adhesion molecules. The expression of Ttyh1 also resulted in a statistically significant

increase in the rate of cell migration. It is possible that this increase was the result of changes in F-actin polymerization dynamics at focal adhesion sites. The Ttyh1 protein appears to associate with the F-actin cytoskeleton and traverse the cell membrane thereby forming a direct link between the cytoskeleton and the ECM. It is possible that the Ttyh1 protein modulates the rate of cell migration by facilitating F-actin polymerization at focal adhesion sites. These findings strengthen the argument that Ttyh1 may be a modulator of early focal adhesion formation, and demonstrate the close association of the Ttyh1 protein with cell adhesion and migration.

Integrins and other membrane components of focal adhesions can be delivered to adhesion assembly sites via microtubule driven membrane traffic (Bretscher 1996). It has been shown that blocking vesicle transport along microtubules inhibits cell spreading and delivery of integrins to the cell membrane (Roberts et al. 2001). In Ttyh1-expressing cells, microtubules tended to be polarized towards the membrane and terminated directly behind Ttyh1 filopodia. The Ttyh1-GFP protein was highly co-localized with α-tubulin close to the nucleus and could be seen in discrete packages along microtubules as they radiated out towards the membrane. It is very likely that Ttyh1, along with other focal adhesion components, is transported to the membrane via microtubules.

Evidence suggests that growth cone filopodia in neural cells act as chemosensors which can influence the direction of growth cone migration (Miller et al. 1995). These filopodia have been described as long distance sensors that can guide axons by manipulating growth cone motility (Oakley and Tosney 1993). Filopodia at the leading edge of growth cones contain F-actin, while the core contains polarized microtubules (Lee and Kolodziej 2002). The orientation of microtubules and the extension of F-actin beyond the cell membrane in Ttyh1 expressing cells seemed to mimic observations in neuronal growth cones. To test whether Ttyh1 filopodia shared similarities with growth cones, antibodies to early growth cone markers were used to analyse Ttyh1-expressing cells. Although staining did occur along some filopodia, it was not sufficient to make a direct correlation to nascent neuronal growth cones. The expression of Ttyh1 in neuronal

cell types followed by growth cone analysis would need to be investigated before any association between Ttyh1 filopodia and axonal growth cones could be concluded.

Integrins are capable of acting synergistically with cell membrane receptor systems to finely modulate cell adhesive activities in response to environmental signals (Schmid and Anton 2003), and membrane bound adhesion molecules have been shown to trigger synapse formation (Fu et al. 2003). The action of these adhesion molecules is not limited to initial contact formation but can also perform the function of specific target recognition (Shen et al. 2004). In this group of experiments the Ttyh1 protein was observed moving towards the cell membrane via polarized microtubules in a similar way to cell adhesion molecules. The Ttyh1 protein was incorporated into the cell membrane as predicted, and led to the generation of F-actin rich projections similar to those generated by the expression of F-actin bundling proteins. These projections appeared to facilitate the formation of direct cytoskeletal connections between cells. The Ttyh1 protrusions are likely to have been generated by the same mechanism as the protrusions induced by α5 integrin expression, and may implicate Ttyh1 as a focal complex molecule. The Ttyh1 protein co-localized with α5 integrin, was highly upregulated in nascent focal adhesions and led to an increase in the rate of cell migration in Ttyh1-expressing cells. The Ttyh1 protein fulfils the criteria expected of a membrane bound protein that mediates cell adhesion. Future experiments should be aimed at the elucidation of signalling pathways involved in the generation of the filopodia. The use of nocodazol to disrupt microtubules could verify whether Ttyh1 was carried to the cell membrane in a microtubule dependent manner, and whether the F-actin structures were reliant on microtubule polarization. The disruption of F-actin structures using cytochalasin could be used to confirm or refute the hypothesis that the increased rate of cell migration in Ttyh1-GFP expressing cells is dependent on Ttyh1-induced actin polymerization.

Chapter 4

Detection of Endogenous Ttyh1 by Immunohistochemistry

4.1 Introduction

The aim of the work presented in this section was to visualize endogenously expressed Ttyh1 by immunohistochemical analysis (IHC) to make possible a comparison with the ectopically expressed protein. The study of ectopically expressed Ttyh1 generated information regarding the localization of Ttyh1, some associated molecules and some functional data. However, it was necessary to confirm that this information was also applicable to the endogenously expressed protein in its native tissue. Previous experiments revealed that Ttyh1 was present in whole brain lysates, but it could not be detected in available cell lines by Western blotting. The N- and C-terminal antibodies were previously shown to accurately detect the Ttyh1 protein by IHC when it was expressed in HEK293 cells using the p-N1-Ttyh1 plasmid. It is known that protein detection by IHC is more sensitive than Western blot analysis, so this technique was applied in an attempt to identify Ttyh1 in cell lines, primary neuronal cultures and *in situ* using cryosectioned rat brain. Detection of Ttyh1 was considered to be specific if both antibodies detected the protein, fluorescence could be blocked by competitive binding of the primary antibody to its cognate antigen peptide, and if the fluorescence was absent in the presence of secondary antibody alone.

4.2 Materials and methods

4.21 Culture of prenatal rat brain cells

Prenatal rat pups were removed from the placenta and decapitated using a scalpel or scissors as described elsewhere (Romijn et al. 1988). The entire head was washed twice in 70 % ethanol for 10 seconds. Heads were suspended in 5 ml of DMEM containing 10 % FCS under sterile conditions followed by trituration, first with a 25 ml pipette, then a 10 ml pipette and finally with a 5 ml pipette to dissociate cells from brain tissue. The tissue was allowed to sediment at 37°C for 5 minutes and supernatant was decanted into a 75 cm^2 flask containing 20 ml of DMEM with 10 % FCS. Cells were cultured overnight at 37°C in a humidified 5 % CO_2 atmosphere. The following day, non-adherent cells were removed by washing with PBS pre-heated to 37°C, and culture medium was replaced.

4.22 Preparation of substrates for neuronal culture

The following protocol was used to prepare 24-well cell culture plates and glass coverslips prior to use as substrates for neuronal cell culture. Round glass coverslips (13 mm, ProSciTech, Germany) were cleaned in concentrated HCl (5 min), rinsed overnight in a continuous flow of water, rinsed in distilled water, then rinsed twice in 100 % ethanol and stored in 100 % ethanol until use. The coverslips were individually flame dried and placed in wells of a 24-well plate. A substrate coating solution was prepared consisting of 0.1 mg/ml of poly-D-lysine plus 0.5 mg/ml of rat tail collagen. To provide a substrate for island cultures, a glass microatomizer (Fisher Scientific, USA) was used to spray a fine mist of the coating solution onto the coverslips. These were allowed to dry in a laminar flow hood and were then placed into the wells of the culture plate. A few drops of culture medium were added to each well so that it just covered the surface of the coverslips. The neuronal culture medium consisted of 870 mg of DMEM/HEPES (Sigma, Australia) dissolved in 50 ml of MilliQ H_2O (pH 7.3), 50 ml of DMEM/bicarbonate (Sigma, Australia), 2 ml of B27 supplement (Gibco, Australia), 22 µM of L-alanine, 5.53 µM of L-asparagine-HCl, 0.2 µM of lipoic acid, 67.4 µM of L-proline, 0.25 µM of vitamin B12, 0.67 µM of zinc sulphate, 1 ml of 100× penicillin/streptomycin (10,000 units of penicillin, 10 mg of streptomycin per ml (Sigma, Australia)) and 5 ml of heat-inactivated FCS. The final pH of the culture medium was adjusted to 7.5 using NaOH. Prepared plates were incubated at 37°C in a 5 % humidified CO_2 atmosphere overnight. The medium was removed immediately before adding cell suspensions to the wells.

4.23 Culture of new born rat hippocampal cells

Newborn Evans or Wistar rat pups were anesthetised with Fluothane before decapitation and brain dissection. Hippocampi were removed under dissection solution (125 mM NaCl, 3 mM KCl, 2 mM $CaCl_2$, 1 mM $MgCl_2$, 25 mM HEPES pH 7.4, 10 mM glucose, 25 mM sorbitol, pre-warmed to 37°C). The CA1 region of the hippocampus was dissected out after cutting the ends off the "jelly roll" structure and gently unrolling it. The dentate-CA3 end of the sheet was sliced off and discarded and the remaining CA1 region was cut into approximately 1 mm square blocks. The tissue pieces were transferred to a 25 cm^2 tissue culture flask containing enzyme solution (2 ml Hank's

Balanced Salt Solution (BSS), 2.2 mM EDTA pH 7.0, 1.5 mg L-cysteine, 13.4 μM 2-mercaptoethanol, 200 units lyophilized papain, pre-incubated at 37°C for 30 minutes and made up to 10 ml with Hank's BSS). The flask was placed in a 37°C water bath and gently agitated for 30 minutes. A lightly flame-polished Pasteur pipette was used to transfer the tissue pieces to a 15 ml sterile tube. Tissue pieces were allowed to settle before the supernatant was removed and discarded. Tissue was rinsed three times with warmed culture medium (125 mM NaCl, 3 mM KCl, 2 mM $CaCl_2$, 1 mM $MgCl_2$, 25 mM HEPES pH7.4, 10 mM glucose, 25 mM sorbitol) and allowed to settle before discarding the supernatant from each rinse. A 1 ml aliquot of culture medium was added, and the tissue was gently triturated 3-4 times. Tissue was allowed to settle, and the supernatant was collected into a 15 ml tube. This procedure was repeated 6 times, each time triturating more vigorously, until the tissue was dissociated giving a total of 6 ml of cell suspension. Phase bright cells were counted using a haemocytometer and diluted to 8×10^4 cells/ml. An aliquot of 0.5 ml of cell suspension was added to each well of a freshly prepared 24-well plate and incubated at 37°C in a humidified 5 % CO_2 atmosphere.

4.24 Neuronal culture scratch assay to induce a Ttyh1 response

Hippocampal cell cultures were grown in a 24-well plate until they were approximately 80 % confluent. Two scratches were made through the cultures by pressing a yellow pipette tip down on the substrate and moving it from one side of the well to the other. Cells were fixed at 0, 1, 6, 12, 24 and 48 hours followed by IHC analysis using the AP1 antibody to detect any Ttyh1 response to the injury.

4.25 Preparation of rat brain cryosections

Rats were anesthetized with pentobarbital (50 mg/kg; intraperitoneal) (Rosenberg et al. 2001). The chest cavity was sectioned on ice to expose the heart, and the left atrium nicked with a scalpel. A 25G needle was inserted immediately into the right ventricle and PBS was pumped through using a peristaltic pump to clear the blood. When clear PBS flowed from the left atrium the pump was turned off and the vacuum tube inserted into PBS containing 4 % paraformaldehyde. The pump was then turned back on and perfusion continued until the body stiffened. The brain was dissected out and post-fixed in 4 %

paraformaldehyde for 3 hours at 4°C. Cryo-protection was implemented by placing the brain in PBS containing 30 % sucrose and incubating at 4°C overnight. This was diluted 1:2 with Optimal Cutting Temperature medium (OCT) and incubated at 4°C overnight, then diluted again 1:4 in OCT and incubated at 4°C overnight. The brain was then placed in pure OCT and incubated at 4°C overnight followed by freezing at -80°C. Thin (10 μm) slices were cut from the anterior to the posterior of the brain using a cryostat. Slices were air-dried before being subjected to immunohistochemical analysis.

4.3 Results

4.31 Absence of endogenous Ttyh1 in cell lines

Available cell lines were analysed for possible expression of the Ttyh1 protein following overnight serum starvation and stimulation with phorbol ester (200 ng/ml), forskolin (40 μg/ml), EGF (50 ng/ml) or NGF (50 ng/ml). The cell lines analysed were human embryonic kidney (HEK293), mouse fibroblast-like (Swiss3T3), retinal pigmented epithelial (ARPE-19), Chinese hamster ovary (CHO), African Green Monkey kidney fibroblast (COS-7), neuroblastoma (IMR-32), neuroblastoma (Kelly), rat pheochromocytoma (PC-12), and neuroblastoma (SK-N-SH) cells. The PC-12 cells were analysed before and after NGF-induced neuron-like differentiation but no Ttyh1 expression was detected (Fig. 4.1). The ARPE-19 cell line expressed an unknown protein at the cell membrane where Ttyh1 may be expected to localize. However, the addition of up to 1 mg/ml of peptide antigen 802 to the AP1 antibody prior to use did not block detection of the protein (Fig. 4.2). In fact, the addition of antigen caused a bright background and enhanced the fluorescence of all cellular proteins including the unknown membrane protein. The AP2 antibody did not detect this protein, and it was later exposed as an artefact due to direct secondary antibody binding which was further enhanced by the addition of the 802 peptide antigen. No Ttyh1 expression was detected in the other cell lines, thus confirming previous results from Western blot analyses and EST expression data.

4.32 Endogenous Ttyh1 in prenatal rat brain cultured cells

Preliminary experiments involving detection of endogenous Ttyh1 in cultured neuronal cells were conducted using cells from whole dissociated prenatal rat heads. The day following dissociation and seeding of primary brain cells into culture plates, cells were analysed by IHC using antibodies AP1 and AP2. Bright immuno-reactive spots were detected on cell bodies and along axon-like structures by both antibodies (Fig. 4.3). The spots were specifically blocked by the incubation of antibodies with 500 μg/ml of their respective cognate peptide antigens prior to use. They were not blocked by the addition of non-antigenic peptide (peptide 806 with AP1 and peptide 802 with AP2) to the antibodies, and were absent when secondary antibody alone was used. The general background fluorescence was increased by the addition of peptide 802 to the AP1 antibody but the bright spots were almost completely blocked (Fig. 4.3). In subsequent IHC experiments using cells which had been cultured for several passages, the Ttyh1 spots could no longer be detected.

4.33 Endogenous Ttyh1 in hippocampal neurons and astrocytes

Primary hippocampal cell cultures were analysed following immunohistochemical staining using the N- and C-terminal Ttyh1 antibodies. Ttyh1 was detected along neuronal axons in discrete spots in a very similar pattern to those observed during exogenous expression studies (Figs. 4.4 and 4.5). The spots were concentrated near the zenith of angles in substrate-bound axons, were detected by both antibodies, could be blocked by the addition of 200 μg/ml of antigen peptide to the antibodies prior to use, and were absent in the presence of secondary antibody alone. Similar spots were also observed in what appeared to be astrocytes, and substrate bound deposits were observed behind migrating astrocytes (Fig. 4.6). The Ttyh1 protein appeared to be concentrated near the cell membrane in small protrusions, and to leave a fine trail of substrate bound deposits of consecutive dots similar to those observed following Ttyh1 expression in HEK293 cells (Fig. 4.7). Photographs of endogenous Ttyh1 were taken with long open-aperture times of around 5 seconds as the staining was quite faint.

4.34 Neuronal culture scratch assay

It was difficult to ascertain whether there had been any upregulation of Ttyh1 in response to the scratch injury. The only possible Ttyh1 response was observed at the 1 hour time point where it appeared that cells retreating from the wound showed a slight increase in the brightness of antibody staining at the membrane near the trailing edge of cells. Small trails of what appeared to be endogenous Ttyh1 were also observed behind trailing edge filopodia, though these trails were not necessarily a response to the injury. No upregulation was observed at any other time point.

4.35 Endogenous Ttyh1 in rat brain slices

In situ immunochemistry performed on thin (10 μm) rat brain slices revealed small dots of Ttyh1 around the hippocampus (Fig. 4.8). In rare cases, similar dots were observed at the interface between cells in areas where the cell matrix appeared slightly less dense than in the surrounding tissue (Fig. 4.9). The native Ttyh1 protein was detected independently by each antibody and the observed dots could be blocked by the pre-incubation of each antibody with 200 μg/mL of its antigen peptide.

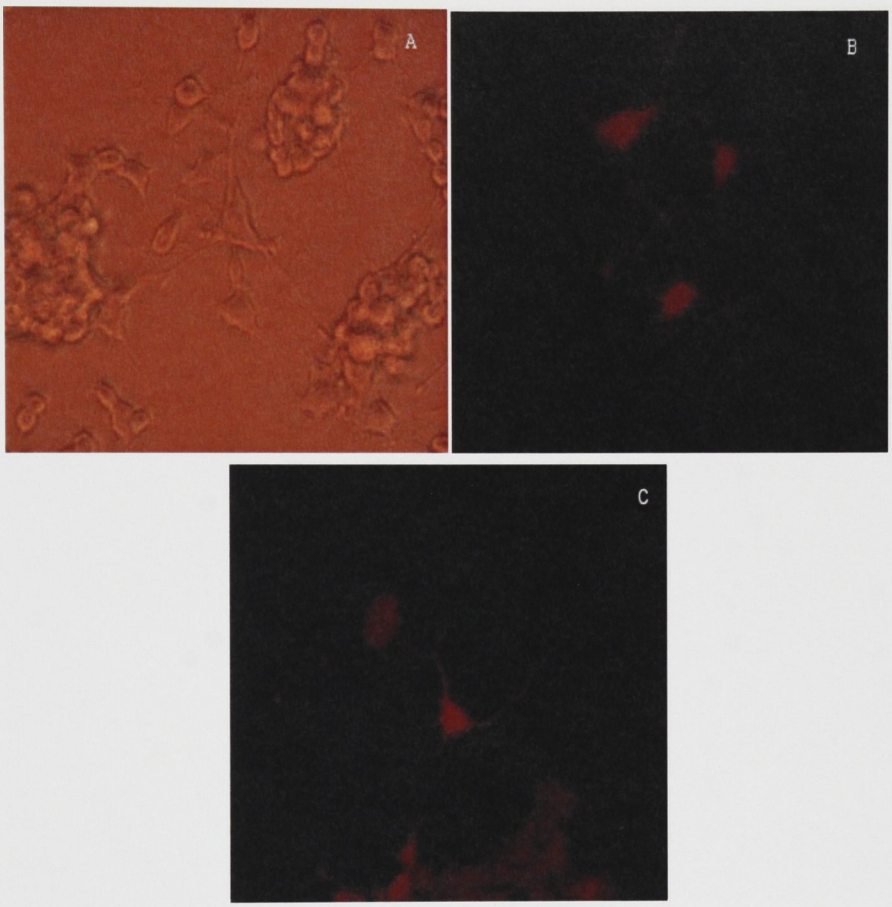

Fig. 4.1 The figure shows images of PC-12 cells which did not endogenously express the Ttyh1 protein (A) A phase contrast image of PC-12 cells following NGF-induced neuron-like differentiation. (B) A confocal image of PC-12 cells following immunohistochemical analysis using the AP1 antibody followed by a Texas Red conjugated secondary antibody revealed no Ttyh1 protein. (C) A confocal image of PC-12 cells stained with secondary antibody alone showed similar staining to that observed in the presence of the AP1 antibody.

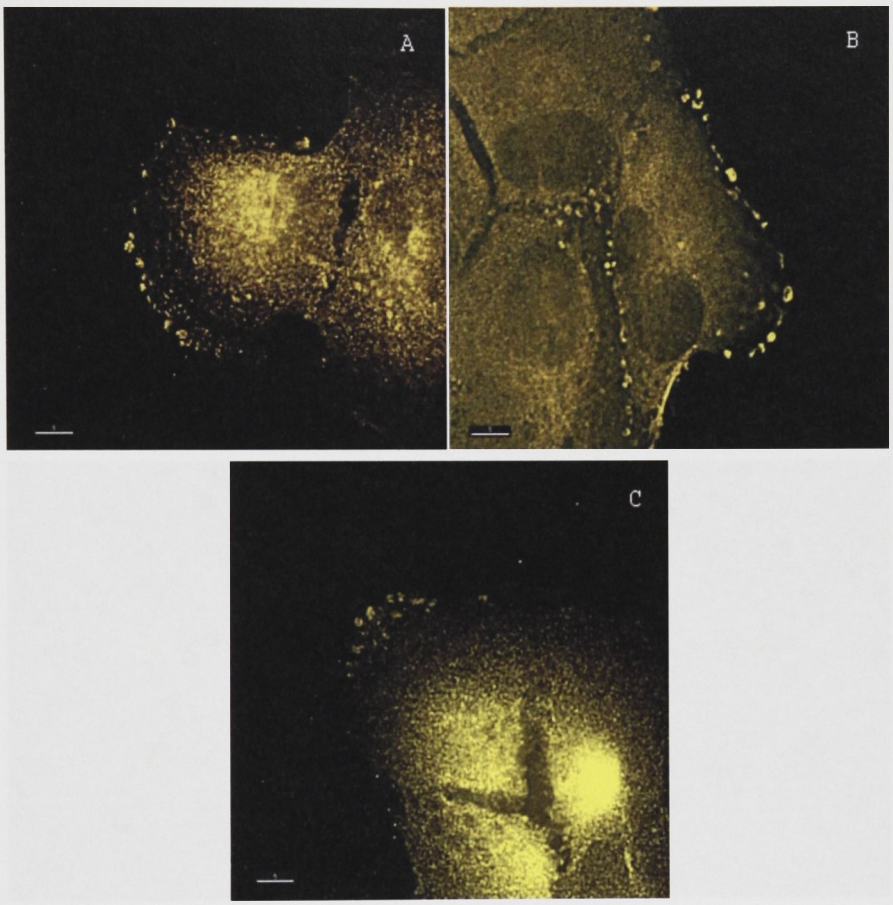

Fig. 4.2 The figure shows confocal images of ARPE-19 cells analysed using the AP1 antibody which detected an unknown membrane-localized protein. (A) Staining using a 1:100 concentration of AP1 detected a protein with Ttyh1-like localization. (B) Blocking of the AP1 antibody with up to 1 mg/ml of peptide 802 prior to use enhanced the fluorescence of the unknown protein. (C) The secondary anti-sheep antibody alone detected the unknown protein but with slightly less fluorescence. Scale bars represent 5 μm.

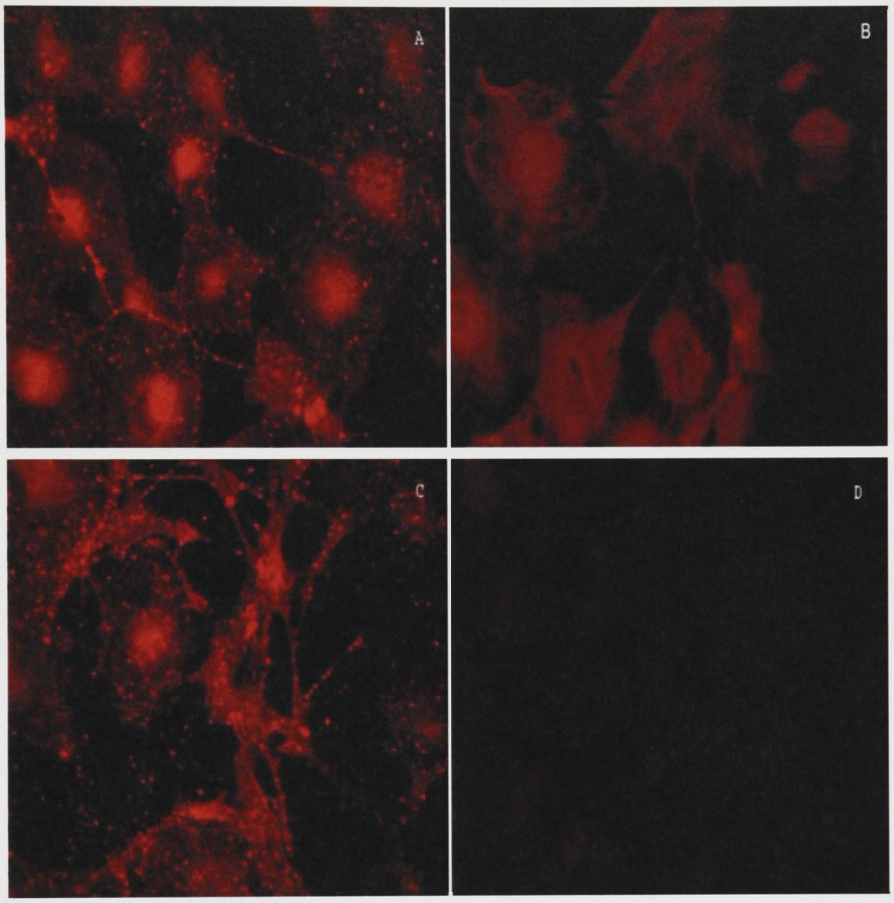

Fig. 4.3 The figure shows confocal images of preliminary experiments showing endogenous Ttyh1 in prenatal rat head cultured cells. (A) Cells showed Ttyh1 in dots along axon-like structures following IHC staining using AP1. (B) Staining was blocked by the addition of the 802 peptide antigen. (C) A similar staining pattern was detected using AP2. (D) Staining with AP2 was blocked by the addition of the 806 peptide antigen. Secondary antibody alone did not detect the protein.

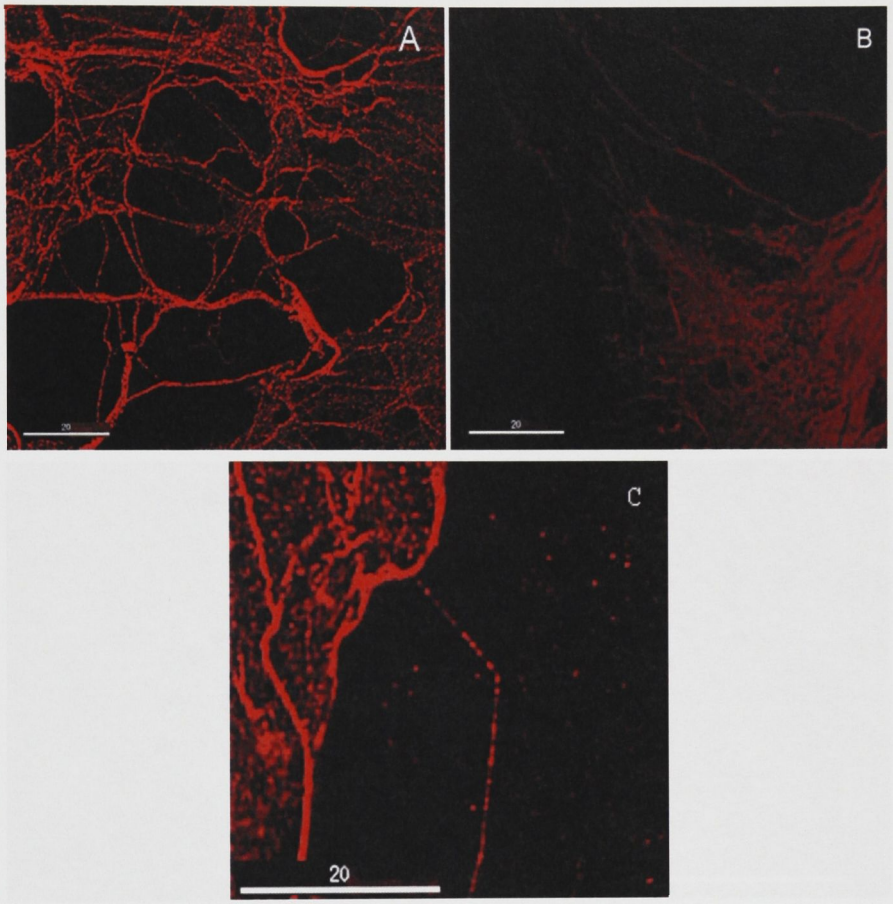

Fig. 4.4 The figure shows de-convoluted confocal images of the detection of endogenous Ttyh1 in primary rat hippocampal cultured cells using affinity-purified antibody AP1. (A) Ttyh1 was expressed in small dots along axons in a similar pattern to that observed in Ttyh1-GFP expression studies. (B) Detection was blocked by the addition of 200 μg/mL of the peptide antigen 802. (C) A close-up view of a single axon emphasizes the characteristic pattern of Ttyh1 dots. Scale bars represent 20 μm.

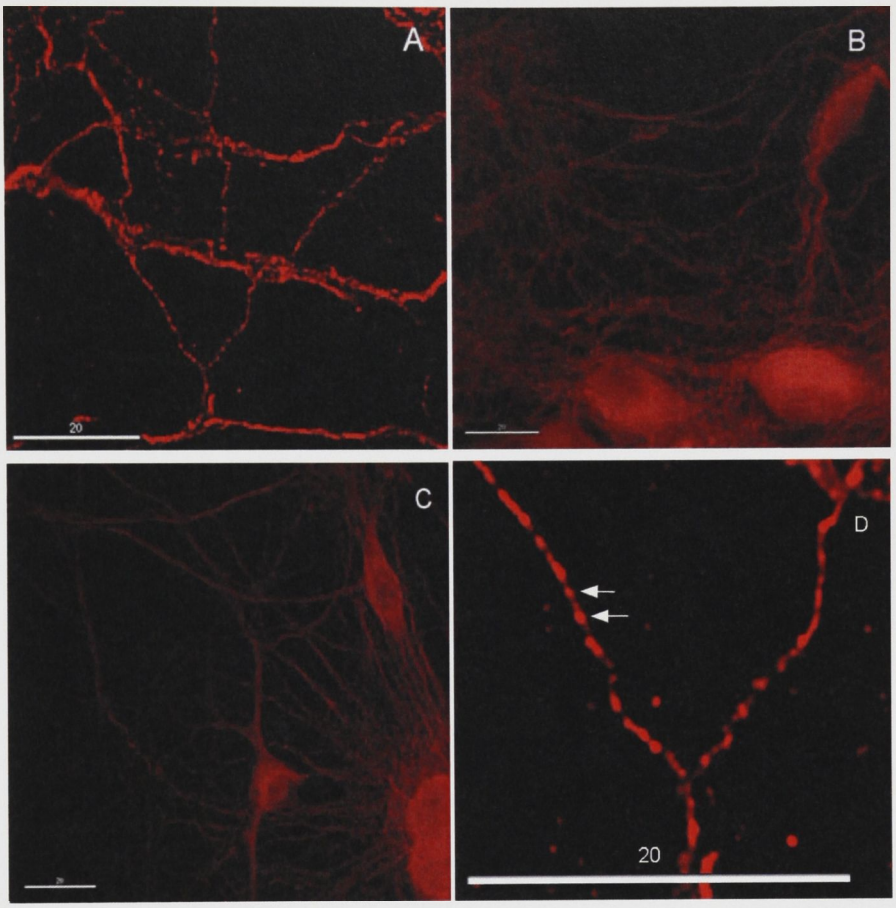

Fig. 4.5 The figure shows de-convoluted confocal images of the detection of endogenous Ttyh1 in primary rat hippocampal cultured cells using antibody AP2. (A) Ttyh1 was expressed in small dots along axons in a similar pattern to that observed using AP1. (B) Detection was blocked by the addition of 200 μg/mL of the peptide antigen. (C) The Ttyh1 dots were absent following staining with the secondary antibody alone. (D) A close-up view emphasizes the characteristic pattern of Ttyh1 dots. Scale bars represent 20 μm.

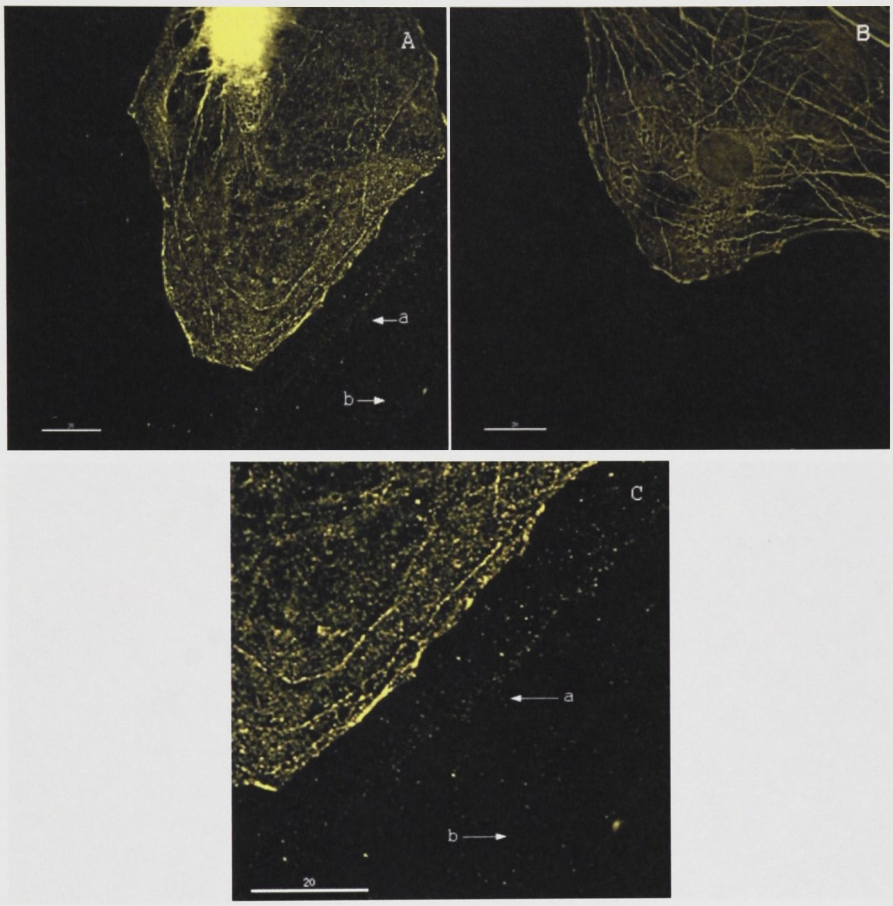

Fig. 4.6 The figure shows de-convoluted confocal images of the detection of endogenous Ttyh1 in primary rat hippocampal cultures which revealed possible Ttyh1 trails behind migrating astrocytes. (A) An astrocyte analysed using AP1 leaving what appears to be a Ttyh1 trail bound to the substrate. (B) The trails were absent following the addition of the peptide antigen. (C) A close-up view reveals the outlines of (a) small protrusions and (b) Ttyh1 trails. Scale bars represent 20 μm.

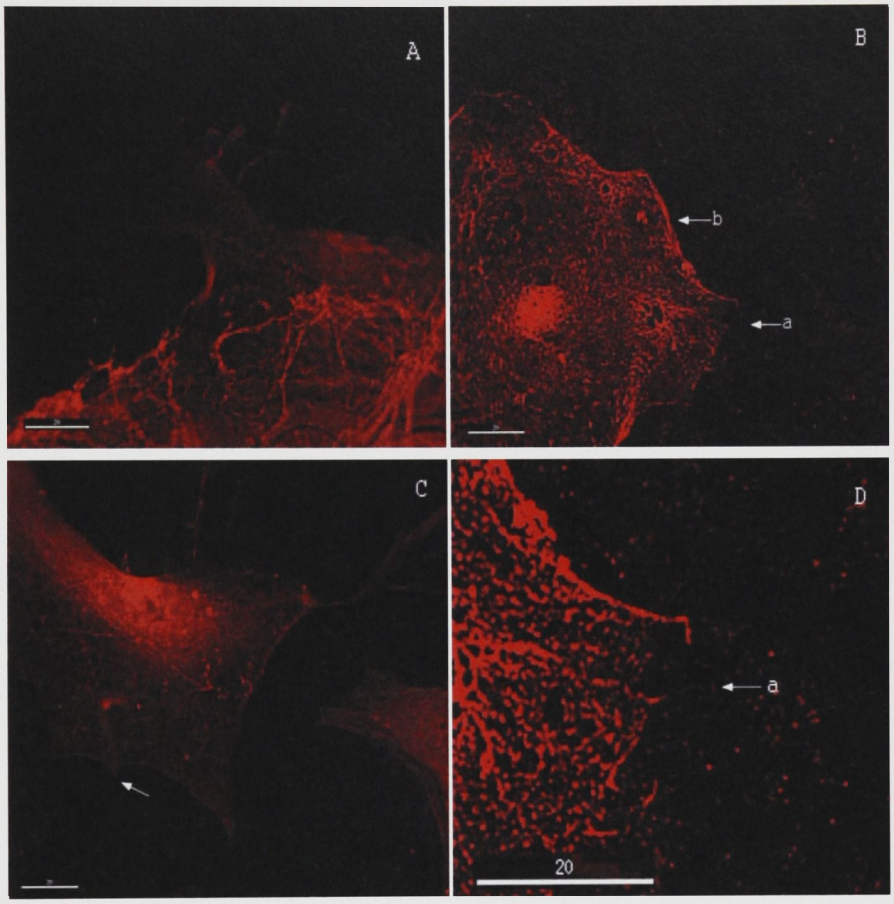

Fig. 4.7 The figure shows de-convoluted confocal images of a neuron scratch assay stained with AP1 which showed possible Ttyh1 staining at the 1 hour time point. (A) Time point 0 hours. (B) The time point at 1 hour showed fluorescence in (a) a small protrusion and (b) along the retracting membrane. (C) The time point at 6 hours showed no fluorescence in the protrusions. (D) A close-up view of the 1 hour time point showing a Ttyh1 trail extending beyond the small protrusion. Scale bars represent 20 μm.

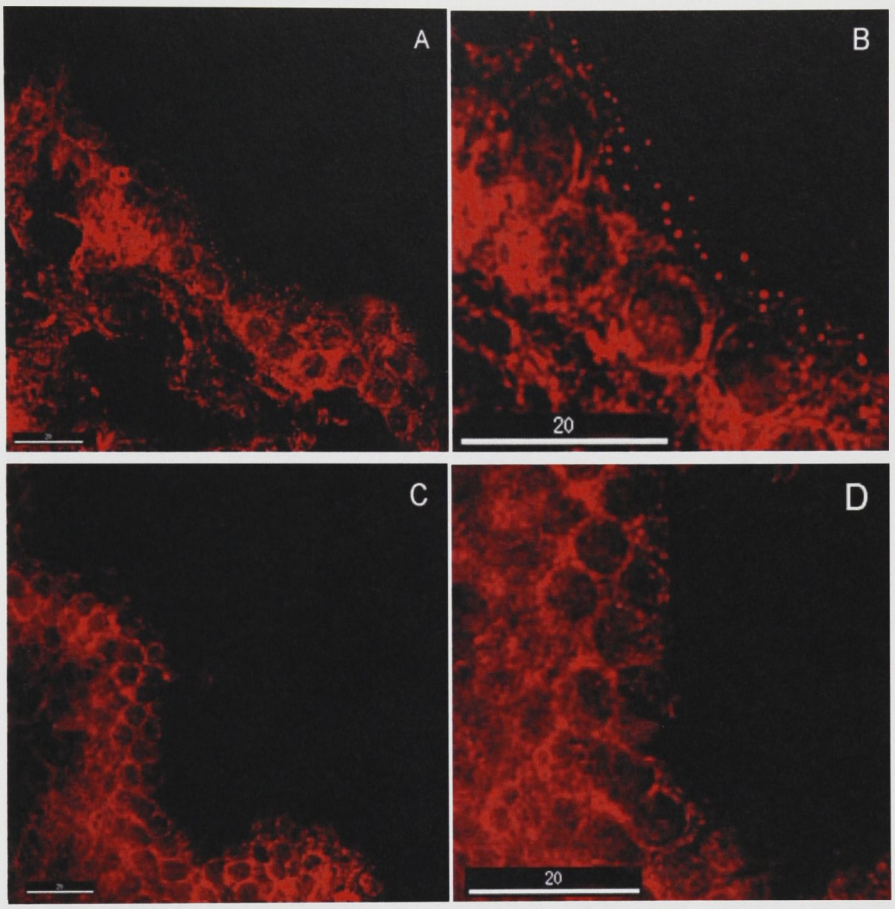

Fig. 4.8 The figure shows de-convoluted confocal images of the detection of Ttyh1 in 10 μm thick anterior to posterior (coronal) rat brain slices using antibody AP2. (A) Ttyh1 dots were detected at the external boundary of the hippocampus. (B) A close-up view of the Ttyh1 staining. (C) The dots of staining were mostly blocked by the addition of antigenic peptide. The remaining staining is likely to be non-specific. (D) A close-up view of the peptide-blocked staining near the edge of the hippocampus. Scale bars represent 20 μm.

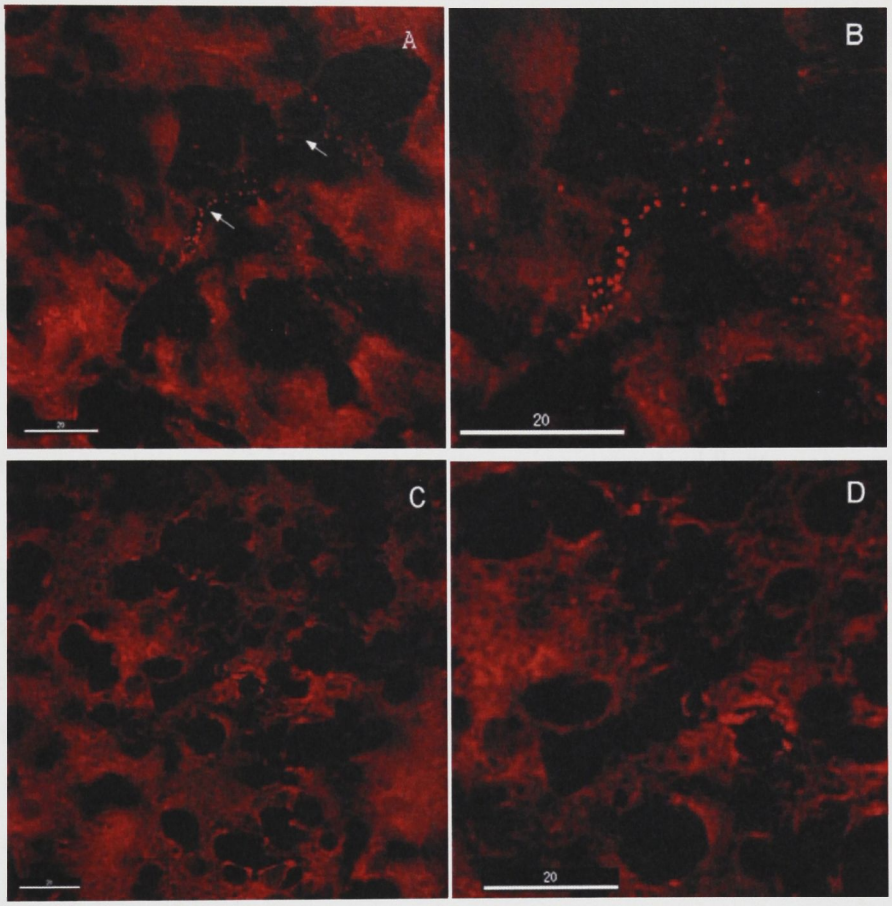

Fig. 4.9 The figure shows de-convoluted confocal images of the detection of Ttyh1 in 10 μm thick anterior to posterior rat brain slices using antibody AP1. (A) Ttyh1 was expressed in dots at cell interfaces (arrows) and around the hippocampus (not shown). (B) A close-up view of the Ttyh1 dots between cells. (C) The staining was blocked by the addition of peptide antigen. (D) A close-up view of the staining after peptide blocking. Scale bars represent 20 μm.

4.4 Discussion

Analysis of available EST data indicated that the expression of Ttyh1 in tissues was specific to the brain and testes with very little expression elsewhere (Rae et al. 2001; Matthews et al. 2007). The results presented here support the EST data by revealing that the Ttyh1 protein was not expressed in any of the cell lines tested, with the exception of primary neuronal cultures. A considerable amount of time was spent investigating the unknown membrane protein detected in ARPE-19 cells as it was not immediately apparent that this immunostaining was an artefact. Initially the protein could only be detected using AP1 with the addition of its cognate peptide antigen. It was not until the image-enhancing deconvolution process was applied to confocal microscopic images that the artefact was detected using the secondary antibody alone. Brighter fluorescence using AP1 when it was combined with peptide 802 is likely to have occurred due to the tendency of the hydrophobic peptide 802 to bind to cellular proteins, thereby making the artefact appear brighter and facilitating detection using a standard light microscope.

Each of the anti-peptide antibodies was successfully used to detect what appeared to be the Ttyh1 protein in primary prenatal rat head cultured cells. The criteria used to eliminate false positives were fulfilled, as the addition of the antigenic peptide abolished detection, and the protein was not visible using the secondary antibody alone. Since the staining was similar to that observed previously in Ttyh1-GFP expression studies, it is likely that this protein is endogenous Ttyh1. A matter of concern was that in prenatal brain cultures, the Ttyh1 protein was only detectable within the first couple of days following cell plating and after this time Ttyh1 was not detectable. The most likely cause of this phenomenon was that the cells were cultured in DMEM containing 10 % FCS without supplements to promote neuronal cell survival or proliferation. Since the entire prenatal head was triturated to isolate cells, many fibroblasts and other cell types would have been present in the culture. These cell types can proliferate in culture, and would quickly become more abundant than any neuronal cells present. Another possibility is that protein expression was down-regulated in the absence of native ECM molecules required to maintain Ttyh1 expression.

In postnatal rat hippocampal cultures, a protein was detected in spots along neuronal axons using both antibodies, and the detected protein satisfied the criteria to be considered genuine endogenous Ttyh1. Upon close inspection the Ttyh1 protein was shown to be expressed in small dots along axons which were very similar to those observed in Ttyh1-GFP expression studies. The Ttyh1 protein was concentrated at probable adhesion sites along axons similar to those observed in Ttyh1-induced filopodia which co-localized with α5 integrin. There were also many substrate-bound particles that were detected using both Ttyh1 antibodies. The substrate-bound particles appeared to have been deposited by migrating astrocytes as the trailing edge of cells moved forward. A simple scratch assay performed to determine whether Ttyh1 was upregulated following monolayer disruption revealed that Ttyh1 was slightly concentrated at the cell membrane after one hour and that the substrate-bound trails were deposited by cells as they moved away from the injury. Small protrusions exist at the trailing edge of migratory astrocytes, and Ttyh1 deposits are likely to have been formed in a similar fashion to those observed in expression studies. The Ttyh1 protein was only detected at the one hour time point following the scratch assay which implicates it in a possible early cell migration event. No obvious upregulation was observed as the cells moved into the scratch over a 48 hour period. These results imply that Ttyh1 is unlikely to be required at the leading edge of cells after early migration events, though further investigation would be required to confirm this.

Since Ttyh1 was detected along neuronal axons and at the cell membrane of astrocytes, it is possible that Ttyh1 mediates the interaction between the two cell types by facilitating adhesion events or cytoskeletal linking. The expression pattern observed in neurons and astrocytes was difficult to detect and required long camera open aperture times. However, the localization of endogenous Ttyh1 and the substrate-bound deposits were almost identical to those observed in expressed Ttyh1-GFP studies. It is probably safe to consider the results obtained during exogenous expression experiments to be applicable to the endogenous protein in its native context. The endogenous expression of Ttyh1 *in situ* was quite difficult to detect and it was only shown to be expressed around the hippocampus and occasionally at the interface between cells. It is likely that the low

level of detection in rat brain slices was due to insufficient access for the antibodies to detect the Ttyh1 protein. A modified IHC protocol may be necessary when probing brain tissue as the relatively high level of detection by Western blotting and in neuronal cell cultures was not observed in brain slices. An alternative Ttyh1-expressing tissue, such as testes, could be included to confirm *in situ* results, along with a non-Ttyh1-expressing tissue, such as liver. A more powerful and tissue-specific permeablisation buffer could facilitate antibody access to the Ttyh1 protein. Alternatively, antibodies directed against the loop region, which is predicted to protrude out of the cell membrane, may facilitate detection if N- and C-terminal conformation or splicing is not conducive to antibody binding.

The experimental results presented in this chapter have confirmed that among the available cell lines, the expression of the Ttyh1 protein was limited to neuronal cell types. Endogenous expression of the native protein has been shown to correspond to the results obtained during Ttyh1-GFP studies. Ttyh1 was expressed in dots along neuronal axons, at likely adhesion points in axons and at the trailing edge of migrating astrocytes where substrate-bound trails were deposited. In thin brain slices Ttyh1 was detected at the interface between cells and around the hippocampus. It is likely that results derived from exogenous Ttyh1 expression studies are applicable to the localization and function of the endogenous protein.

Chapter 5

General Discussion

5.1 Expression of the mammalian Ttyh1 protein

The work described in this thesis was directed at elucidating the cellular function of the mammalian Ttyh1 protein. The Ttyh1 protein is a member of a novel group of mammalian proteins related to the protein encoded by the *D. melanogaster* tty gene (Campbell et al. 1993). These proteins contain five potential membrane spanning regions arranged in a characteristic 2-2-1 pattern (Campbell et al. 2000; Rae et al. 2001). Phylogenetic analysis shows that multiple tty-related genes have arisen via separate gene duplications in the vertebrate (three genes, with further gene duplications in fish and amphibians), insect (two genes in *D. melanogaster* and *A. gambiae*), slime mould (two genes in *D. discoideum*) and plant lineages (four genes in *A. thaliana*) (Matthews et al. 2007). Although the *D. melanogaster* tty gene is not essential for viability, its absence could contribute to the severe phenotype observed when the embryonic lethal fliI gene was deleted, along with tty and several other nearby non-vital genes. The concomitant transgenic replacement of fliI rescued the lethality of this knockout (Campbell et al. 1993; Maleszka et al. 1996); however, the absence of Tty and several other genes may have caused the reduced viability and uncoordinated behaviour observed in flies that survived to adulthood (Maleszka et al. 1996). Expression of Ttyh2 is up-regulated in renal cell carcinoma, and it has been suggested that Ttyh2 may be a cell surface receptor mediating binding of integrins (Rae et al. 2001). EST expression profiles indicate that all the human and mouse tty-related genes are expressed strongly in the brain and eye, with the exception of Ttyh2 which is weakly expressed in the latter. Ttyh1 expression appears to be substantially restricted to neural tissue and testis, whereas Ttyh2 and Ttyh3 are expressed in a significantly broader range of tissues.

5.2 Two splice variants of endogenous Ttyh1

The existence of C-terminal variants of rat Ttyh1 derived by alternative splicing of mRNA, as occurs in the mouse, was supported by our Western blot data using antibodies directed against N- and C-terminal peptides of Ttyh1. Given the consistency with which two bands were detected by the N-terminal antibody, it is possible that modification of the C-terminus leads to an altered peptide target in the 51 kDa Ttyh1 isoform which cannot be detected by the C-terminal antibody. It is also possible that an alternative form

of the N-terminus exists in the native protein. This modification may not be so dramatic since the N-terminal antibody can still detect the same 49 kDa band that is detected by the C-terminal antibody. These results suggest that in rat brain there are two major splicing variants of Ttyh1 leading to two distinct isoforms of the Ttyh1 protein, one which contains the AP2 C-terminus and one which has an altered C-terminus.

5.3 The Ttyh1 protein may be directly associated with F-actin

The results presented here have validated the pEGFP-N1-Ttyh1 and p-N1-Ttyh1 expression vectors for the ectopic expression of Ttyh1-GFP and Ttyh1, respectively, in human and mouse cell lines. The cytoskeleton was identified as a possible Ttyh1-associated structure, in part because solubilisation of the cell membrane using Triton-X100 based lysis buffer was not sufficient to free the Ttyh1 protein from brain tissue. The addition of 0.3 % SDS to the lysis buffer released Ttyh1 into the supernatant, indicating that Ttyh1 was associated non-covalently with a Triton-X100 insoluble cellular component (Patton et al. 1989). The Ttyh1 protein was immunoprecipitated from brain and cell lysates that contained 0.1-0.3 % SDS using AP1, AP2 and a generic anti-GFP antibody. The exogenously expressed Ttyh1-GFP fusion protein was successfully immunoprecipitated from HEK293 cells using the AP1 antibody, and was subsequently immunoblotted using the AP2 antibody. This result confirmed that both antibodies were functioning as intended as they were immuno-reactive to the same expressed Ttyh1 protein. Several unidentified Ttyh1-associated proteins were detected by co-immunoprecipitation and silver staining, although their low concentration did not facilitate analysis by standard mass spectrometry. Extremely sensitive techniques such as MALDI-TOF mass spectrometry may be sufficient to directly identify these co-immunoprecipitated proteins.

5.4 Migration trails implicate Ttyh1 in cell adhesion

It was previously shown that fibroblasts deposit extracellular matrix components along their migration trails (Chen 1981; Halfter et al. 1990), and it has been suggested that these trails may be subsequently utilized by other cells for pathfinding (Halfter et al. 1990). Components of the trails include lipids, integrins and fibronectin (Regen and

Horwitz 1992; Palecek et al. 1996, 1998). GFP derivatives of the adhesion components α5-integrin, paxillin and α-actinin in CHO, B2 and K1 cells have been used to show that α5-integrin is deposited in fibres by migrating cells, but that these fibres lack paxillin and α-actinin (Laukaitis et al. 2001). Similarly, vinculin, talin and F-actin are not deposited in the integrin-rich trails behind motile chicken fibroblasts (Regen and Horwitz 1992) indicating considerable specificity of the deposited material. Integrin is deposited by a process described as membrane ripping, which leaves the α5β1 integrin complex attached to the substrate (Palecek et al. 1996). The formation of these macroaggregates is thought to depend on actin cytoskeleton disruption leading to the fragmentation of cylindrical cell extensions into periodic chains of pearls (Bar-Ziv et al. 1999).

We used the expression of a Ttyh1-GFP fusion protein in HEK293 cells to verify cellular localization. The Ttyh1-GFP protein was initially concentrated in perinuclear regions suggestive of localization to the Golgi apparatus, and after a 36 hour period it had localized to the peripheral membrane. Ttyh1-GFP was observed along regions of cell extension and was highly concentrated at the tips of filopodia, particularly at the interface of the peripheral membrane and the underlying substrate. Removal of the GFP reading frame to allow expression of the Ttyh1 gene without GFP did not affect the localization of the protein or the induction of filopodia, demonstrating that these were specific effects of the expression of Ttyh1. If the function of Ttyh1 involves the identification or deposition of substrate bound environmental cues, the peripheral membrane, and particularly filopodial extensions, would be a logical area for the transmembrane protein to be expressed. Therefore, it is possible that Ttyh1 is involved in providing or detecting substrate-bound environmental cues to facilitate communication with neighbouring cells or path finding.

It has previously been shown that the upregulation of F-actin bundling proteins such as fascin (Yamashiro et al. 1998) and villin (Frank et al. 1990) causes dramatic changes in cell morphology, and results in the formation of long, spiky protrusions at the cell membrane. It is likely that the filopodia play a sensory role in cells, and the induction of similar filopodia by the over-expression of receptors such as SREC substantiates this

claim (Shibata et al. 2004). Ttyh1-induced filopodia were F-actin rich and extended away from the trailing edge of migrating cells, with substrate-bound Ttyh1 deposits extending in chains of dots out past the tips of protrusions. The part of the protrusion that actually contained F-actin was always attached to the cell body, and even when apparently intact filament-like Ttyh1 protrusions were deposited, they did not contain F-actin. When F-actin retracted back into the cell it left protrusions without a supporting backbone. This is likely to have contributed to the disintegration of the substrate-bound membrane upon cell locomotion owing to the adhesive contacts below the filopodia. In fact, F-actin was only observed throughout filopodia by using a fast-fixing method to preserve structures quickly during cell fixation. This may account for the lack of up-regulated active small GTPases that might be expected if an increase in total F-actin was induced by Ttyh1 expression. It is likely that a synaptogenic cell adhesion molecule would be concentrated at the tips of synapses to facilitate heterophilic adhesion between axons and other cell types (Kim et al. 2006). The cytosolic region would be expected to interact with scaffold proteins to enable a coupling of adhesion events with the recruitment of synaptic proteins (Kim et al. 2006). With regard to localization and cytoskeletal interaction, the Ttyh1 protein fulfils the criteria that would be expected of a membrane bound receptor or cell adhesion molecule.

5.5 Deposits of Ttyh1 co-localize with integrin

The Ttyh1-induced protrusions appeared to extend onto the substrate and form focal contacts. The Ttyh1 protein itself was nearly always observed above CD49e, the human homologue of α5-integrin, implying close proximity to focal complexes. If exogenous Ttyh1 expression led to the induction of filopodia that formed focal adhesions inappropriately, they may not have been able to release upon cell migration, thereby causing cytoskeletal disruption and the observed membrane ripping effect. The localization of protrusions to the trailing edge of migrating cells is likely to have been the result of protrusions attaching to the substrate as the cell moved forward. If the cell continued to migrate, the attached protrusion would stretch out from the trailing edge, break off, and leave a substrate-bound deposit. This model was clearly demonstrated by real-time photographic imaging of live Ttyh1-expressing cells. As cells moved along the

substrate with filopodia stretching out from the rear, adherent protrusions were torn from the substrate, recoiled towards the cell body and left a Ttyh1-rich deposit behind on the substratum.

The Ttyh1 migration trails were reminiscent of the integrin-rich trails deposited by motile fibroblasts and suggested that Ttyh1 was spatially and perhaps functionally associated with integrins. Analysis of substrate-bound Ttyh1 filopodia showed that Ttyh1-GFP was highly concentrated at the tips of filopodia, at points of trajectory change and where filopodia made contact with one another. For a sharp angle to form in filopodia, it would be necessary to attach the structure to the substrate at the angle's zenith. It would be safe to assume that adhesion sites exist at these points of trajectory change, which is exactly where Ttyh1-GFP was concentrated. These small dots of concentrated Ttyh1 in the filopodia were shown to co-localize with CD49e integrin, implying that Ttyh1 was specifically targeted to areas of integrin-mediated focal adhesion. In a recent publication, the expression of α5 integrin appears to have induced the formation of long, branched filopodia, though this induction may have been overlooked and was not discussed in the paper (Laukaitis et al. 2001). Since (a) the expression of Ttyh1 results in the formation of filopodia, (b) the expression of α5 integrin induces very similar filopodia and (c) Ttyh1 co-localizes with α5 integrin, it is possible that both proteins are eliciting the induction of filopodia via a common, cell adhesion-associated signalling pathway.

Integrins are capable of acting synergistically with cell membrane receptor systems to finely modulate cell adhesive activities in response to environmental signals (Schmid and Anton 2003), and membrane bound adhesion molecules have been shown to trigger synapse formation (Fu et al. 2003). The action of these adhesion molecules is not limited to initial contact formation but can also perform the function of specific target recognition (Shen et al. 2004). Mice that express null mutations in genes for many of the α- and β-integrin subunits show a wide range of distinct phenotypes, indicating that many of the integrins have specific functions with less overlap than previously thought

(Sheppard 2000). A complete understanding of the association of integrins with Ttyh1 requires further investigation.

5.6 The expression of Ttyh1 causes microtubule polarization

The expression of Ttyh1 had an effect on the conformation of the cytoskeletal microtubules in HEK293 cells. In control cells, the paths of microtubules were directed through the cytoplasm towards the cell membrane, but then ran along parallel to the membrane in most cases. In areas where microtubules were turned towards the membrane, short protrusions were formed, though these occasions were rare in comparison with Ttyh1-expressing cells. The majority of microtubules near the periphery in Ttyh1-expressing cells were orientated towards the membrane and, in many cases, long Ttyh1-induced filopodia projected onto the substrate from near the tips of microtubules. Distinct Ttyh1-rich dots were coincident with microtubules around the nucleus and extended along the microtubules from the Golgi to the cell membrane. It is very likely that Ttyh1, along with other focal adhesion components, is transported to the membrane via microtubules where its integration into the membrane leads to the induction of actin-rich filopodia. Microtubule polarization towards the membrane is known to occur at the core of neuronal growth cones during axon extension (Lee and Kolodziej 2002). In growth cones, filopodia at the leading edge contain F-actin whereas the core contains polarized microtubules. The actin-microtubule interface is crucial for the regulation of cell dynamics during morphogenesis and cell motility.

Analysis of cell-cell interactions between Ttyh1-expressing cells and neighbouring cells revealed that filopodia making contact with other cells often formed a thick cable of F-actin, and that Ttyh1 was expressed throughout the cable. The Ttyh1 protein was highly concentrated at the interface between the F-actin cables and the contacted cell, suggesting a role for Ttyh1 in the formation of adhesive contacts between the cells. If two cells were to make contact via a Ttyh1 projection, mechanical forces could convey information to both cells thereby facilitating cell-cell communication. In addition, Ttyh1 was up-regulated directly behind filopodia in regions of cell-cell contact where the protrusions mediated the formation of direct cytoskeletal F-actin links between cells. In

many instances it appeared that Ttyh1 filopodia had somehow opened a pore in the membrane of contacted cells to facilitate the formation of F-actin bridges between the cells. The observation that Ttyh1-GFP deposits were also left on the cell membrane of cells which had been in contact with filopodia implies that a substantial mechanical force had been developed between the cells in order to cause the membrane ripping events. It would be useful to over-express Ttyh1 in neuronal cell types that express endogenous Ttyh1 to see if similar cables and filopodia are formed.

5.7 The putative anion channel activity of Ttyh1

There is substantial evidence that the actin cytoskeleton is involved in the gating of volume regulatory anion channels (VRAC) in several cell types (Moustakas et al. 1998). It has been well documented that VRAC are positively-regulated by the disruption of F-actin, although negative modulations have also been reported (Jakab et al. 2002). The destabilization of actin polymers promotes the activation of Cl^- currents with biophysical and pharmacological characteristics that overlap those of VRAC in cultured cortical astrocytes (Lascola and Kraig 1996). However, the most recent investigation has ruled out the possibility that actin cytoskeleton disassembly plays a direct role in VRAC regulation (Benfenati et al. 2007). In the latter study, the aquaporin (AQP) family of water channels were used to investigate VRAC currents. The AQP channels are a specialized family of related proteins encompassing at least 11 members in mammals (Verkman 2005), with AQP4 most abundantly expressed in the brain (Amiry-Moghaddam and Ottersen 2003). Under experimental gene knockout conditions, there was no difference in basal conductance between control siRNA- and AQP4siRNA-knockout astrocytes in which the actin cytoskeleton had been altered (Nicchia et al. 2005). Furthermore, a prolonged incubation in the presence of cytochalasin D caused deregulation of the actin cytoskeleton, as revealed by extreme changes in cell morphology, but did not alter VRAC current. Similarly, the treatment of astrocytes with the re-polymerizing agent, jasplakinolide, did not restore the hypotonicity-mediated current in AQP4siRNA astroglia (Benfenati et al. 2007). Collectively, these results demonstrated that VRAC are not gated by F-actin mediated mechanisms.

Since both osmotic and pressure differences activate I_{cl} swelling, it could be argued that the channel is gated by membrane tension. However, tension generated by the same osmotic or pressure difference would, in accordance with Laplace's law, differ substantially between cells with different shapes. A stretch-activated channel in any given cell would experience a different gating signal from surrounding cells, depending on its shape, for the same osmotic or pressure gradient. Mechanically activated anion channels have a very large conductance (~300 ps), but are different from volume-activated channels (Nilius et al. 1997). These channels are believed to be activated directly by mechanical force as mechanosensory responses often occur on a sub-millisecond time scale which is faster than would be permitted by a second messenger system (Suksarev and Corey 2004).

We found that the cDNA of the hTtyh1sv splice variant which was used in the ion channel study by Suzuki and Mizuno (2004) lacked exon 11 of the more common transcripts, and contained a number of frameshift alterations that may have affected its function (Matthews et al. 2007). The hTtyh1sv gene sequence was isolated from a retinal library, and RT-PCR revealed that mTtyh1, but not mTtyh1sv, is expressed in the hippocampus and hypothalamus (Suzuki 2005). The most compelling evidence of chloride channel activity in a Tty-related protein is for Ttyh3. However, Ttyh3 is most distantly related to Ttyh1 and Ttyh2 (Suzuki 2005, Matthews et al. 2007), contains six transmembrane segments (Suzuki 2005) and is expressed in a wide range of non-neural tissues (Matthews et al. 2007). Data suggest that Ttyh1sv may function independently of the canonical Ttyh1 isoform (Suzuki 2005), and therefore an association with the chloride channel activity detected in Ttyh3 cannot be made. Known anion channels have been shown to exhibit a negative grand average of hydropathy score, whereas Ttyh1 has a positive score which would be highly unusual for an anion channel (Millar et al. 2001). A recent paper identified Ttyh1 expression in the superior olivary complex of the mammalian auditory brainstem (Nothwang et al. 2006). If Ttyh1 was to cause a large swelling-induced Cl^- current this would suggest a role in cell volume regulation. However, the role of the canonical Ttyh1 isoforms in neurons may be different from the maxi-Cl^- channel activity observed in the splice variant, as intracellular chloride

concentration is very tightly regulated in neurons owing to its importance in inhibitory neurotransmission (Ben-Ari 2002).

It is possible that the observed whole cell maxi-Cl^- activity caused by the Ttyh1 splice variant was a secondary effect of cytoskeletal disruption leading to the activation of endogenous VRAC. We have shown that the canonical form of Ttyh1 can induce F-actin polymerization and is upregulated in focal adhesions. If an abnormal form of Ttyh1 was expressed in cells, this would be likely to have an effect on F-actin dynamics and may facilitate disruption of cytoskeletal-membrane connections at lower osmotic pressures than in the control cells. This could result in the indirect activation of VRAC and cause the observed Cl^- currents. These results may actually substantiate the evidence presented here that Ttyh1 is a transmembrane F-actin binding protein. If the Ttyh1 protein exhibits any chloride channel activity, it is more likely to be induced by ECM adhesion-mediated mechanical activation than by osmotic pressure considering that it is expressed almost exclusively in neural tissues. Further work is necessary to determine whether common variants of Ttyh1 exhibit ion channel activity.

5.8 Ttyh1 localizes to focal adhesions and affects cell migration

When focal complexes form in the vicinity of lamellipodia which flank the cell body, they fuse together at the trailing edge to create large, oval shaped adhesions resembling complete focal adhesions (Anderson et al. 1996). The lateral adhesions are mobile, transient, and are drawn towards the flanks of the cell body in a sliding motion which is driven by the contractile bundles of laterally orientated actin filaments (Anderson et al. 1996; Lee et al. 1994). Rear detachment is known to be a rate-limiting step in cell migration (Anderson et al. 1996), and filopodia have been associated with cells that move directionally (Ribeiro et al. 2002). There is also evidence that cellular extensions participate in guided migration (Rorth 2003). Nascent focal adhesions that formed at the rear of Ttyh1-GFP expressing cells appeared to sequester Ttyh1-GFP from the surrounding focal complexes and cytoplasm. Ttyh1-GFP became highly concentrated in the new focal adhesions and remained dynamically associated with them as cells migrated. The expression of Ttyh1-GFP in HEK293 cells resulted in a significantly

increased rate of cell migration. Since the Ttyh1 protein traverses the cell membrane, associates with the F-actin cytoskeleton and co-localizes with integrins, it may mediate the connection between specific integrin subunits and the cytoskeleton. It is possible that the Ttyh1 protein modulates the rate of cell migration by facilitating F-actin polymerization at focal adhesion sites.

On occasions where cells had been mechanically removed from the substrate, clear Ttyh1-GFP footprints remained attached depicting the outline of where the cell had been. This exemplifies the strength of the association between the Ttyh1 protein and cell adhesion molecules. It has previously been reported that knockouts of the non-vital genes dodo, penguin and tweety in *Drosophila* results in reduced viability. When knockouts of multiple non-vital genes in the flightless locus were performed, flies that survived to adulthood were uncoordinated, sluggish and rarely lived for longer than two days (Maleszka et al. 1996). Although the Tty gene is not essential for viability and its removal does not result in a dramatic phenotype, a comparison with knockout studies of known neural adhesion molecules reveals similar behavioural abnormalities and possible genetic redundancy.

Considerable research has been conducted with the aim of describing phenotypes associated with synaptic cell adhesion molecules in the brain (Tomasiewicz et al. 1993, Cremer et al. 1994, Polo-Parada et al. 2004). Neural cell adhesion molecules (NCAMs) were the first Ig superfamily members to be described that were involved in cell adhesion at the synapse (Barbas et al. 1988). These are a family of three alternatively spliced transmembrane proteins which have been shown to mediate homophilic adhesion and neurite outgrowth (Niethammer et al. 2002). Surprisingly, even the complete knockout of all three NCAMs in mice does not result in a severe phenotype, but rather in a reduction in brain size and poor spatial learning capabilities (Cremer et al. 1994). Synapses are preferentially established on neurons which express NCAMs (Dityatev et al. 2004), but impaired synapse formation in NCAM knockout cells can be rescued by the expression of any one of the major NCAM isoforms (Dityatev et al. 2004) highlighting the redundancy that exists between these related genes. The L1 cell adhesion molecule is also a member

of the Ig superfamily, is expressed in the brain and exhibits homophilic and heterophilic cell adhesion properties (Kamiguchi et al. 1998). The L1 membrane protein has been shown to mediate pre-synaptic and post-synaptic cell adhesion, and to promote axon outgrowth (Lemmon et al. 1989). Knockout of L1 results in an increased rate of embryonic lethality, reduced postnatal survival (Dahme et al. 1997) and abnormalities in spatial learning and exploratory behaviour (Demyanenko et al. 2001).

The reduced viability and uncoordinated or sluggish behaviour associated with Tty knockout in *Drosophila* (Maleszka et al. 1996) may be comparable to the phenotypes observed after knockout of known neural adhesion molecules. Studies have suggested that these molecules are not essential for the formation of central synapses but instead are likely to be involved in differentiation or activity-driven remodelling (Polo-Parada et al. 2004, Dityatev et al. 2004). The compensatory mechanisms of neural cell adhesion molecules may be responsible for the lack of a severe phenotype. Since there are at least two separate isoforms of Tty expressed in *Drosophila*, it is possible that the subtle phenotype observed after Tty knockout was due to similar redundancy between the Tty genes. The behavioural abnormalities observed after the knockout of known neural adhesion molecules are similar to those observed after Tty knockout. These data support the hypothesis that Ttyh1 functions as a neural cell adhesion molecule.

5.9 Endogenous Ttyh1 is expressed in neurons and astrocytes

We detected endogenous Ttyh1 immunohistochemically in cultured hippocampal neurons, astrocytes and in thin brain slices. Ttyh1 was expressed around the hippocampus and occasionally in regions where cells appeared less dense than in the surrounding tissue. In neurons, Ttyh1 was detected in dots along axons in a pattern which was very similar to that observed in the filopodial structures induced by Ttyh1 expression in HEK293 cells. Our results support EST data as the Ttyh1 protein was not detected in any of the cell lines tested, with the exception of primary neuronal cultures. The Ttyh1 protein was concentrated at probable adhesion sites along axons similar to those observed in Ttyh1-induced filopodia which co-localized with α5 integrin. There were also many substrate bound particles detected using the N- and C-terminal Ttyh1 antibodies that

appear to have been deposited by the trailing edge of migrating astrocytes. Small protrusions exist at the trailing edge of astrocytes and endogenous Ttyh1 deposits appear to be formed in a similar manner to those observed during expression studies. It is probably safe to consider the results obtained in exogenous expression experiments to be applicable to the localization and function of the endogenous protein in its native context.

The early evolutionary origin of the tty family, leading to its occurrence in organisms without nerve cells, indicates that Ttyh1 has been recruited during evolution for a specific nervous system function from non-neural tissues. The Ttyh1 protein is expressed along neuronal axons, is highly expressed at cell-matrix and cell-cell interfaces, and can induce morphological changes in the actin cytoskeleton. It is closely associated with integrins and can influence the rate of cell migration. The knockout of Tty, and other genes in the flightless locus, results in a phenotype that is comparable to those observed following the knockout of known neural cell adhesion molecules. It is likely that Ttyh1 is an F-actin-associated cell adhesion molecule or receptor that can influence neuronal adhesion and F-actin cytoskeletal dynamics, thereby affecting migration and cell communication in the mammalian brain.

Further studies on the biological function of Ttyh1 should be aimed at identifying a phenotype by inactivating the Ttyh1 gene and its isoforms in a mammalian model system. Investigations could initially be carried out using *C. Elegans* as the model system as there is only one copy of the Tty gene in this organism, and compensatory mechanisms due to gene redundancy could be avoided. The signalling pathways involved in the generation of the filopodia should be examined in wild type and Ttyh1 knockout cells to determine where Ttyh1 is involved. The mutation of known signalling intermediates and identification of mutations which affect the formation of Ttyh1-induced cellular projections would help to shed further light on the regulation and detailed biological role of this protein.

References

Abercrombi, M., Heaysman, J. E. and Pegrum S. M. (1971) Adhesion plaques associated with the production of a daughter cell in Euglypha (Testacea; Potozoa). Exp. Cell Res. 67, 359-367.

Allen, W. E., Jones, G. E., Pollard, J. W. and Ridley, A. J. (1997) Rho, Rac and Cdc42 regulate actin organization and cell adhesion in macrophages. J. Cell Sci. 110, 707-720.

Amiry-Moghaddam M. and Ottersen O. P. (2003) The molecular basis of water transport in the brain. Nat. Rev. Neurosci. 4, 991-1001.

Anderson, K. I. and Cross, R. (2000) Contact dynamics in keratocyte motility. Curr. Biol. 10, 253-260.

Anderson, K. I., Wang, Y. L. and Small J. V. (1996) Coordination of protrusion and translocation of the keratocyte involves rolling of the cell body. J. Cell Biol. 134, 1209-1218.

Avnur, Z., Small, J. V. and Geiger, B. (1983) Actin-independent association of vinculin with the cytoplasmic aspect of the plasma membrane in cell-contact areas. J. Cell Biol. 96, 1622-1630.

Balaban, N. Q., Schwartz, U. S., Riveline, D., Goichberg, P., Tzur, G., Sabanay, I., Mahalu, D., Safran, S., Bershadsky, A., Addadi, L. and Geiger, B. (2001) Force at single focal adhesions determines their assembly: A study using elastic micro-patterned substrates. Nat. Cell Biol. 3, 466-472.

Barbas, J. A., Chaix, J. C., Steinmetz, M. and Goridis, C. (1988) Differential splicing and alternative polyadenylation generates distinct NCAM transcripts and proteins in the mouse. EMBO J. 7, 625-632.

Bar-Ziv, R., Tlusty, T., Moses, E., Safran, S. A. and Bershadsky, A. (1999) Pearling in cells: A clue to understanding cell shape. Proc. Natl. Acad. Sci. USA 96, 10140-10145.

Benfenati, V., Nicchia, G. P., Svelto, M., Rapisarda, C., Frigeri, A. and Ferroni, S. (2007) Functional down regulation of volume regulated anion channels in AQP4 knockdown cultured rat cortical astrocytes. J. Neurochem. 100, 87-104.

Beningo, K. A., Dembo, M., Kaverina I., Small, J. V. and Wang, Y. L. (2001) Nascent focal adhesions are responsible for the generation of strong propulsive forces in migrating fibroblasts. J. Cell Biol. 153, 881-888.

Bershadsky A., Chausovsky, E., Becker, A., Lyubimova A. and Geiger B. B. (1996) Involvement of microtubules in the control of adhesion-dependent signal transduction. Curr. Biol. 6, 1279-1289.

Bretscher, A. (1999) Regulation of a cortical structure by the ezrin-radixin-moesin protein family. Curr. Opin. Cell Biol. 11, 109-116.

Bretscher, M. S. (1996) Moving membrane up to the front of migrating cells. Cell 85, 465-467.

Brock, J., Midwinter, K., Lewis, J. and Martin, P. J. (1996) Healing of incisional wounds in the embryonic chick wing bud: characterization of the actin purse-string and demonstration of a requirement for Rho activation. J. Cell Biol. 135, 1097-1107.

Brown, N. H. (1994) Null mutations in the alpha PS2 and beta PS integrin subunit genes have distinct phenotypes Dev. 120, 1221-1231.

Burridge, K., Fath K., Kelly T., Nuckolls G. and Turner C. (1988) Focal adhesions: transmembrane junctions between the extracellular matrix and the cytoskeleton. Annu. Rev. Cell Biol. 4, 487-525.

Campbell H. D., Kamei M., Claudianos C., Woollatt E., Sutherland G. R., Suzuki Y., Hida M., Sugano S. and Young I. G. (2000) Human and mouse homologues of the Drosophila

melanogaster tweety (tty) gene: A novel gene family encoding predicted transmembrane proteins. Genomics 68, 89-92.

Campbell H. D., Schimansky T., Claudianos C., Ozsarac N., Kasprzak A. B., Cotsell J. N., Young I. G., de Couet H. G. and Miklos G. L. (1993) The Drosophila melanogaster flightless-I gene involved in gastrulation and muscle degeneration encodes gelsolin-like and leucine-rich repeat domains, and is conserved in Caenorhabditis elegans and human. Proc. Natl Acad. Sci. USA 90, 11386-11390.

Carton, I., Hermans, D. and Eggermont J. (2003) Hypertonicity induces membrane protrusions and actin remodeling via activation of small GTPases Rac and cdc42 in Rat-1 Fibroblasts Am. J. Physiol. Cell Physiol. 285, 935-944.

Chen, W. T. (1981) Mechanism of retraction of the trailing edge during fibroblast movement J. Cell Biol. 90, 187-200.

Chrzanowska-Wodnicka, M. and Burridge, K. (1996) Rho-stimulated contractility drives the formation of stress fibers and focal adhesions J. Cell Biol. 133, 1403-1415.

Clark, K. A., McGrail, M. and Beckerle, M. C. (2003) Analysis of PINCH function in Drosophila demonstrates its requirement in integrin-dependent cellular processes. Dev. 130, 2611-2621.

Cramer, L. P. and Mitchison, T. J. (1995) Myosin is involved in postmitotic cell spreading J. Cell Biol. 131, 179-189.

Cremer, H., Lange, R., Christoph, A., Plomann, M., Vopper, G., Roes, J., Brown, R., Baldwin, S., Kraemer, P., Scheff, S., Barthels, D., Rajewsky, K. and Wille, W. (1994) Inactivation of the N-CAM gene in mice results in size reduction of the olfactory bulb and deficits in spatial learning. Nature 367, 455-459.

Curtis, A. S. G. (1964) The Mechanism Of Adhesion Of Cells To Glass: A Study by Interference Reflection Microscopy J. Cell Biol. 20, 199-215.

Dahme, M., Bartsch, U., Martini, R., Anliker, B., Schachner, M. and Mantei, N. (1997) Disruption of the mouse L1 gene leads to malformations of the nervous system. Nat. Genet. 17, 346-349.

Danjo, Y and Gipson, I. K. (1998) Actin 'purse string' filaments are anchored by E-cadherin-mediated adherens junctions at the leading edge of the epithelial wound, providing coordinated cell movement
J. Cell Sci. 111, 3323-3332.

Danowski, B. A. (1989) Fibroblast contractility and actin organization are stimulated by microtubule inhibitors. J. Cell Sci. 93, 255-266.

Demyanenko, G. P., Shibata, Y. and Maness, P. F. (2001) Altered distribution of dopaminergic neurons in the brain of L1 null miceDev. Brain Res. 126, 21-30.

De Nichilo, M. O. and Yamada, K. M. (1996) Integrin alpha(v)beta(5)-dependent Serine Phosphorylation of Paxillin in Cultured Human Macrophages Adherent to Vitronectin.J. Biol. Chem. 271, 11016-11022.

Dityatev, A., Dityateva, G., Sytnyk, V., Delling, M., Toni, N., Nikonenko, I., Muller, D. and Schachner M. (2004) Polysialylated neural cell adhesion molecule promotes remodeling and formation of hippocampal synapses.J. Neurosci. 24, 9372-9382.

Drees, B. E., Andrews, K. M. and Beckerle, M. C. (1999) Molecular dissection of zyxin function reveals its involvement in cell motility. J. Cell Biol. 147, 1549-1559.

Drees, B. E., Friederich, E., Fradelizi, J., Louvard, D., Beckerle, M. C. and Golsteyn, R. M. (2000) Characterization of the interaction between zyxin, and members of the

Ena/vasodilator-stimulated phosphoprotein family of proteins. J. Biol. Chem. 275, 22503-22511.

D'souza, S. E., Ginsberg, M. H. and Plow, E. F. (1991) Arginyl-glycyl-aspartic acid (RGD): a cell adhesion motif. Trends Biochem. Sci. 16, 246-250.

Dunn, G. A. (1980) The locomotory machinery of fibroblasts. Eur. J. Cancer 16, 6-8.

Felsenfeld, D. P., Schwartzberg, P. L., Venegas, A., Tse, R. and Sheetz, M. P. (1999) Selective regulation of integrin-cytoskeleton interactions by the tyrosine kinase Src. Nat. Cell Biol. 1, 200-206.

Frank, Z., Footer, M. and Bretscher, A. (1990) Microinjection of villin into cultured cells induces rapid and long-lasting changes in cell morphology but does not inhibit cytokinesis, cell motility or membrane ruffling. J. Cell Biol. 111, 2475-2485.

Franzke, C. W., Tasanen, K., Borradori, L., Huotari, V. and Bruckner-Tuderman, L. (2004) Shedding of collagen XVII/BP180: structural motifs influence cleavage from cell surface. J. Biol. Chem. 279, 24521-24529.

Furukawa, R. and Fechheimer, M. (1997) The structure, function, and assembly of actin filament bundles. Int. Rev. Cytol. 175, 29-90.

Fu, Z-Y., Washbourne, P., Ortinski, P. and Vicini, S. (2003) Functional excitatory synapses in HEK293 cells expressing neuroligin and glutamate receptors. J. Neurophysiol. 90, 3950-3957.

Geiger, B. (1979) A 130K protein from chicken gizzard: its localization at the termini of microfilament bundles in cultured chicken cells.Cell 18, 193-205.

Gloushankova, N. A., Alieva, N. A., Krendel, M. F., Bonder, E. M., Feder, H. H., Vasiliev, J. M. and Gelfand, I. M. (1997) Cell–cell contact changes the dynamics of lamellar activity in nontransformed epitheliocytes but not in their ras-transformed descendants. Proc. Natl. Acad. Sci. U.S.A. 94, 879-883.

Graus-Porta, D., Blaess, S., Senften, M., Littlewood-Evans, A., Damsky, C., Huang, Z., Klein, R., Schittny, J. C. and Muller, U. (2001) Beta1-class integrins regulate the development of laminae and folia in the cerebral and cerebellar cortex. Neuron 31, 367-379.

Goebl, M. G. and Petes, T. D. (1986) Most of the yeast genomic sequences are not essential for cell growth and division. Cell 46, 983-992.

Hall, A. (1998) Rho GTPases and the actin cytoskeleton. Science 279, 509-514.

Hansen, M. D. H. and Beckerle, M. C. (2006) Opposing roles of zyxin/LPP ACTA repeats and the LIM domain region in cell-cell adhesion. J. Biol. Chem. 281, 16178-16188.

Heath, J.P. and Holifield, B.F. (1993) On the mechanisms of cortical actin flow and its role in cytoskeletal organisation of fibroblasts. Symp. Soc. Exp. Biol. 47, 35-56.

Hobert, O., Schilling, J. W., Beckerle, M. C., Ullrich, A. and Jallal B. (1996) SH3 domain-dependent interaction of the proto-oncogene product Vav with the focal contact protein zyxin. Oncogene 12, 1577-1581.

Izzard, C. S. and Lochner, L. R. (1980) Formation of cell-to-substrate contacts during fibroblast motility: an interference-reflexion study. J. Cell Sci. 42, 81-116.

Jacinto, A., Wood, W., Balayo, T., Turmaine, M., Martinez-Arias, A. and Martin, P. (2000) Dynamic actin-based epithelial adhesion and cell matching during Drosophila dorsal closure.Curr. Biol. 10, 1420-1426.

Jakab, M., Furst, J., Gschwentner, M., Botta, G., Garavaglia, M. L., Bazzini, C., Rodighiero, S., Meyer, G., Eichmueller, S., Woll, E., Chwatal, S., Ritter, M. and Paulmichl, M. (2002) Mechanisms sensing and modulating signals arising from cell swelling.Cell Physiol. Biochem. 12, 235-258.

Johnson, N. and Varshavsky, A. (1994) Split ubiquitin as a sensor of protein interactions in vivo. Proc. Natl. Acad. Sci. USA 91, 10340-10344.

Kadrmas, J. L., Smith, M. A., Clark, K. A., Pronovost, S. M., Muster, N., Yates, J. R. and Beckerle, M. C. (2004) The integrin effector PINCH regulates JNK activity and epithelial migration in concert with Ras suppressor 1. J. Cell Biol. 167, 1019-1024.

Kamiguchi, H., Hlavin, M. L. and Lemmon, V. (1998) Role of L1 in neural development: what the knockouts tell us. Mol. Cell Neurosci. 12, 48-55.

Kaverina, I., Rottner, K. and Small J. V. (1998) Targeting, capture, and stabilization of microtubules at early focal adhesions. J. Cell Biol. 142, 181-190.

Kaverina I., Krylyshkina, O., Gimona, M., Beningo, K., Wang, Y. L. and Small, J. V. (2000) Enforced polarisation and locomotion of fibroblasts lacking microtubules. Curr. Biol. 10, 739-742.

Kaverina I., Krylyshkina, O. and Small, J. V. (1999) Microtubule targeting of substrate contacts promotes their relaxation and dissociation. J. Cell Biol. 146, 1033-1044.

Kim, S., Burette, A., Chung, H. S., Kwon, S. K., Woo, J., Lee, H. W., Kim, K., Kim, H., Weinberg, R. J. and Eunjoon, K. (2006) NGL family PSD-95-interacting adhesion molecules regulate excitatory synapse formation. Nat. Neurosci. 9, 1294-1301.

Kirfel, G., Rigort, A., Borm, B. and Herzog, V. (2004) Cell migration: mechanisms of rear detachment and the formation of migration tracks. Eur. J. Cell Biol. 83, 717-724.

Kyte, J. and Doolittle, R. F. (1982) A simple method for displaying the hydropathic character of a protein. J. Mol. Biol. 157, 105-132.

Lascola, C. D. and Kraig, R. P. (1996) Whole-cell chloride currents in rat astrocytes accompany changes in cell morphology. J. Neurosci. 16, 2532-2545.

Lauffenberger, D.A. and Horwitz, A.F. (1996) Cell migration: a physically integrated molecular process. Cell 84, 359-369.

Laukaitis, C. M., Webb, D. J., Donais, K. and Horwitz, A. F. (2001) Differential dynamics of alpha 5 integrin, paxillin, and alpha-actinin during formation and disassembly of adhesions in migrating cells. J. Cell Biol. 153, 1427-1440.

Lee, J., Ishihara, A., Oxford, G., Johnson, B. and Jacobson, K. (1999) Regulation of cell movement is mediated by stretch-activated calcium channels. Nature 400, 382-386.

Lee, J. and Jacobson, K. (1997) The composition and dynamics of cell-substratum adhesions in locomoting fish keratocytes. J. Cell Sci. 110, 2833-2844.

Lee, S. and Kolodziej, P. A. (2002) Short Stop provides an essential link between F-actin and microtubules during axon extension. Dev. 129, 1195-1204.

Lee, J., Leonard, M., Oliver, T., Ishihara, A. and Jacobson, K. (1994) Traction forces generated by locomoting keratocytes. J. Cell Biol. 127, 1957-1964.

Lemmon, V., Farr K. L. and Lagenaur C. (1989) L1-mediated axon outgrowth occurs via a homophilic binding mechanism. Neuron 2, 1597-1603.

Li, S., Bordoy, R., Stanchi, F., Moser, M., Braun, A., Kudlacek, O., Wewer, U. M., Yurchenco, P. D. and Fassler, R. (2005) PINCH1 regulates cell-matrix and cell-cell

adhesions, cell polarity and cell survival during the peri-implantation stage. J. Cell Sci. 118, 2913-2921.

Li, S., Butler, P., Wang, Y., Hu, Y., Han, D. C., Usami, S., Guan, J. L. and Chien, S. (2002) The role of the dynamics of focal adhesion kinase in the mechanotaxis of endothelial cells. PNAS 99, 3546-3551.

Li, S., Harrison, D., Carbonetto, S., Fassler, R., Smyth, N., Edgar, D. and Yurchenco, P. D. (2002) Matrix assembly, regulation, and survival functions of laminin and its receptors in embryonic stem cell differentiation. J. Cell Biol. 157, 1279-1290.

Li, F., Zhang, Y. and Wu, C. (1999) Integrin-linked kinase is localized to cell-matrix focal adhesions but not cell-cell adhesion sites and the focal adhesion localization of integrin-linked kinase is regulated by the PINCH-binding ANK repeats. J. Cell Sci. 112, 4589-4599.

Liang, X., Zhou, Q., Li, X., Sun, Y., Lu, M., Dalton, N., Ross, Jr, J. and Chen, J. (2005) PINCH1 plays an essential role in early murine embryonic development but is dispensable in ventricular cardiomyocytes. Mol. Cell Biol. 25, 3056-3062.

Maleszka, R., Hanes, S. D., Hackett, R. L., DeCouet, H. G. and Miklos, G. L. G. (1996) The Drosophila melanogaster dodo (dod) gene, conserved in humans, is functionally interchangeable with the ESS1 cell division gene of Saccharomyces cerevisiae. Proc. Natl. Acad. Sci. USA 93, 447-451.

Matthews, C. A., Shaw, J. E., Hooper, J. A., Young, I. G., Crouch, M. F. and Campbell, H. D. (2007) Expression and evolution of the mammalian brain gene Ttyh1. J. Neurochem. 100, 693-707.

Maxfield, F. R. (1993) Regulation of leukocyte locomotion by Ca^{2+}. Trends Cell Biol. 3, 386-391.

Milan, M., Perez, L. and Cohen, S. M. (2002) Short-range cell interactions and cell survival in the Drosophila wing.Dev. Cell 2, 797-805.

Millar, H. A., Sweetlove, L. J., Giege, P. and Leaver, C. J. (2001) Analysis of the Arabidopsis mitochondrial proteome. Plant Physiol. 127, 1711-1727.

Miller, J., Fraser, S. E. and McClay, D. (1995) Dynamics of thin filopodia during sea urchin gastrulation. Dev. 121, 2501-2511.

Moorman, J. P., Luu, D., Wickham, J., Bobak, D. A. and Hahn, C. S. (1999) A balance of signaling by Rho family small GTPases RhoA, Rac1 and Cdc42 coordinates cytoskeletal morphology but not cell survival. Oncogene 18, 47-57.

Moustakas, A., Theodoropoulos, P. A., Gravanis, A., Haussinger, D. and Stournaras, C. (1998) The cytoskeleton in cell volume regulation. Contrib. Nephrol. 123, 121-134.

Nayal, A., Webb, D. J. and Horwitz, A. F. (2004) Talin: an emerging focal point of adhesion dynamics. Curr. Opin. Cell Biol. 16, 94-98.

Neyfakh, A. A. and Svitkina, T. M. (1983) Isolation of focal contact membrane using saponin. Exp. Cell Res. 149, 582-586.

Nicchia, G. P., Srinivas, M., Li, W., Brosnan, C. F., Frigeri, A. and Spray, D. C. (2005) New possible roles for aquaporin-4 in astrocytes: cell cytoskeleton and functional relationship with connexin43. FASEB J. 19, 1674-1676.

Niethammer, P., Delling, M., Sytnyk, V., Dityatev, A., Fukami, K. and Schachner, M. (2002) Cosignaling of NCAM via lipid rafts and the FGF receptor is required for neuritogenesis. J. Cell Biol. 157, 521-532.

Oakley, R. A. and Tosney, K. W. (1993) Contact-mediated mechanisms of motor axon segmentation. J. Neurosci. 13, 3773-3792.

Onfelt, B., Purbhoo, M. A., Nedvetzki, S., Sowinski, S. and Davis, D. M. (2005) Long-distance calls between cells connected by tunneling nanotubules. Sci. STKE. Dec 6; (313):pe55.

Palecek, S. P., Huttenlocher, A., Horwitz, A. F. and Lauffenburger, D. A. (1998) Physical and biochemical regulation of integrin release during rear detachment of migrating cells. J. Cell Sci. 111, 929-940.

Palecek S. P., Schmidt C. E., Lauffenburger D. A. and Horwitz A. F. (1996) Integrin dynamics on the tail region of migrating fibroblasts. J. Cell Sci. 109, 941–952.

Pantaloni, D., Le Clainche, C. and Carlier, M. F. (2001) Mechanism of actin-based motility. Science 292, 1502-1506.

Patton, W. F., Dhanak, M. R. and Jacobson, B. S. (1989) Differential partitioning of plasma membrane proteins into the triton X-100-insoluble cytoskeleton fraction during concanavalin A-induced receptor redistribution. J. Cell Sci. 92, 85-91.

Pederson, S. F., Prenen, J., Droogmans, G., Hoffmann, E. K. and Nilius, B. (1998) Separate swelling- and Ca2+-activated anion currents in Ehrlich ascites tumor cells. J. Membr. Biol. 163, 97-110.

Pelham, R. J. and Wang, Y. L. (1999) High resolution detection of mechanical forces exerted by locomoting fibroblasts on the substrate. Mol. Biol. Cell 10, 935-945.

Polo-Parada, L., Bose, C. M., Plattner, F. and Landmesser, L. T. (2004) Distinct roles of different neural cell adhesion molecule (NCAM) isoforms in synaptic maturation revealed by analysis of NCAM 180 kDa isoform-deficient mice. J. Neurosci. 24, 1852-1864.

Rae F. K., Hooper J. D., Eyre H. J., Sutherland G. R., Nicol D. L. and Clements J. A. (2001) TTYH2, a human homologue of the Drosophila melanogaster gene tweety, is located on 17q24 and upregulated in renal cell carcinoma. Genomics 77, 200-207.

Rathke, P.C., Osbourn, M. and Webber K. (1979) Immunological and ultrastructural characterization of microfilament bundles: polygonal nets and stress fibers in an established cell line. Eur J. Cell Biol. 19:40-48.

Ribeiro, C., Ebner, A. and Affolter, M. (2002) In vivo imaging reveals different cellular functions for FGF and Dpp signaling in tracheal branching morphogenesis. Dev. Cell 2, 677-683.

Ritzenthaler, S., Suzuki, E. and Chiba, A. (2000) Postsynaptic filopodia in muscle cells interact with innervating motoneuron axons. Nat. Neurosci. 3, 1012-1017.

Riveline, D., Zamir, E., Balaban, N. Q., Schwartz, U. S., Ishizaki, T., Narumia, S., Kam, Z., Geiger, B. and Bershadsky, A. D. (2001) J. Cell Biol. 153, 1175-1186.

Roberts, M., Barry, S., Woods, A., Van Der Sluijs P. and Norman, J. (2001) Focal contacts as mechanosensors: externally applied local mechanical force induces growth of focal contacts by an mDia1-dependent and ROCK-independent mechanism. Curr. Biol. 11, 1392-1402.

Romijn H. J., de Jong, B. M. and Ruijter, J. M. (1988) A procedure for culturing rat neocortex explants in a serum-free nutrient medium. J. Neurosci. Methods. 23, 75-83.

Rorth, P. (2003) Communication by touch: role of cellular extensions in complex animals. Cell 112, 595-598.

Rosenberg, G. A., Cunningham, L. A., Wallace, J., Alexander, S., Estrada, E. Y., Grossetete, M., Razhagi, A., Miller, K. and Gearing A. (2001) Immunohistochemistry of matrix

metalloproteinases in reperfusion injury to rat brain: activation of MMP-9 linked to stromelysin-1 and microglia in cell cultures. Brain Res. 893, 104-112.

Rossiter, H., Alon, R. and Kupper, T. S. (1997) Selectins, T-cell rolling and inflammation. Mol. Med. Today 3, 214-222.

Rost, B., Fariselli, P. and Casadio, R. (1996) Topology prediction for helical transmembrane segments at 95% accuracy. Prot. Sci. 7, 1704-1718.

Rottner, K., Behrendt, B., Small, J. V. and Wehland, J. (1999) VASP dynamics during lamellipodia protrusion. Nat. Cell Biol. 1, 321-322.

Rottner, K., Hall, A. and Small, J. V. (1999) Interplay between Rac and Rho in the control of substrate contact dynamics. Curr. Biol. 9, 640-648.

Rottner, K., Krause, M., Gimona, M., Small, J. V. and Wehland, J. (2001) Zyxin is not colocalized with vasodilator-stimulated phosphoprotein (VASP) at lamellipodial tips and exhibits different dynamics to vinculin, paxillin, and VASP in focal adhesions. Mol. Biol. Cell 12, 3103-3113.

Sakai, T., Li, S., Docheva, D., Grashoff, C., Sakai, K., Kostka, G., Braun, A., Pfeifer, A., Yurchenco, P. D. and Fassler, R. (2003) Integrin-linked kinase (ILK) is required for polarizing the epiblast, cell adhesion, and controlling actin accumulation. Genes Dev. 17, 926-940.

Schmid, R. S. and Anton, E. S. (2003) Role of integrins in the development of the cerebral cortex. Cereb. Cortex 13, 219-224.

Schoenwaelder, S. M. and Burridge, K. (1999) Bidirectional signaling between the cytoskeleton and integrins. Curr. Opin. Cell Biol. 11, 274-286.

Sheetz, M. P., Felsenfeld, D. P. and Galbraith, C. G. (1998) Cell migration: regulation of force on extracellular-matrix-integrin complexes. Trends Cell Biol. 8, 51-54.

Sheetz, M.P., Felsenfeld, D., Galbraith, C.G. and Choquet, D. (1999) Cell migration as a five-step cycle. Biochem. Soc. Symp. 65, 233-243.

Shen, K., Fetter, R. D. and Bargmann, C. I. (2004) Synaptic specificity is generated by the synaptic guidepost protein SYG-2 and its receptor, SYG-1. Cell 116, 869-881.

Shibata, M., Ishii, J., Koizumi, H., Shibata, N., Dohmae, N., Takio, K., Adachi, H., Tsujimoto, M. and Arai, H. (2004) Type F scavenger receptor SREC-I interacts with advillin, a member of the gelsolin/villin family, and induces neurite-like outgrowth. J. Biol. Chem. 279, 40084-40090.

Shutt, D. C., Wessels, D., Wagenknecht, K., Chandrasekhar, A., Hitt, A. L., Luna, E. J. and Soll, D. R. (1995) Ponticulin plays a role in the positional stabilization of pseudopods. J. Cell Biol. 131, 1495-1506.

Small, J. V. (1981) Organization of actin in the leading edge of cultured cells: influence of osmium tetroxide and dehydration on the ultrastructure of actin meshworks. J. Cell Biol. 695-705.

Small, J. V. and Celis, J. E. (1978) Direct visualization of the 10-nm (100-A)-filament network in whole and enucleated cultured cells. J. Cell Sci. 31, 393-409.

Small, J. V., Rottner K., Kaverina I. and Anderson K. I. (1998) Assembling an actin cytoskeleton for cell attachment and movement. Biochim. Biophys. Acta 1404, 271-481.

Soriano, P. (1995) Gene Targeting in ES Cells. Annu. Review Neurosci. 18, 1-18.

Spaargaren, M. and Bos, J. L. (1999) Rab5 induces Rac-independent lamellipodia formation and cell migration. Mol. Biol. Cell 10, 3239-3250.

Stagljar, I., Korostensky, C., Johnsson, N. and Heesen, S. (1998) A genetic system based on split-ubiquitin for the analysis of interactions between membrane proteins in vivo. Proc. Natl. Acad. Sci. 95, 5187-5192.

Stokes, C. L., Rupnick, M. A., Williams, S. K. and Lauffenburger, D. A. (1990) Chemotaxis of human microvessel endothelial cells in response to acidic fibroblast growth factor. Lab. Invest. 63, 657-668.

Sukharev, S. and Corey, D. P. (2004) Mechanosensitive Channels: Multiplicity of Families and Gating Paradigms Sci. STKE 219, 1-24.

Suter, B., Auerbach, D. and Stagljar, I. (2006) Yeast-based functional genomics and proteomics technologies: the first 15 years and beyond. Biotechniques 40, 625-644.

Suzuki, M. (2005) The Drosophila tweety family: molecular candidates for large-conductance Ca2+-activated Cl- channels. Exp. Physiol. 91, 141-147.

Suzuki M. and Mizuno A. (2004) A novel human Cl(-) channel family related to Drosophila flightless locus. J. Biol. Chem. 279, 22461-22468.

Svitkina, T. M., Verkhovsky, A. B., McQuade, K. M. and Borisy, G. G. (1997) Analysis of the actin-myosin II system in fish epidermal keratocytes: mechanism of cell body translocation. J. Cell Biol. 139, 397-415.

Takenawa, T. and Miki, H. (2001) WASP and WAVE family proteins: key molecules for rapid rearrangement of cortical actin filaments and cell movement. J. Cell Sci. 114, 1801-1809.

Tilly, B. C., Edixhoven, M. J., Tertoolen, L. G. J., Morii, N., Saitoh, Y., Narumiya, S. and de Jong, H. R. (1996) Activation of the osmo-sensitive chloride conductance involves P21rho and is accompanied by a transient reorganization of the F-actin cytoskeleton. Mol. Biol. Cell 7, 1419-1427.

Tomasiewicz, H., Ono, K., Yee, D., Thompson, C., Goridis, C., Rutishauser, U. and Magnuson, T. (1993) Genetic deletion of a neural cell adhesion molecule variant (N-CAM-180) produces distinct defects in the central nervous system. Neuron 11, 1163-1174.

Toomre, D. and Manstein, D. J. (2001) Lighting up the cell surface with evanescent wave microscopy. Trends Cell Biol. 11, 298-303.

Vasiliev, J. M. and Gelfand, I. M. (1976) in Cell Motility, Cold Spring Harbour Laboratory, Cold Spring Harbour, NY, pp. 279-304.

Verkman, A. S. (2005) More than just water channels: unexpected cellular roles of aquaporins. J. Cell Sci. 118, 3225-3232.

Vicente-Manzanares, M., Webb, D. J. and Horwitz, A. R. (2005) Cell migration at a glance. J. Cell Sci. 118, 4917-4919.

Watanabe, N., Kato, T., Fujita, A., Ishizaki, T. and Narumiya S. (1999) Cooperation between mDia1 and ROCK in Rho-induced actin reorganization. Nat. Cell. Biol. 1, 136-143.

Watanabe, N. and Mitchison, T. J. (2002) Single-molecule speckle analysis of actin filament turnover in lamellipodia. Science 295, 1083-1086.

Waterman-Storer, C. M., Worthylake, R. A., Liu, B. P., Burridge, K. and Salmon, E. D. (1999) Microtubule growth activates Rac1 to promote lamellipodial protrusion in fibroblasts. Nat. Cell Biol. 1, 45-50.

Werb, Z. and Yan, Y. (1998) A cellular striptease act. Science 282, 1279-1280.

Wollert, T., DePina, A. S., Thompson, R. F. and Langford, G. M. (2002) Ca(2+) effects on myosin-II-mediated contraction of pseudo-contractile rings and transport of vesicles in extracts of clam oocytes. Biol. Bull. 203, 206-208.

Wulfkuhle, J. D., Donina, I. E., Stark, N. H., Pope, R. K., Pestonjamasp, K. N., Niswonger, N. L. and Luna, E. J. (1999) Domain analysis of supervillin, an F-actin bundling plasma membrane protein with functional nuclear localization signals. J. Cell Sci. 112, 2125-2136.

Yamamoto, S., Higuchi, Y., Yoshiyama, K., Shimizu, E., Kataoka, M., Hijiya, N. and Matsuura, K. (1999) ADAM family proteins in the immune system. Immunol. Today 20, 278-284.

Yamashiro, S., Yamakita, Y., Ono, S. and Matsumura, F. (1998) Fascin, an actin-bundling protein, induces membrane protrusions and increases cell motility of epithelial cells. Mol. Biol. Cell 9, 993-1006.

Yang, J. T., Rayburn, H. and Hynes, R. O. (1995) Cell adhesion events mediated by alpha 4 integrins are essential in placental and cardiac development. Development 121, 549-560.

Zamir, E. and Geiger B. (2001) Molecular complexity and dynamics of cell-matrix adhesions. J. Cell Sci. 114, 3583-3590.

Zamir, E., Katz, M., Posen, Y., Erez, N., Yamada, K. M., Katz, B. Z., Lin, S., Lin, D. C., Bershadsky, A., Kam, Z. and Geiger, B. (2000) Dynamics and segregation of cell-matrix adhesions in cultured fibroblasts. Nat. Cell Biol. 2, 191-196.

Zervas, C. G., Gregory, S. L. and Brown, N. H. (2001) Drosophila integrin-linked kinase is required at sites of integrin adhesion to link the cytoskeleton to the plasma membrane. J. Cell Biol. 152, 1007-1018.

Zhang, Y., Guo, L., Chen, K. and Wu, C. (2002) A critical role of the PINCH-integrin-linked kinase interaction in the regulation of cell shape change and migration. J. Biol. Chem. 277, 318-326.

Zicha, D., Dobbie, I. M., Holt, M. R., Monypenny, J., Soong, D. Y. H., Gray, C. and Dunn, G. A. (2003) Rapid actin transport during cell protrusion. Science 300, 142-145.